

Copyright
by
Madhavi Malladi
2007

**The Dissertation Committee for Madhavi Malladi certifies that this is the
approved version of the following dissertation:**

**Regulation of DIAP1 function by *Drosophila* Omi and the N-end rule
pathway.**

Committee:

Shawn B. Bratton, Supervisor

Janice A. Fischer

Edward M. Mills

Dean G. Tang

Carla Vandenberg

**Regulation of DIAP1 function by *Drosophila* Omi and the N-end rule
pathway.**

by

Madhavi Malladi, B.S.; M.S.

Dissertation

Presented to the Faculty of the Graduate School of
The University of Texas at Austin
in Partial Fulfillment
of the Requirements
for the Degree of

Doctor of Philosophy

The University of Texas at Austin

December 2007

Dedication

To my husband, Srinivas, for all his love and support.

Acknowledgements

I would like to thank my mentor, Dr. Shawn B. Bratton, for his constant guidance, encouragement, constructive criticism and inspiration through out my graduate studies. He was there for me at all times and looked out for me. I will always seek advice and inspiration from him and hope that our relationship continues like this forever.

I would like to thank Dr. Janice Fischer, Dr. Edward (Ted) Mills, Dr. Dean Tang and Dr. Carla Vandenberg for being on my dissertation committee and providing helpful suggestions and comments.

I would also take this opportunity to thank Dr. John Richburg, for his valuable scientific advice and for sharing his passion for photography with me.

I am grateful to the members of Bratton and Mills lab for their friendship and help with this work. Especially, I would like to thank Shankar Vardarajan and Jae kyoung Son (Jay) for making lab a fun place.

Finally, I would like to thank Srinivas, and my family members for all their support without which this endeavor would not have been successful.

Regulation of DIAP1 function by *Drosophila* Omi and the N-end rule pathway.

Publication No. _____

Madhavi Malladi, Ph.D.

The University of Texas at Austin, 2007

Supervisor: Shawn B. Bratton

The molecular mechanisms of apoptosis are evolutionarily-conserved with caspases being the chief executioners of this process. Though key regulators of apoptosis, including caspases, inhibitor of apoptosis (IAP) proteins, and IAP antagonists exist in both mammals and flies, there are reportedly mechanistic differences in the way the apoptotic process is executed. One of the differences pertains to the importance of mitochondrial permeabilization for caspase activation. Herein, we demonstrate that dOmi, a *Drosophila* homologue of the serine protease Omi/HtrA2, is a developmentally-regulated mitochondrial intermembrane space protein that undergoes processive cleavage *in situ* to generate two distinct inhibitor of apoptosis (IAP) binding motifs. Depending upon the pro-apoptotic stimulus, mature dOmi is then differentially released into the cytosol, where it binds selectively to the baculovirus IAP repeat 2 (BIR2) domain in *Drosophila* IAP1 (DIAP1) and displaces the initiator caspase DRONC. This interaction alone, however, is insufficient to promote apoptosis, as dOmi fails to displace the effector caspase DrICE from the BIR1 domain in DIAP1. Rather, dOmi alleviates DIAP1 inhibition of all caspases by proteolytically degrading DIAP1 and induces apoptosis both

in cultured cells and in the developing fly eye. Thus, we demonstrate for the first time in flies that mitochondrial permeabilization not only occurs during apoptosis, but also results in the release of a *bona fide* pro-apoptotic protein.

DIAP1, in addition to being regulated by dOmi, is also regulated by RING-dependent autoubiquitination and by the N-end rule degradation (NERD) pathway. Despite decreasing the cellular levels of DIAP1, the NERD pathway enhances its anti-apoptotic function through an unknown mechanism(s). Herein, we show for the first time that the NERD pathway facilitates *trans*-ubiquitination and degradation of IAP antagonist bound to DIAP1. Indeed, Grim is *trans*-ubiquitinated in an Ubr1-dependent manner and requires its interaction specifically with the BIR1 domain of DIAP1. These results demonstrate that similar to RING domain-dependent ubiquitination, the NERD pathway regulates not only the levels of DIAP1, but also of the levels of IAP antagonists bound to it.

Table of Contents

List of Figures	xiii
List of Tables.....	xv
List of Illustrations.....	xvi
List of Abbreviations.....	xvii
Chapter 1: Introduction	1
1.1 Background.....	1
1.2 Programmed cell death in mammals.....	2
1.2.1 Caspases.....	4
1.2.2 Inhibitor of Apoptosis proteins (IAPs).....	8
1.2.3 IAP antagonists.....	9
1.2.3.1 Smac/Diablo.....	10
1.2.3.2 Omi/Htra2.....	11
1.3 Key regulators of <i>Drosophila</i> apoptosis.....	14
1.4 Mechanisms of <i>Drosophila</i> apoptosis.....	20
1.4.1 Regulation of caspases by DIAP1.....	21
1.4.1.1 Mechanisms of Dronc inhibition	21
1.4.1.2 Mechanisms of DrICE inhibition.....	25
1.4.2 IAP antagonists and DIAP1.....	28
1.4.2.1 Differential regulation of DIAP1 by IAP antagonists.....	28
1.4.2.2 The RHG proteins regulate the levels of DIAP1.....	29
1.4.2.3 IBM-independent roles of the RHG proteins.....	30

1.4.2.4	DIAP1 regulates the expression of RHG proteins through its E3 ligase activity.....	31
1.4.3	Regulation of DIAP1 by caspases	32
1.4.3.1	Cleavage of DIAP1 by Dronc	32
1.4.3.2	DrICE cleavage promotes N-end rule-dependent degradation of DIAP1.....	32
1.4.4	Role of mitochondria in <i>Drosophila</i> apoptosis	37
1.5	Significance of studying apoptosis.....	40
1.6	Significance of studying apoptosis in <i>Drosophila</i>	43
1.7	Dissertation Objectives.....	43
Chapter 2: Methods and materials		46
2.1	Methods and materials for chapter 3.....	46
2.1.1	Bacterial and fly expression constructs.....	46
2.1.2	Cell culture and transfections.....	47
2.1.3	Cell death assays.....	47
2.1.4	<i>Drosophila</i> genetics.....	48
2.1.5	Developmental expression of dOmi.....	48
2.1.6	RNA interference of dOmi.....	49
2.1.7	Subcellular fractionation of <i>Drosophila</i> embryos.....	49
2.1.8	Subcellular localization of dOmi by immunofluorescence.....	50
2.1.9	Mitochondrial release of cytochrome c and dOmi.....	51
2.1.10	GST-DIAP1 pulldown assays.....	52

2.1.11	Displacement of DrICE and DRONC from DIAP1.....	53
2.1.12	Effector caspase (DEVDase) activity assays.....	54
2.1.13	$\Delta\psi_m$ measurements.....	54
2.1.14	DNA fragmentation assay.....	55
2.1.15	Recombinant protein expression.....	55
2.1.16	dOmi protease assays.....	56
2.1.17	Ubiquitination assays.....	57
2.1.18	Structural modeling.....	57
2.2	Methods and materials for chapter 4.....	58
2.2.1	Strains and culture media.....	58
2.2.2	Plasmid construction.....	58
2.2.3	Yeast transformation.....	59
2.2.4	Degradation analysis of the ubiquitin-fusion proteins.....	60
2.2.5	Degradation analysis of the Grim protein.....	60
2.2.6	Viability assays.....	61
2.2.7	Cell culture and transfections.....	61

Chapter 3: *Drosophila* Omi, a mitochondrial-localized IAP antagonist and

proapoptotic serine protease 63

3.1	Introduction.....	63
3.2	Results.....	66
3.2.1	dOmi is a <i>Drosophila</i> Omi/HtrA2 homologue.....	66

3.2.2	dOmi contains an N-terminal targeting sequence that is proteolytically removed during mitochondrial import.....	69
3.2.3	Mature dOmi contains two IBMs and is developmentally-regulated in flies.....	75
3.2.4	Mature dOmi is released from mitochondria during apoptosis via caspase-dependent and -independent mechanisms.....	80
3.2.5	Mature dOmi induces cell death in S2 cells and in the developing fly eye, primarily through its serine protease activity.....	85
3.2.6	The IBMs in dOmi interact selectively with the BIR2 domain in DIAP1 and displace the initiator caspase DRONC.....	86
3.2.7	dOmi alleviates DIAP1 inhibition of caspases by proteolytically degrading DIAP1.....	96
3.3	Discussion.....	99

Chapter 4: Caspase cleavage of DIAP1 promotes N-end rule-dependent *trans*-ubiquitination and degradation of the IAP antagonist Grim

4.1	Introduction.....	103
4.2	Results.....	106
4.2.1	An N-degron form of DIAP1-BIR1 leads to Grim degradation.....	106
4.2.2	Grim is <i>trans</i> -ubiquitinated by Ubr1 an a critical lysine following their association with DIAP1-BIR1.....	114
4.2.3	Cleavage of DIAP1 by Dronc generated a BIR1 fragment that more readily promotes <i>trans</i> -ubiquitination of Grim.....	116

4.3	Discussion.....	119
	Chapter 5: Concluding remarks	125
	References	134
	Vita	154

List of Figures

Figure 3.1	<i>Drosophila</i> Omi is an HtrA family member.....	67
Figure 3.2	<i>Drosophila</i> and mammalian Omi are similar at tertiary structural level.....	68
Figure 3.3	dOmi has two putative cleavage sites after the transmembrane domain.....	71
Figure 3.4	Full-length dOmi is processed into two mature forms.....	73
Figure 3.5	dOmi is a mitochondrial resident protein.....	74
Figure 3.6	Mature dOmi binds DIAP1 <i>via</i> two distinct IBMs.....	77
Figure 3.7	Processing of dOmi occurs in the mitochondria.....	78
Figure 3.8	Expression of dOmi is developmentally regulated.....	79
Figure 3.9	STS and UVB irradiation induce caspase-dependent and -independent MOMP in S2 cells.....	81
Figure 3.10	dOmi, similar to cytochrome c, is released into cytosol in a caspase-dependent and –independent manner in S2 cells.....	82
Figure 3.11	Overexpression of full-length dOmi sensitizes cells to STS treatment....	83
Figure 3.12	Knock down of dOmi by RNAi decreases the caspase activation after STS treatment.....	84
Figure 3.13	Mature dOmi induces cell death in S2 cells.....	87
Figure 3.14	Mature dOmi causes eye ablation phenotype when expressed in <i>Drosophila</i> eye.....	88
Figure 3.15	Mature dOmi binds to the BIR2 domain in DIAP1.....	90

Figure 3.16	The IBM of $\Delta 79$ -dOmi shows exhibits differential binding to the BIR1 and BIR2 domains of DIAP1.....	91
Figure 3.17	Mature dOmi cannot displace BIR1 domain bound active Drice.....	92
Figure 3.18	Mature dOmi displaces the BIR2 domain bound initiator caspase DRONC.....	94
Figure 3.19	dOmi proteolytically degrades DIAP1.....	98
Figure 4.1	Grim stability is dependent on caspase activation.....	108
Figure 4.2	N-degron form of DIAP1 is degraded in an Ubr1-dependent manner...	110
Figure 4.3	N-degron form of DIAP1 promotes <i>trans</i> -degradation of Grim.....	112
Figure 4.4	Difference in the Grim levels are not a consequence of cell death.....	113
Figure 4.5	<i>Trans</i> -degradation of Grim requires its interaction with the BIR1 domain of DIAP1.....	115
Figure 4.6	<i>Trans</i> -degradation of Grim requires an intact lysine at position 136.....	117
Figure 4.7	<i>Trans</i> -degradation of Grim occurs in an Ubr1-dependent manner.....	118
Figure 4.8	<i>Trans</i> -degradation of Grim requires binding to BIR1 domain of DIAP1 only.....	120

List of Tables

Table 3.1	The IBM of mature dOmi has less affinity towards BIR2 domain in DIAP1 relative to Rpr-IBM.	95
-----------	--	----

List of Illustrations

Illustration 1.1	Cell death pathway in <i>C.elegans</i>	3
Illustration 1.2	Simplified overview of intrinsic apoptotic pathway in mammals...	5
Illustration 1.3	Classification of Bcl-2 family members.....	7
Illustration 1.4	An overview of apoptotic pathway in <i>Drosophila</i>	15
Illustration 1.5	Regulation of <i>Drosophila</i> apoptosis by DIAP1.....	22
Illustration 1.6	Comparison of mammalian and <i>Drosophila</i> caspases.....	24
Illustration 1.7	Two proposed models depicting the mechanisms of DrICE inhibition.....	27
Illustration 1.8	Regulation of DIAP1 by caspases.....	34
Illustration 1.9	A simplified overview of the NERD pathway.....	36
Illustration 3.1	Model of dOmi import across the outer mitochondrial membrane and processing within the intermembrane space (IMS).....	70
Illustration 4.1	Scheme representing the ubiquitin-fusion proteins used to generate DIAP1 proteins with either a stabilizing or destabilizing N- terminal residue.....	109
Illustration 4.2	Model depicting the mechanisms involved in the ubiquitin- mediated degradation of the pro-apoptotic proteins by DIAP1...	122

List of Abbreviations

Ala	Alanine
AMC	7-Amino-4-methylcoumarin
Apaf-1	Apoptosis Protease Activating Factor-1
Asn	Asparagine
Arg	Arginine
Asp	Aspartic acid
Ate1	Arginine protein tRNA Transferase
Bcl-2	B Cell Lymphoma-2
BH	Bcl-2 Homology
BIR	Baculoviral Inhibitor of apoptosis Repeat
CARD	Caspase Recruitment Domain
Caspase	CysteinyI Aspartic Acid-specific Proteases
CED	Cell-Death abnormal
cIAP-1	Cellular Inhibitor of Apoptosis Protein-1
cIAP-2	Cellular Inhibitor of Apoptosis Protein-2
CuSO ₄	Copper Sulfate
Cys	Cysteine
Dark	<i>Drosophila</i> Apaf-1 Related Killer
Dcp-1	Death Caspase-1
DebcI	Death Executioner for Bcl-2 homolog
DEVD	L-aspartyl-L-glutamyl-L-valyl-l-aspartic acid
DHFR	Dihydro Folate Reductase
Diablo	Direct IAP Binding protein with low pI
DIAP1	<i>Drosophila</i> Inhibitor of Apoptosis 1
DMSO	Dimethyl-Sulfoxide
DNA	Deoxyribonucleic acid
DTT	1, 4-Dithiothreitol
EDTA	Ethylene Diamine TetraAcetic acid
Egl	Egg-Laying defective
ER	Endoplasmic Reticulum
EST	Expressed Sequence Tag
dOmi	<i>Drosophila</i> Omi
dsRNA	double-stranded ribonucleic acid
Dredd	Death-related CED-3
DrICE	<i>Drosophila</i> Interleukin-1 β -Converting Enzyme
Dronc	<i>Drosophila</i> Nedd-2 like caspase
FITC	Fluorescein Isothiocyanate
GFP	Green Fluorescent Protein
GH3	Grim Helix-3
Gly	Glycine
Glu	Glutamic acid
GMR	Glass-Mediated Response
GSH	Glutathione

GST	Glutathione-S-Transferase
HA	Hemagglutinin
HEPES	N-[2-hydroxyethyl]piperazine-N'-[2-ethanesulfonic acid]
Hid	Head Involution Defective
His	Histidine
HSV	Herpes Simplex Virus
HtrA2	High Temperature Requirement 2
IAP	Inhibitor of Apoptosis
IBM	IAP Binding motif
Ile	Isoleucine
IPTG	isopropyl β -D-thiogalactoside
Leu	Leucine
MEFs	Mouse Embryonic Fibroblasts
Met	Methionine
mnd2	Motor Neuron Degeneration 2
MOMP	Mitochondrial
Morgue	Modifier of <i>reaper</i> and <i>grim</i> , Ubiquitously Expressed
MTS	Mitochondrial Targeting Sequence
NAIP	Neuronal Apoptosis Inhibitory Protein
NBD	Nucleotide Binding Domain
NERD	N-End Rule-dependent Degradation
Ni-NTA	Nickel-Nitrilotriacetic Acid
NTAN1	N-terminal Amino Hydrolyase enzyme 1
PAGE	PolyAcrylamide Gel Electrophoresis
PARP	Poly (ADP-ribose) Polymerase
PBS	Phosphate Buffered Saline
PCR	Polymerase Chain Reaction
PI	Propidium Iodide
PMSF	Phenyl Methyl Sulfonyl Fluoride
Phe	Phenyl Alanine
Pro	Proline
RING	Really Interesting New Gene
RNAi	Ribonucleic Acid Interference
Rpr	Reaper
RT-PCR	Reverse Transcriptase- Polymerase Chain Reaction
SD	Synthetic Defined
SDS	Sodium Dodecyl Sulfate
Ser	Serine
Smac	Second mitochondria-derived activation of caspase
STS	Staurosporine
<i>th</i>	<i>thread</i>
Trp	Tryptophan
Tyr	tyrosine
Ub	Ubiquitin
UEV	Ubiquitin-conjugating enzyme E2 Variant
Ura	Uracil

UV	Ultraviolet
Val	Valine
WT	Wild-type
XIAP	X-linked Inhibitor of Apoptosis Protein
ZVAD-fmk	zVal-Ala-Asp-fluoro-methyl ketone
$\Delta\psi_m$	Mitochondrial Permeability transition

Chapter 1: Introduction

1.1 Background

Apoptosis or programmed cell death is critical for various aspects of development including the removal of structures with transient functions, tissue sculpting and morphogenesis (Vaux and Korsmeyer, 1999). In adult multi-cellular organisms, it plays a pivotal role not only in maintaining tissue homeostasis but also in the removal of damaged cells and immune cells that have the potential to harm the organism (Opferman and Korsmeyer, 2003). Cells undergoing apoptosis exhibit morphological characteristics such as cell shrinkage, plasma membrane blebbing, chromatin condensation, nuclear membrane breakdown, and formation of small vesicles known as apoptotic bodies. Subsequently, phagocytes rapidly engulf these apoptotic bodies thus avoiding a potential inflammatory response (Kerr et al., 1972). Necrosis, on the other hand, is a form of cell death caused by accidental injury and is distinguished by morphological features like cytoplasmic swelling, disruption of various organelles, and loss of membrane integrity. In contrast to apoptosis, necrotic cell death initiates an inflammatory response due to the rupturing of the cell and subsequent release of the cytoplasmic contents (Kerr et al., 1972).

Elegant studies by Horvitz, Brenner, and Sulston in *C. elegans* have led to the characterization of the molecular mechanism of apoptosis. During hermaphrodite development in *C. elegans*, 131 of the 1090 cells generated die by programmed cell death (Sulston et al., 1983). Genetic screens have identified four important loci that perturb

this programmed cell death mechanism: *ced-3* (*ced* for cell-death abnormal), *ced-4*, *ced-9*, and *egl-1* (*egl* for egg-laying defective)(Conradt and Horvitz, 1998; Ellis and Horvitz, 1986; Hengartner et al., 1992; Yuan and Horvitz, 1992) (Illustration 1.1). The *ced-3* locus encodes a pro-apoptotic cysteine protease, the chief executioner of apoptosis, which exists as a zymogen in healthy cells (Xue et al., 1996; Yuan et al., 1993). The *ced-4* locus encodes an adaptor protein that is required for activation of CED-3. The homotypic interaction between CED-3 and CED-4 is required for the activation of the former (Seshagiri and Miller, 1997). However, in healthy cells CED-4 is sequestered due to its interaction with an anti-apoptotic protein, CED-9 (Chinnaiyan et al., 1997; Spector et al., 1997; Wu et al., 1997). The cell death pathway is initiated when pro-apoptotic EGL-1 disrupts the CED-9: CED-4 interaction thereby allowing CED-4 to activate CED-3 (Conradt and Horvitz, 1998; Yan et al., 2004a). Activation of CED-3 leads to cleavage of several cellular substrates ultimately leading to apoptosis (Nicholson et al., 1995)(Illustration 1.1). Analogous to *C. elegans*, mammals also have similar key regulators thus emphasizing the evolutionarily-conserved nature of apoptosis (Hengartner, 1996).

1.2 Programmed cell death in mammals

The apoptotic pathways in mammals can be categorized as either intrinsic or extrinsic based on the origin of death stimuli (Jiang and Wang, 2004). The intrinsic pathway is initiated due to a death stimuli originating within the cell such as oncogene activation or DNA damage whereas, the extrinsic pathway is triggered upon binding of

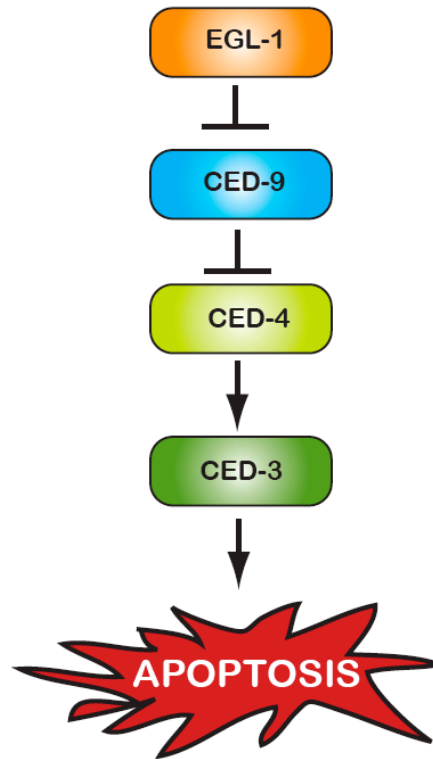


Illustration 1.1 Cell death pathway in *C.elegans*.

The activation of CED-3, through CED-3:CED-4 is required for the execution of apoptosis. However, in healthy cells the CED-4 is sequestered due to its interaction with CED-9. Upregulation of EGL-1 in response to apoptic stimuli, leads to the disruption of CED-4:CED-9 interaction. This is achieved by the binding of EGL-1 to CED-9 thereby, liberating CED-4, which subsequently activates CED-3. Once CED-3 is active it cleaves several cellular substrates ultimately leading to cell death.

extracellular death ligands to cell-surface death receptors. Irrespective of the nature of the stimulus, activation of CED-3 like cysteine proteases is required for carrying out both the pathways (Danial and Korsmeyer, 2004; Riedl and Salvesen, 2007).

1.2.1 Caspases

Caspases, a highly conserved family of cysteine proteases, are the chief executioners of apoptosis (Hengartner, 1996). These proteases have an active site cysteine and cleave their substrates after an Asp residue and hence the name caspases (cysteine-dependent Asp-specific proteases) (Alnemri et al., 1996). Caspases contain an N-terminal prodomain, followed by a large subunit, and a C-terminal small subunit. They are divided into two categories based on their hierarchy of activation: initiator caspases (caspase-2, -8, -9, and -10) characterized by the presence of long N-terminal prodomains, and effector caspases (caspase-3, -6, and -7) with short prodomains (Riedl and Shi, 2004). In response to an apoptotic stimulus, caspases that exist as zymogens are activated either proteolytically or through conformational changes (Shi, 2006). Initiator caspases are activated first and they in turn activate effector caspases by cleaving them at specific internal aspartic acid residues thus leading to a cascade of caspase activation. Once activated, the effector caspases cleave a broad spectrum of cellular targets, which ultimately leads to cell death (Riedl and Salvesen, 2007) (Illustration 1.2).

Generally in the intrinsic pathway, caspase activation requires mitochondrial outer membrane permeabilization (MOMP). MOMP is regulated by the Bcl-2 family members, which are classified as either pro- or anti-apoptotic (Illustration 1.3). Anti-

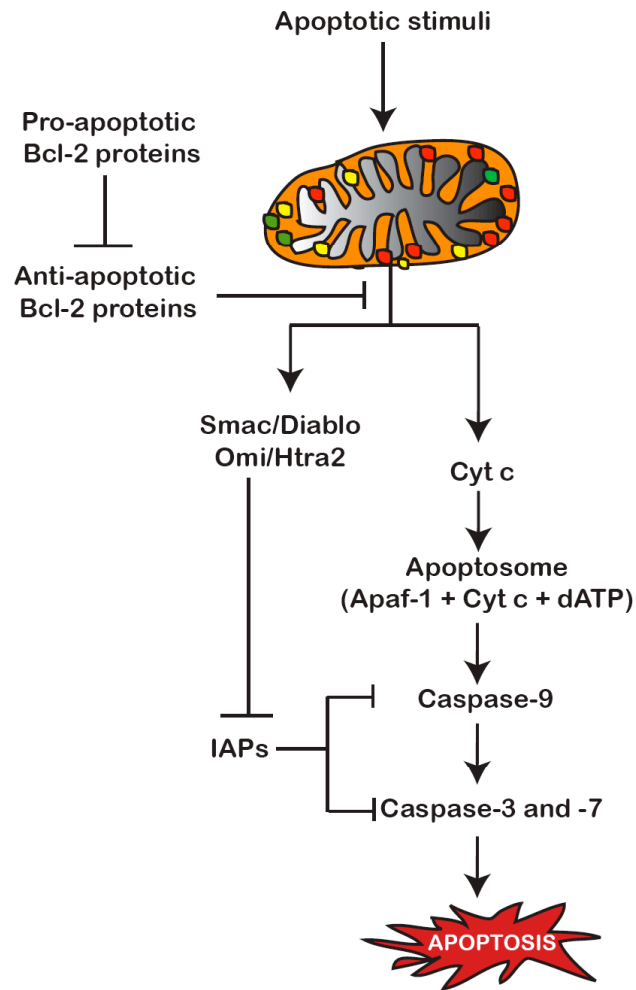


Illustration 1.2 **Simplified overview of intrinsic apoptotic pathway in mammals.**

Upon the receipt of an apoptotic stimulus, pro-apoptotic Bcl-2 members cause MOMP thereby leading to the release of pro-apoptotic factors such as cytochrome c (cyt c), Smac/Diablo, and Omi/HtrA2. The adaptor protein, Apaf-1, along with cyt c and dATP forms an oligomeric complex called the apoptosome, which in turn recruits caspase-9 thereby leading to its activation. Once the initiator caspase-9 is activated, it cleaves the effector caspase-3, which subsequently cleaves various cellular substrates leading to apoptosis. Active caspases-9, -3 and -7 are further inhibited by IAPs with the help of their BIR domains. The IAP antagonists, Smac/Diablo and Omi/HtrA2, bind to IAPs through their N-terminal IBMs consequently leading to caspase displacement.

apoptotic Bcl-2 proteins such as Bcl-2, Bcl-X_L, and MCL-1, which are homologous to CED-9 of *C.elegans*, are characterized by the presence of four Bcl-2 homology (BH) domains (BH1-4). Pro-apoptotic Bcl-2 members are further divided into two categories based on the number of BH domains: multi-domain pro-apoptotic members containing three BH domains (BH1-3) and BH3-only members (Illustration 1.3). Anti-apoptotic Bcl-2 members inhibit the multi-domain pro-apoptotic Bcl-2 proteins, the critical players required for MOMP, by binding and sequestering them. In response to apoptotic stimuli the BH3-only members like Bid and Bim activate the multi-domain pro-apoptotic Bcl-2 proteins like Bax and Bak leading to MOMP. As a consequence of MOMP several inter-membrane space resident proteins such as cytochrome c are released into the cytosol (Danial and Korsmeyer, 2004). The released cytochrome c then binds to an adaptor molecule, Apoptotic protease activating factor-1 (Apaf-1), the mammalian homolog of CED-4 (Zou et al., 1997). Apaf-1 comprises of an N-terminal caspase recruitment domain (CARD), a nucleotide binding domain (NBD), and a series of C-terminal WD-40 repeats. Apaf-1, upon binding to cytochrome c through its WD-40 repeats, interacts with ATP/dATP via its NBD (Acehan et al., 2002). Apaf-1 bound to cytochrome c and dATP forms a heptameric complex termed the apoptosome (Acehan et al., 2002; Cain et al., 2000; Cain et al., 1999) (Illustration 1.2). These interactions reveal the CARD domain of Apaf-1, thus making it competent to bind the prodomain of caspase-9, the mammalian homolog of CED-3 (Acehan et al., 2002; Cain et al., 2000; Cain et al., 1999; Rodriguez and Lazebnik, 1999; Zou et al., 1997). Procaspase-9 once recruited to the apoptosome is activated and also undergoes self-processing in the linker region between the large and

Anti-apoptotic Bcl-2 subfamily



Pro-apoptotic multi-domain Bcl-2 subfamily



Pro-apoptotic BH3-only Bcl-2 subfamily

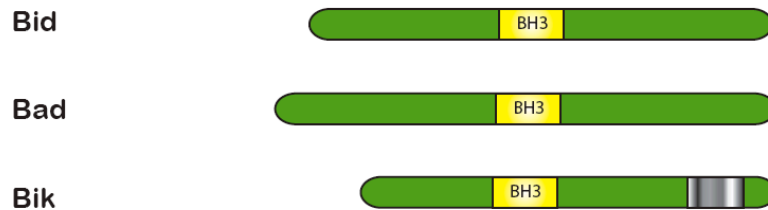


Illustration 1.3 Classification of Bcl-2 family members

Bcl-2 family members are classified into anti- or -pro apoptotic family members. Anti-apoptotic Bcl-2 family members are characterized by the presence of four Bcl-homology (BH) domains: BH1, BH2, BH3 and BH4. Pro-apoptotic multi-domain Bcl-2 subfamily members have BH1-3 domains, which are held in check by interactions with anti-apoptotic Bcl-2 family members. Upon receiving apoptotic stimulus, multi-domain proteins activate BH3-only subfamily members that are required for causing MOMP.

small subunits (Srinivasula et al., 1998). The active caspase-9 bound to apoptosome further cleaves and activates effector caspases like caspase-3, which in turn cleaves several intracellular substrates thus leading to apoptosis (Li et al., 1997) (Illustration 1.2).

1.2.2 Inhibitor of Apoptosis proteins (IAPs)

In mammals, the activated caspases are further regulated by a conserved IAP family of proteins such as X-linked IAP (XIAP), cellular inhibitor of apoptosis protein-1 (cIAP-1), cIAP-2, melanoma IAP (ML-IAP)/Livin, neuronal apoptosis-inhibitory protein (NAIP), Bruce/Apollon, and Survivin (Salvesen and Duckett, 2002). The IAPs were first identified in baculoviruses and are often characterized by the presence of one to three baculoviral IAP repeat (BIR) motifs and sometimes a really interesting new gene (RING) domain (Clem and Miller, 1994; Salvesen and Duckett, 2002). The BIR is an ~ 70 residue zinc-binding domain which plays an important role in protein-protein interactions. The RING domain, which also comprises of a zinc-binding motif, plays an important role in the ubiquitin ligase (E3) activity of the IAPs. In general, the RING domain-containing proteins catalyze ubiquitination and thereby regulate the stability of several proteins as well as themselves. Therefore, the presence of a RING domain in IAPs provides an important link between the ubiquitin signaling pathway (USP) and the regulation of apoptosis. Apart from the BIR and RING domains, cIAP1 and cIAP2 also have a CARD domain whose role in apoptosis remains uncharacterized (Salvesen and Duckett, 2002).

One of the well-characterized IAPs in mammals, XIAP, consists of three BIR domains (BIR1-3) and a C-terminal RING domain (Duckett et al., 1996; Uren et al., 1996). The BIR domains play an important role in binding to caspases thereby inhibiting their activity. The BIR3 domain of XIAP binds exclusively to the processed caspase-9 through the N-terminus of the small subunit thereby potentially inhibiting its activity (Huang et al., 2001; Srinivasula et al., 2001). With respect to the effector caspases-3 and -7, the linker region between the BIR1 and BIR2 domains of XIAP plays an important role in binding and inhibiting the caspase activity. The linker region binds to the active site of the effector caspases thereby preventing access to substrates (Chai et al., 2001a; Huang et al., 2001; Riedl et al., 2001). The E3 ubiquitin ligase activity of the XIAP RING domain regulates apoptosis through ubiquitination of pro-apoptotic molecules such as caspases (Morizane et al., 2005; Suzuki et al., 2001b). The E3 ligase activity of XIAP is also directed towards itself, thus regulating its own levels (Yang et al., 2000).

1.2.3 IAP antagonists

In cells undergoing apoptosis, the inhibition of caspases by IAPs is removed by a group of proteins called IAP antagonists (Illustration 1.2). The IAP antagonists have a characteristic IAP-binding motif (IBM), which comprises of an unmodified alanine residue at the N-terminus. The IBM of an IAP antagonist is required for its interaction with the BIR domain of the IAPs. Either removal of the IBM or mutation of the N-terminal residues to glycines completely abolishes the binding of IAP antagonists to the BIR domains in IAPs. IAP antagonists inhibit the function of IAPs by either displacing

already bound caspases or by preventing BIR:caspase interactions (Salvesen and Duckett, 2002; Vaux and Silke, 2003).

The IAP antagonists characterized so far in mammals are mitochondrial inter-membrane space resident proteins. Despite their localization to mitochondria, mammalian IAP antagonists are nuclear encoded genes. After translation the precursor proteins are targeted to the mitochondria via a classical mitochondrial-targeting signal (MTS) present at their N-termini. In mitochondria, the MTSs are removed to generate mature proteins with IBMs at the new N-termini. Upon MOMP, these proteins are released into the cytosol where they neutralize the inhibitory function of IAPs (Vaux and Silke, 2003). Two of the extensively studied mammalian IAP antagonists include, Smac (second mitochondria-derived activator of caspase)/Diablo (direct IAP binding protein with low pI) (Du et al., 2000; Verhagen et al., 2000) and Omi/HtrA2 (High temperature requirement A2) (Hegde et al., 2002; Martins et al., 2002; Suzuki et al., 2001a; Verhagen et al., 2002).

1.2.3.1 Smac/Diablo

Smac/Diablo, in its mature form ($\Delta 55$ -Smac), inhibits the function of XIAP primarily through its N-terminal IBM, which comprises of the residues Ala-Val-Pro-Ile (Du et al., 2000; Verhagen et al., 2000). The N-terminal Ala of the IBM binds into a hydrophobic pocket in the BIR2 and BIR3 domains of XIAP (Liu et al., 2000; Srinivasula et al., 2000). As described earlier XIAP can inhibit both caspase-9 and caspase-3 through its interactions with the BIR domains (Salvesen and Duckett, 2002). Smac/Diablo,

through its IBM, antagonizes XIAP by displacing the bound caspases. The N-terminus of the caspase-9 small subunit and the IBM of Smac/Diablo compete for the hydrophobic pocket in the BIR3 domain, thereby decreasing the ability of XIAP to bind and inhibit caspase-9 (Wu et al., 2000). Similarly, XIAP inhibition of caspase-3 is also neutralized by the interaction of Smac/Diablo to the BIR2 domain (Chai et al., 2000; Scott et al., 2005). Smac/Diablo in turn can also be regulated by XIAP. *In vitro* studies have demonstrated that XIAP can inhibit the function of Smac/Diablo by RING-dependent ubiquitination thereby promoting its degradation in a proteasome-dependent manner (MacFarlane et al., 2002; Morizane et al., 2005).

1.2.3.2 Omi/HtrA2

Omi/HtrA2 belongs to the HtrA family of serine proteases that are well conserved from bacteria to humans (Clausen et al., 2002). Omi/HtrA2 has an N-terminal MTS, a transmembrane domain, protease domain, and a C-terminal PDZ domain. The N-terminal MTS targets Omi/HtrA2 to mitochondria, where cleavage after the transmembrane domain releases mature Omi/HtrA2 ($\Delta 133$ Omi) into the inter-membrane space with an N-terminal IBM, Ala-Val-Pro-Ser (Hegde et al., 2002; Martins et al., 2002; Suzuki et al., 2001a; Verhagen et al., 2002). The protease domain has an active site, which is comprised of a catalytic triad: Ser-306, His-198, and Asp-228. Mutating the critical amino acids of the catalytic triad abolishes the protease activity of the enzyme. Structural data suggests that the C-terminal PDZ acts as a lid over the active site thus regulating the protease activity by restricting its access to substrates (Li et al., 2002). In

agreement with this data, removal of the PDZ domain enhances the activity of the enzyme (Jones et al., 2003; Li et al., 2002). As the PDZ domain acts as a lid over the active site, it has also been suggested that binding of certain activating peptides (or proteins) to the PDZ domain could cause a conformational change within the tertiary structure and allow access to the active site (Martins et al., 2003). Mature Omi/HtrA2 exists as a homo-trimeric protein with Phe-149 critical for oligomerization. It has been demonstrated that trimerization also regulates protease activity by orienting the PDZ domains into a conformation that allows for easy access of substrates to the active site of the enzyme (Li et al., 2002).

During apoptosis, Omi/HtrA2 is released into the cytosol as a consequence of MOMP. Similar to Smac/Diablo, Omi/HtrA2 then relieves the inhibition of IAPs on caspases by binding to the BIR domains of XIAP (Hegde et al., 2002; Martins et al., 2002; Suzuki et al., 2001a; Verhagen et al., 2002). Omi/HtrA2 also causes caspase-dependent cell death by cleaving IAPs through its serine protease activity (Srinivasula et al., 2003; Yang et al., 2003). Disruption of the protease activity by mutating the active site serine dramatically decreases the ability of Omi/HtrA2 to potentiate cell death, underscoring the importance of its serine protease activity. Addition of the broad-spectrum caspase inhibitor, zVAD-fmk (*N*-benzyloxycarbonyl-Val-Ala-Asp (Ome)-fluoromethylketone), does not completely inhibit the cell death caused by Omi/HtrA2. This suggests that Omi/HtrA2 can also cause cell death in a caspase-independent manner, presumably by cleaving various extra-mitochondrial substrates (Hegde et al., 2002; Suzuki et al., 2001a; Verhagen et al., 2002).

Omi/HtrA2 has also been implicated in neurodegeneration. The mutant *mnd2* (motor neuron degeneration 2) mouse is characterized by muscle wasting, neurodegeneration, and involution of spleen and thymus. This mouse has a missense mutation (Ser at position 276 mutated to Ala) in Omi/HtrA2, which results in a dramatic decrease in its protease activity. Although the aforementioned mutation does not affect the catalytic triad it has been suggested that it disrupts the regulatory function of the PDZ domain by holding it in a locked position (Jones et al., 2003). In agreement with this hypothesis, removal of the PDZ domain on this mutant background enhances the activity of the enzyme. The mitochondria from the *mnd2* mice show increased sensitivity to calcium induced permeability transition ($\Delta\psi_m$) and mitochondrial membrane permeabilization, thus suggesting that mitochondrial dysfunction may be the underlying reason for neurodegeneration. Intriguingly, MEFs (mouse embryonic fibroblasts) isolated from *mnd2* mice show increased apoptosis in response to treatment with stress-inducing agents (Jones et al., 2003). These data strongly suggest that Omi/HtrA2 plays an important housekeeping role in mitochondria, but once released into the cytosol in response to an apoptotic stimuli, it antagonizes IAPs and potentiates cell death.

Similar to *mnd2* mutants, mice lacking the expression of Omi/HtrA2 also exhibit neurodegeneration due to loss of certain striatal neurons. These mice also exhibit Parkinsonian symptoms such as progressive akinesia, lack of coordination, decreased mobility, bended posture, and tremor that eventually leads to their death around 30 days after birth. Upon treatment with mitochondrial stress-inducing agents, MEFs isolated from Omi/HtrA2 *-/-* mice show increased number of mitochondria with abnormal shape

and/or with distorted cristae. Also, MEFs from Omi/HtrA2 $-/-$ mice exhibit a decrease in the levels of citrate synthase relative to wild-type mice suggesting a decrease in the number of mitochondria (Martins et al., 2004). The role of Omi/HtrA2 in mitochondrial function is elevated upon the identification of mutations in four German Parkinson's disease patients. These mutations include Ala141Ser and Gly399Ser, have been shown to affect IAP binding properties and regulatory function of the PDZ domain, respectively (Strauss et al., 2005). However, the exact role of Omi/HtrA2 in mitochondrial maintenance and therefore in neurodegeneration is not yet clear.

1.3 Key regulators of *Drosophila* apoptosis

Apoptosis is an evolutionarily-conserved process with many common features in both vertebrates and invertebrates. In *Drosophila*, similar to mammals, caspases are the chief executioners of apoptosis. The seven *Drosophila* caspases identified so far include Dronc (*Drosophila* Nedd-2-like caspase) (Dorstyn et al., 1999a), Dredd (Death-related ced-3/Nedd2-like) (Chen et al., 1998), Strica (Doumanis et al., 2001; Vernooy et al., 2000), DrICE (*Drosophila* ICE) (Fraser and Evan, 1997), DCP-1 (death caspase-1) (Song et al., 1997), Decay (Dorstyn et al., 1999b), and Damm (Vernooy et al., 2000), with the former three categorized as initiator caspases and the latter as effector caspases.

Dronc is one of the extensively characterized initiator caspases in *Drosophila* (Illustration 1.4). Animals lacking zygotic *Dronc* are defective for programmed cell death and most arrest at an early pupal stage. The *Dronc* mutants also exhibit other cell death-defective phenotypes like the presence of supernumary cells, enlarged brain lobes,

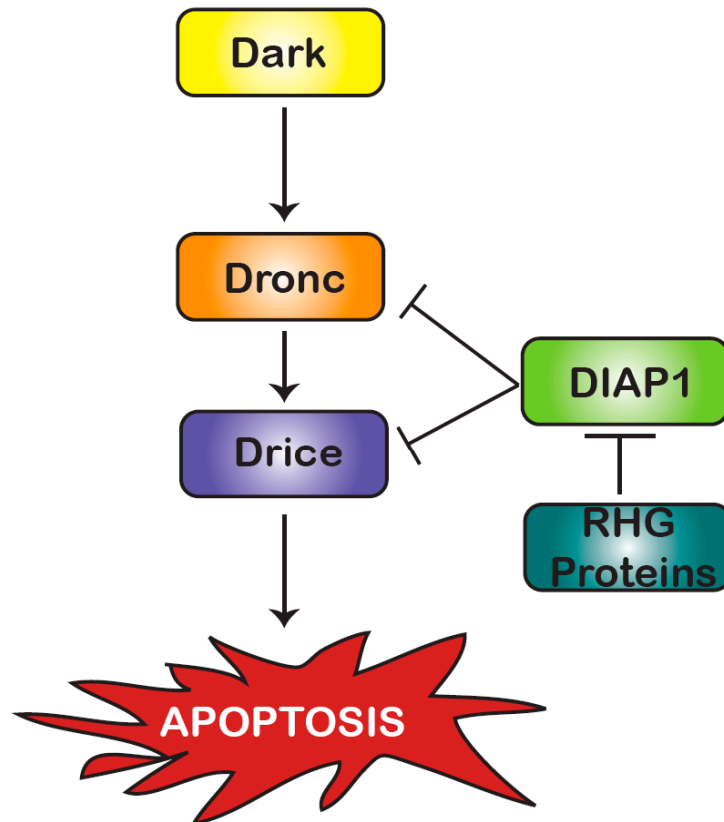


Illustration 1.4 **An overview of apoptotic pathway in *Drosophila*.**

The *Drosophila* adaptor protein, Dark, is required for the activation of the initiator caspase Dronc. Once Dronc is activated it cleaves the effector caspase DrICE, which subsequently cleaves various cellular substrates leading to apoptosis. The caspases Dronc and DrICE are inhibited by IAPs. The RHG proteins bind to IAPs through their N-terminal IBMs, subsequently leading to caspase displacement.

and deformed imaginal discs underscoring the importance of Dronc in apoptosis (Chew et al., 2004; Daish et al., 2004; Waldburger et al., 2005; Xu et al., 2005). Similar to mammalian caspase-9, Dronc also has a CARD domain and requires Dark, a homolog of the adaptor protein Apaf-1, for its activation (Kanuka et al., 1999b; Muro et al., 2002; Muro et al., 2004; Yan et al., 2006). The importance of Dark in programmed cell death is apparent by the fact that the null animals exhibit less apoptosis in the larval brain as well as in embryos (Kanuka et al., 1999b). Also, RNAi of Dark in *Drosophila* S2 cells inhibits most of the caspase-dependent cell death suggesting the requirement of both Dark and caspases for the execution of apoptosis (Kiessling and Green, 2006; Muro et al., 2002; Muro et al., 2004; Zimmermann et al., 2002).

Apart from its apoptotic function, Dronc has also been implicated in other non-apoptotic roles such as compensatory proliferation as well as differentiation of spermatids (Huh et al., 2004a; Huh et al., 2004b). Similarly, Dredd, an initiator caspase characterized by the presence of a death effector-like domain (DED) has been mainly implicated in the activation of innate immunity system (Hultmark, 2003). The function of Strica, an initiator caspase with a serine- and threonine-rich prodomain, remains uncharacterized yet (Doumanis et al., 2001).

DrICE and Dcp-1 are the two well-characterized effector caspases. Similar to their mammalian counterparts, they are activated upon cleavage by initiator caspases such as Dronc (Hawkins et al., 2000; Meier et al., 2000) (Illustration 1.4). Animals lacking DrICE are pupal lethal and exhibit less cell death in the embryonic nervous system, pupal

retinae, and adult wings. Even in response to stress stimuli, the *drice* null mutants show decreased cell death relative to wild-type animals (Muro et al., 2006; Xu et al., 2006). In contrast to animals lacking DrICE, *dcp-1* null mutants develop into normal adults thus implicating DrICE as one of the major effector caspase in *Drosophila* (Laundrie et al., 2003). However, mutants lacking both DrICE and Dcp-1 have severe phenotypes when compared to *drice* null animals thus suggesting a redundant role of Dcp-1 (Muro et al., 2006; Xu et al., 2006). Similar to Dronc, DrICE has also been implicated in non-apoptotic roles such as spermatid differentiation and compensatory proliferation (Muro et al., 2006).

Analogous to mammals, caspase activity in *Drosophila* is tightly regulated by two groups of proteins namely: IAPs and IAP antagonists (Illustration 1.4). Three *Drosophila* IAPs characterized so far include DIAP1 (*Drosophila* IAP 1) (Hay et al., 1995), DIAP2 (Duckett et al., 1996; Hay et al., 1995), and dBruce (Vernooy et al., 2000). Of these DIAP1, the IAP encoded by the *thread* (*th*) locus, is mainly implicated in regulating apoptosis (Hay et al., 1995) (Illustration 1.4). It is characterized by the presence of two BIR domains (BIR1-2) and a C-terminal RING domain (Illustration 1.4A). The C-terminal RING domain is essential for the E3 ubiquitin ligase activity of DIAP1 (Chai et al., 2003a; Olson et al., 2003b). Over expression of DIAP1 in S2 cells blocks cell death in response to apoptotic insults like ultraviolet (UV) irradiation, cycloheximide, and actinomycin treatment (Zimmermann et al., 2002). Conversely, RNAi of DIAP1 in S2 cells results in spontaneous cell death (Igaki et al., 2002; Kiessling and Green, 2006; Muro et al., 2002; Yokokura et al., 2004; Zimmermann et al., 2002). Embryos from

DIAP1 homozygous mutant flies show increased caspase activation and cell death, thus underscoring the importance of DIAP1 as a negative regulator in *Drosophila* apoptosis (Yoo et al., 2002). Unlike DIAP1, DIAP2 is mainly implicated in regulating innate immunity in spite of the presence of three N-terminal BIR domains and a C-terminal RING domain. In contrast to DIAP1 null mutants, which are embryonic lethal, flies lacking DIAP2 are viable and show no increased apoptosis in response to various apoptotic stimuli (Huh et al., 2007; Leulier et al., 2006). Instead, DIAP2 plays an important function in antimicrobial peptide synthesis after infection with gram-negative bacteria (Huh et al., 2007; Leulier et al., 2006). Another atypical fly IAP that participates in the regulation of apoptosis is dBruce. It is distinguished from the other IAPs by the presence of only one BIR domain, which is functionally similar to the BIR1 domain of DIAP1, and a C-terminal ubiquitin conjugating domain, characteristic of an E2 enzyme of ubiquitin signaling pathway, instead of a ubiquitin ligase RING motif (Vernooy et al., 2002).

The first IAP antagonists to be identified in *Drosophila* include Reaper (Rpr), Grim, and Head involution defective (Hid), also referred to as RHG proteins (White et al., 1994) (Illustration 1.4). These were identified in a genetic screen performed to discover novel regulators of apoptosis during embryonic development. The *h99* deletion mutant that lacks the loci for the RHG proteins shows no developmental apoptosis, thus providing strong evidence for the role of these proteins in positively regulating *Drosophila* programmed cell death (White et al., 1994). As discussed earlier, well-characterized mammalian IAP antagonists like Smac/Diablo and Omi/HtrA2 are

mitochondrial-resident proteins and over expression of the full-length proteins sensitize the cells to various apoptotic stimuli (Vaux and Silke, 2003). Unlike mammalian IAP antagonists, the RHG proteins are cytosolic and when over-expressed cause massive apoptosis (Chen et al., 1996; Grether et al., 1995; Hay et al., 1995; White et al., 1994). For instance, ectopic expression of the RHG proteins in the fly eye using GMR (glass-mediated response) promoter causes a severe reduced eye phenotype (Hay et al., 1995; White et al., 1996). Although the *h99* deletion embryos show a drastic decrease in developmental apoptotic phenotype, the mutants lacking individual genes show very modest defects in apoptosis in certain tissues, suggesting a cooperative role for the RHG proteins in promoting cell death in a tissue-specific manner (Grether et al., 1995; Peterson et al., 2002). For instance, *Drosophila* mutants lacking Rpr show apoptotic defects only in neurons and neuroblasts and display an enlarged central nervous system (Peterson et al., 2002). Similarly, mutants lacking Hid show a noticeable decrease in cell death near the head region prior to the completion of head involution and present with extra photoreceptor cells (Grether et al., 1995). However, the decrease in developmental cell death in the absence of the RHG proteins is far more profound compared to mutants lacking an individual locus.

Two more IAP antagonists, Sickie (Christich et al., 2002; Srinivasula et al., 2002; Wing et al., 2002a) and Jafrac2 (Tenev et al., 2002), have been recently identified. Sickie, a cytosolic IAP antagonist, shows a slight increase in apoptosis when over expressed by itself in *Drosophila* S2 cells (Srinivasula et al., 2002). However, it shows an enhanced cell death phenotype when co-expressed with the RHG proteins (Srinivasula

et al., 2002; Wing et al., 2002a) or upon UV irradiation suggesting a synergistic function (Christich et al., 2002). All of the aforementioned IAP antagonists are characterized by the presence of a tetrapeptide N-terminal IBM, which is presumably exposed as the result of the removal of the initiator Met by the enzyme Met-aminopeptidase (Tenev et al., 2002; Vucic et al., 1997). Jafrac2, unlike the other *Drosophila* IAP antagonists, is an endoplasmic reticulum (ER)-resident protein (Tenev et al., 2002). In case of Jafrac2, proteolytic cleavage in the ER subsequent to its translocation generates a neo N-terminus with an IBM. Similar to mitochondrial-resident mammalian IAP antagonists, processed Jafrac2 with an N-terminal IBM is released into cytosol upon the receipt of an ER stress stimulus. In agreement with its apoptotic role, cytosolic expression of the mature Jafrac2, with intact IBM, in both S2 cells as well in the *Drosophila* eye induces enhanced cell death (Tenev et al., 2002).

1.4 Mechanisms of *Drosophila* apoptosis

Apoptosis is a genetically programmed and tightly regulated process. There is a constant interplay between the positive and negative regulators of apoptosis thus forming a well-defined, complex regulatory network. The fate of the cell (whether to die or survive) is dependent upon the balance that ensues as a result of these complex interactions. Below is the description of the interactions that occur between the key regulators of *Drosophila* apoptosis in comparison with their mammalian counterparts.

1.4.1 Regulation of caspases by DIAP1

1.4.1.1 Mechanisms of Dronc inhibition

IAPs play an important role in apoptosis by inhibiting caspases (Salvesen and Duckett, 2002) (Illustration 1.5B). As mentioned earlier, the mammalian procaspase-9 is recruited to the apoptosome, a large caspase activating platform comprised of seven Apaf-1 proteins (Acehan et al., 2002; Rodriguez and Lazebnik, 1999). Activation of procaspase-9 is followed by an auto-processing event between the large and small subunits (Srinivasula et al., 1998). As a result of auto-processing, the IBM (Ala-Thr-Pro-Phe) at the neo N-terminus of the small subunit of caspase 9 is exposed. XIAP inhibits processed caspase-9 by binding to the N-terminal IBM through its BIR3 domain (Srinivasula et al., 2001) (Illustration 1.6). In case of *Drosophila*, DIAP1 also regulates the activity of Dronc, the fly homolog of mammalian caspase-9 (Meier et al., 2000). However, in contrast to caspase-9, activation and autoprocessing of Dronc is not required for its interaction with DIAP1. Rather, DIAP1 binds to the unprocessed form of Dronc through its BIR2 domain, thereby facilitating RING-dependent ubiquitination and degradation (Illustration 1.5B and 1.6). In accordance with this model, animals carrying mutations that impair the E3 ligase activity of DIAP1 enhance the cell death caused by Dronc over expression (Wilson et al., 2002). The region of Dronc essential for binding to BIR2 domain of DIAP1 includes a stretch of 10 amino acids from residues 114 to 123 in the prodomain with the critical residues being Phe-118, Ile-119, Leu-121, and Asn-122 (Illustration 1.6). A non-inhibitable form of Dronc, with the Phe-118 mutated to Asp, shows enhanced cell death when compared to the wild-type version thus suggesting the

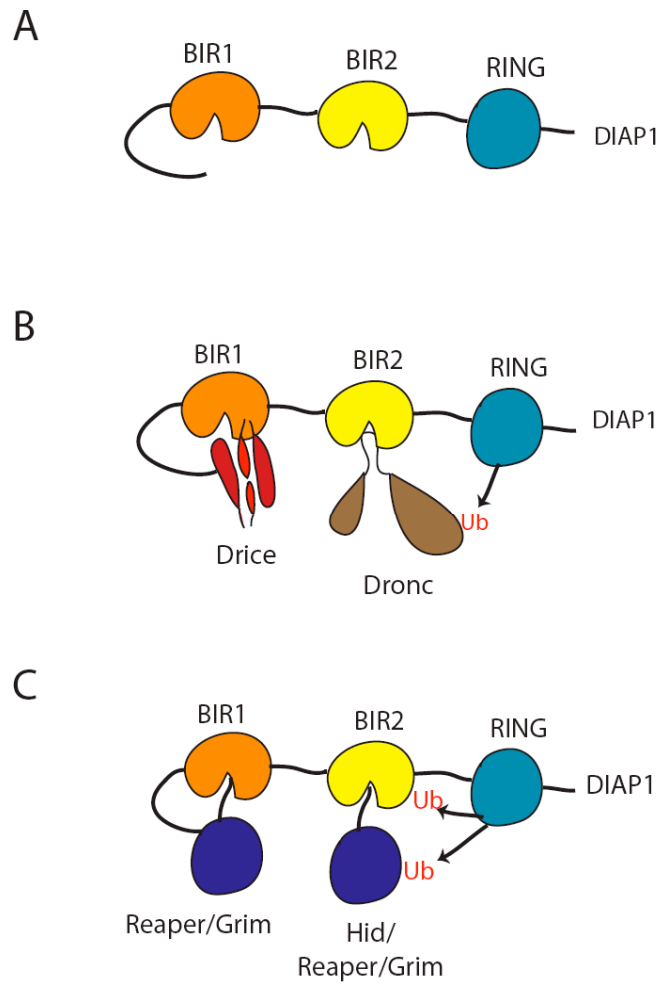


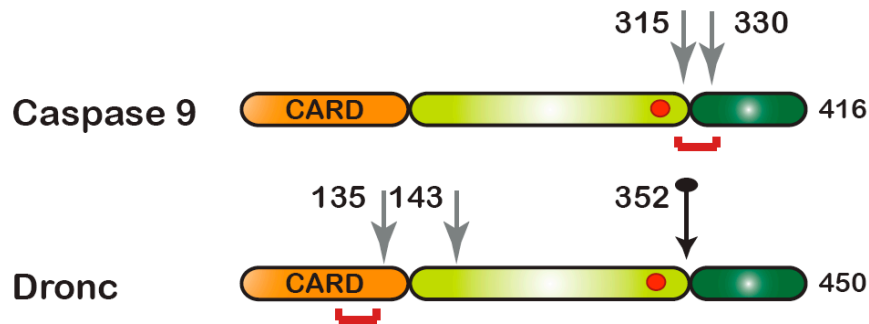
Illustration 1.5 Regulation of *Drosophila* apoptosis by DIAP1.

- (A) DIAP1 is characterized by the presence of two BIR domains (BIR1 and BIR2) and a C-terminal RING domain required for its E3 ligase activity.
- (B) DIAP1 through its BIR2 domain inhibits Dronc by thereby causing RING-dependent ubiquitination. DIAP1 can also inhibit the activity of processed DrICE by binding through its BIR1 domain.
- (C) The RHG proteins bind differentially to the BIR domains of DIAP1. Hid preferentially binds to the BIR2 domain, whereas Reaper and Grim can bind to both the BIR1 and BIR2 domains. The RHG proteins are regulated by ubiquitination in a RING-dependent manner. DIAP1 levels are also regulated by autoubiquitination.

importance of DIAP1 binding for its inhibition (Chai et al., 2003a) . Despite exhibiting a different mode of binding compared to caspase-9, Dronc occupies the same binding groove within DIAP1 as occupied by IAP antagonists. The nature of this interaction thereby facilitates regulation of Dronc activity by the IBM motif of IAP antagonists (Chai et al., 2003a).

In the case of mammalian caspase-9, intra-chain processing between large and small subunits occurs after its recruitment to the apoptosome and is not a pre-requisite for its activation but is necessary for XIAP-mediated inhibition (Bratton et al., 2001; Srinivasula et al., 1998; Srinivasula et al., 2001) (Illustration 1.6). However with regard to Dronc, preliminary data suggest that autocatalytic processing is necessary for Dronc activation. Processing after Asp-352, between the large and small subunits, is presumed to happen within the *Drosophila* apoptosome (Illustration 1.6). This cleavage event changes the conformation of Dronc from a monomeric zymogen form to an active dimeric form (Yan et al., 2006). The dimeric conformation allows a *trans* cleavage event after the Glu-143 resulting in the removal of the prodomain. As the critical residues required for binding to DIAP1 are present in the prodomain, the active form of Dronc is no longer inhibitable (Yan et al., 2006) (Illustration 1.6). This data suggests that unlike in mammals where autoprocessing of caspase-9 enables its inhibition by XIAP, autoprocessing of Dronc makes it uninhibitable by DIAP1 (Srinivasula et al., 2001; Yan et al., 2006). Therefore, DIAP1 primarily reduces the levels of unprocessed Dronc rather than inhibiting the active form.

Initiator Caspases



Effector Caspases

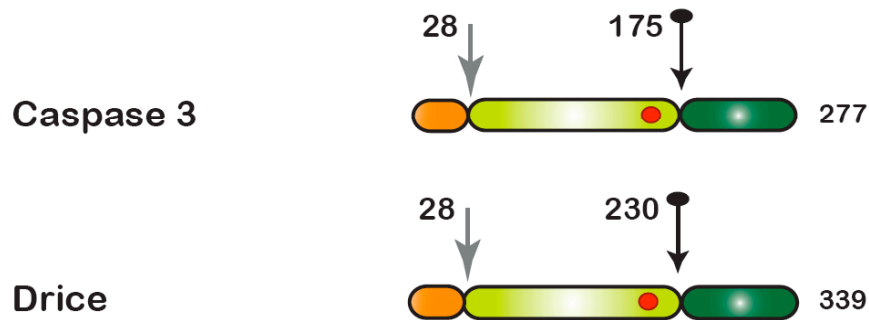


Illustration 1.6 Comparison of mammalian and *Drosophila* caspases.

Initiator caspases are characterized by the presence of long N-terminal pro-domains (orange), followed by large and small subunits. Effector caspases, on the other hand, have very short prodomains. The intra-chain cleavage events necessary for activation are represented by black arrows. Cleavage events that occur after activation either by auto-processing or cleavage by effector caspases are denoted by gray arrows. Red lines represent the regions necessary for IAP-mediated inhibition of initiator caspases. The red circles in the large subunits represent the active sites of the enzyme.

In the case of mammalian caspase-9, cleavage by effector caspase-3 after the Asp-330 results in removal of the N-terminal IBM of the small subunit (Illustration 1.6). Therefore, caspase-3 initiates a feedback amplification loop by rendering the processed caspase-9 incapable of XIAP inhibition (Bratton et al., 2002; Srinivasula et al., 2001). In *Drosophila*, DrICE also processes Dronc after Asp-135, which separates the prodomain from the large subunit (Chai et al., 2003a). Therefore, cleavage of Dronc by itself or by DrICE results in the removal of prodomain thereby transforming it into a DIAP1-uninhibitable form and initiating a feedback amplification loop similar to that in mammals (Chai et al., 2003a; Yan et al., 2004b) (Illustration 1.6).

1.4.1.2 Mechanisms of DrICE inhibition

Similar to mammalian XIAP, DIAP1 also inhibits the effector caspases DrICE and Dcp-1 thereby preventing them from cleaving substrates (Kaiser et al., 1998; Wang et al., 1999). Prior to their cleavage by the initiator caspases, caspases-3 and -7 exist in a dimeric catalytically-incompetent conformation. Cleavage between the large and small subunits by initiator caspases leads to rearrangement of the subunits to form a catalytically active enzyme (Chai et al., 2001b). XIAP then inhibits the effector caspases by binding to their active sites and occluding substrate entry (Chai et al., 2001a; Huang et al., 2001; Riedl et al., 2001). Similar to mammalian caspase-3 and -7, DrICE is also cleaved by Dronc in between large and small subunits thereby leading to its activation (Hawkins et al., 2000). Apart from the intra-chain cleavage, DrICE is also cleaved after Asp-28 presumably by autoprocessing. This cleavage leads to the exposure of an IBM

domain, Ala-Leu-Gly-Ser (amino acids 29-32), at the neo N-terminus of the large subunit (Tenev et al., 2005) (Illustration 1.6). Both these cleavage events play an important role in the inhibition of DrICE by DIAP1. Present data suggests that DrICE binds to DIAP1 in a bimodular fashion, which involves both active site as well as an IBM-like motif generated at position 29 (Tenev et al., 2005). But, many questions regarding the order of events and the mechanisms that lead to DrICE inhibition are still unanswered.

One of the mechanisms that remain unclear is the requirement of DIAP cleavage for DrICE inhibition. Once activated DrICE cleaves DIAP1 after Asp-20 (Ditzel et al., 2003; Yan et al., 2004b) (Illustrations 1.7 & 1.9A). Although the cleavage of DIAP1 by DrICE is well established, the mechanism by which this cleavage affects DrICE inhibition is under debate. Studies by Yan et al. (2004) suggest that the BIR1 domain of DIAP1 is in an auto-inhibitory state prior to DrICE cleavage and therefore removal of the first twenty amino acids is a prerequisite for DrICE inhibition (Illustration 1.7). However, other studies suggest that binding of DrICE precedes the cleavage event (Tenev et al., 2007; Tenev et al., 2005) (Illustration 1.7). This argument was based on the observation that the uncleavable mutant form of DIAP1 (Asp20Ala) is still able to bind DrICE. Also, the DIAP1 mutant (Cys80Gly) which is unable to interact with DrICE, can no longer act as a substrate for DrICE (Tenev et al., 2007). Thus, the importance of DIAP1 cleavage for its ability to inhibit DrICE remains unclear.

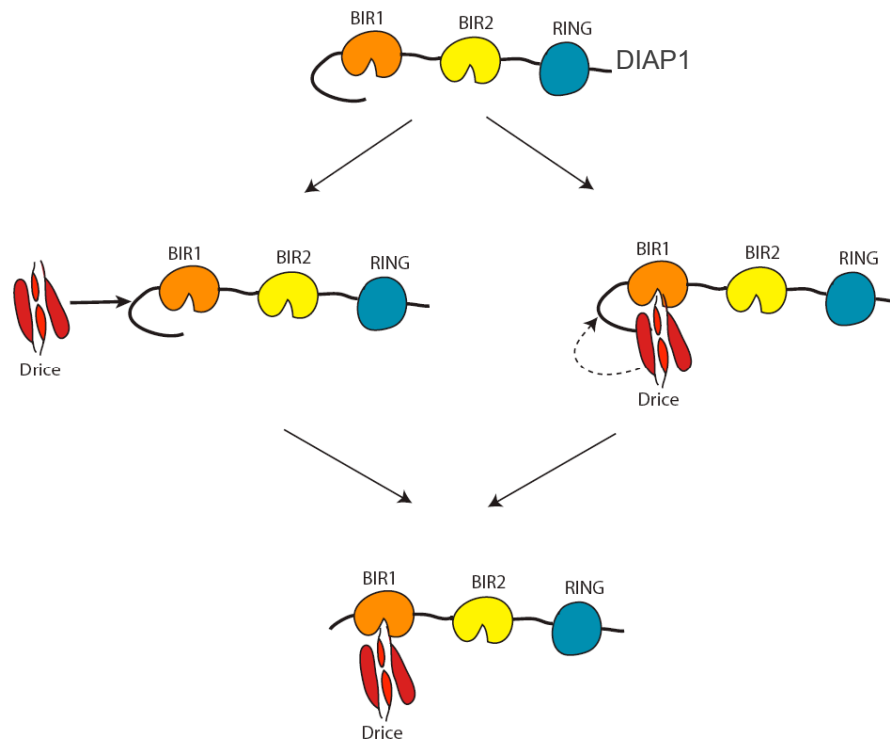


Illustration 1.7 Two proposed models depicting the mechanisms of DrICE inhibition.

By binding through its BIR1 domain, DIAP1 inhibits the effector caspase DrICE. DrICE once activated cleaves DIAP1 after Asp-20. One model (left side) suggests that the N-terminal fragment occludes binding of active DrICE to the DIAP1-BIR1 and therefore cleavage at position 20 is a prerequisite for efficient DrICE inhibition. Another model (right side) suggests that DrICE binding to the BIR1 domain is required for the cleavage after Asp-20.

1.4.2 IAP antagonists and DIAP1

1.4.2.1 Differential regulation of DIAP1 by IAP antagonists

The three extensively studied IAP antagonists of *Drosophila*, Rpr, Hid, and Grim (RHG proteins), antagonize DIAP1 by binding to its BIR domains and thereby causing displacement of caspases (Wang et al., 1999). Similar to mammalian IAP antagonists, the *Drosophila* RHG proteins inhibit DIAP1 primarily through their N-terminal IBMs. Although all the IAP antagonists have a conserved IBM, characterized by the presence of an N-terminal Ala, they show differential selectivity for the BIR1 and BIR2 domains in DIAP1 (Zachariou et al., 2003)(Illustration 1.5C). These differences are attributable to the binding affinities of the RHG proteins for these BIR domains. The four amino acids at the neo N-terminus of RHG proteins include Ala-Val-Ala-Phe, Ala-Val-Pro-Phe, and Ala-Ile-Ala-Tyr, respectively with the major determinant of the binding affinities being the residue at position 3 (Wu et al., 2001; Yan et al., 2004b). In DIAP1-BIR2, residues Leu-270 and Trp-286 are required for binding to the IBM of the IAP antagonists. Hid, with a Pro at position 3, makes more van der Waals contacts with Leu-270 and Trp-286, compared to Rpr and Grim which contain an Ala at this position. As a consequence, Hid has six-fold higher affinity ($K_d = 0.041 \mu\text{M}$) for the BIR2 domain of DIAP1 when compared to Grim ($K_d = 0.241 \mu\text{M}$) (Wu et al., 2001). Within the BIR1 domain of DIAP1, Trp-103 is critical for interacting with the RHG proteins. However, Pro-3 in Hid sterically clashes with Trp-103 in DIAP1-BIR1, compared to Grim, which has an Ala at this position. This decreases the affinity of Hid for the BIR1 domain of DIAP1 (K_d s: Hid = $0.76 \mu\text{M}$, Grim = $0.12 \mu\text{M}$, and Rpr = $0.27 \mu\text{M}$) (Yan et al., 2004b). Similarly, Jafrac2

and Sickie have a preference for binding to the BIR2 domain relative to the BIR1 domain (Srinivasula et al., 2002; Tenev et al., 2002).

As mentioned previously, DrICE and Dronc also show preferential binding to BIR1 and BIR2 domains respectively (Wilson et al., 2002; Zachariou et al., 2003) (Illustration 1.5B). Due to variations in the disassociation constants of the RHG proteins, their ability to relieve the inhibition of initiator and effector caspases by DIAP1 is different. For instance, Hid plays an important role in displacing the initiator caspase Dronc compared to DrICE (Zachariou et al., 2003). Similarly Jafrac2, with a preference for DIAP1-BIR2, potentiates cell death by displacing Dronc (Tenev et al., 2002).

1.4.2.2 The RHG proteins regulate the levels of DIAP1

Apart from displacing caspases, IAP antagonists can also mediate DIAP1 degradation. Similar to other RING domain-containing proteins, the levels of DIAP1 are also regulated by auto-ubiquitination in a RING-dependent manner (Wilson et al., 2002; Yoo et al., 2002). The RHG proteins regulate DIAP1 levels by modulating the rates of auto-ubiquitination (Ryoo et al., 2002; Yoo et al., 2002). However, there is controversy surrounding which of the RHG proteins contribute to increased auto-ubiquitination. Studies by Yoo et al. (2002), suggest that Hid, but not Rpr and Grim, promote degradation of DIAP1 in a RING-domain dependent manner. Conversely, studies by Ryoo et al. (2002) suggest that Rpr, but not Hid, enhances the rate of DIAP1 auto-ubiquitination. The reasons for this disparity remain unresolved.

Another key player that regulates the stability of DIAP1 is Morgue (modifier of *reaper* and *grim*, ubiquitously expressed), an ubiquitin-conjugating enzyme variant (UEV). Morgue regulates cell death by two related mechanisms: firstly, by enhancing the cell death action of Rpr, and secondly, by negatively regulating the levels of DIAP1 presumably by targeting it for ubiquitin-dependent degradation. However, several questions regarding the exact mechanism by which Morgue decreases DIAP1 levels and regulates Rpr-induced cell death remain unanswered (Hays et al., 2002; Wing et al., 2002b).

1.4.2.3 IBM-independent roles of the RHG proteins

IAP antagonists Rpr and Grim can potentiate cell death even in the absence of an intact IBM. One of the mechanisms involves the pro-apoptotic GH3 (Grim Helix-3) domain (also called as RH3 or Trp-block), which includes a short stretch of amino acids that have the propensity to form a BH3-like amphipathic α -helical domain (Claveria et al., 2002; Olson et al., 2003a). The GH3 domain of Grim and Rpr play an important role in their localization to mitochondria. Disruption of the GH3 domain not only prevents mitochondrial localization of Rpr and Grim but also decreases their ability to induce cell death in *Drosophila* S2 cells (Claveria et al., 2002; Olson et al., 2003a). Also, over expression of Grim lacking the GH3 domain in the fly eye under the GMR-promoter shows a decrease in the eye ablation phenotype relative to the wild-type (Claveria et al., 2002). Recent data suggest that the GH3 domain plays an important role in caspase-dependent mitochondrial permeabilization, thus providing a link between the GH3

domain and cell death (Abdelwahid et al., 2007). However, the exact mechanism by which the GH3 domain promotes mitochondrial permeabilization is still unknown.

The IAP antagonist Rpr also regulates IAP levels by promoting global translational repression. Translational repression by Rpr occurs in an IBM-independent manner and also does not require the IAP's E3 ligase activity (Holley et al., 2002). Rpr directly binds to the 40S ribosomal subunit and inhibits cap-dependent, but not IRES (internal ribosomal entry site)-driven mRNA translation. Therefore, Rpr modulates protein synthesis by inhibiting the expression of cap-dependent messages (Colon-Ramos et al., 2006). It is still unclear if Rpr also regulates the expression of additional pro- and anti-apoptotic proteins as a part of this global translational repression mechanism.

1.4.2.4 DIAP1 regulates the expression of RHG proteins through its E3 ligase activity

In response to the antagonizing effects of the RHG proteins, DIAP1 retaliates by causing their degradation. *In vitro* studies demonstrate that, similar to Dronc, the RHG proteins are also direct substrates for the E3 ubiquitin ligase activity of DIAP1 (Illustration 1.5C). Accordingly, mutant Rpr, lacking intact lysine residues is a more potent at inducing cell death when compared to the wild-type Rpr, suggesting that IAP antagonists can also be regulated by the ubiquitin-proteasome system (Olson et al., 2003b). Additionally, cell death caused by the over expression of Rpr and Grim is enhanced in the *th*^{6B} or *th*^{81.03} allelic background. These mutations disrupt the secondary structure of DIAP1's RING domain (Lisi et al., 2000) and suggest that the RING domain

can play an important role in the regulation of caspases and IAP antagonists. However, the cell death caused by Hid is suppressed on the *th*^{6B} or *th*^{81.03} allelic background, suggesting a different mode of regulation (Lisi et al., 2000). One of the possible explanations for this result is that Hid rather than acting as a good substrate for DIAP1 may instead enhance the autoubiquitination of DIAP1 (Yoo et al., 2002).

1.4.3 Regulation of DIAP1 by caspases

1.4.3.1 Cleavage of DIAP1 by Dronc

Both initiator and effector caspases play an important role in DIAP1 regulation. The active initiator caspase Dronc cleaves DIAP1 after Glu-205 which divides DIAP1 into two fragments containing either the BIR1 domain or BIR2-RING domains (Muro et al., 2005; Yan et al., 2004b) (Illustration 1.8A). Both cleaved and uncleaved forms of DIAP1 can bind to the zymogen form of Dronc, but a DIAP1 mutant lacking the cleavage site (Glu205Ala) loses its ability to bind to active form of Dronc. This result suggests that the cleaved form of DIAP1 inhibits Dronc more effectively than the uncleaved form. Moreover, the DIAP1 mutant that cannot be cleaved by Dronc is less anti-apoptotic relative to its wild-type version (Muro et al., 2005).

1.4.3.2 DrICE cleavage promotes N-end rule-dependent degradation of DIAP1

As mentioned earlier, DrICE also cleaves DIAP1 after Asp-20 thereby creating a neo N-terminus containing Asn as the starting residue (Illustrations 1.8A and B). This cleavage decreases the stability of DIAP1 due to its degradation by the N-end rule

pathway (Ditzel et al., 2003). The N-end rule degradation (NERD) pathway involves ubiquitin mediated, proteasome-dependent degradation of proteins based on the identity of the amino acid residue present at the N-terminus (Varshavsky, 2003). In *S. cerevisiae*, the model system in which the NERD pathway was first characterized, the N-terminal amino acids that are classified as “stable” include Cys, Ala, Ser, Thr, Gly, Val, and Met, whereas the remaining amino acids are classified as destabilizing residues. All nascent proteins contain an N-terminal stable Met residue, which is removed by Met-aminopeptidases provided that the second amino acid is a stable residue. When the second amino acid is a destabilizing residue, the Met-aminopeptidases do not act on the first Met. Therefore, in order for a protein to be an N-end rule substrate (N-degron), the pre-N-degron has to be cleaved so that it exposes an N-terminal destabilizing residue (Illustration 1.9). However, all the proteins with an N-terminal destabilizing residue are not identified by the E3 ubiquitin ligase (N-recognin) that binds to N-end rule substrates (Varshavsky, 1996). The amino acids that can directly bind to the N-recognin are called primary destabilizing residues, which are in turn divided into two categories, Type 1 and Type 2. Type 1 destabilizing residues include basic amino acids Arg, Lys, or His and the type 2 residues include hydrophobic amino acids Phe, Leu, Trp, Ile, and Tyr. All the remaining destabilizing residues, which cannot be directly bound to the N-recognin, are classified as either secondary or tertiary destabilizing residues. Proteins with the tertiary destabilizing residues such as Asn and Gln, are acted upon by the enzyme N-terminal-amidohydrolase (NTAN1) and subsequently converted to secondary destabilizing

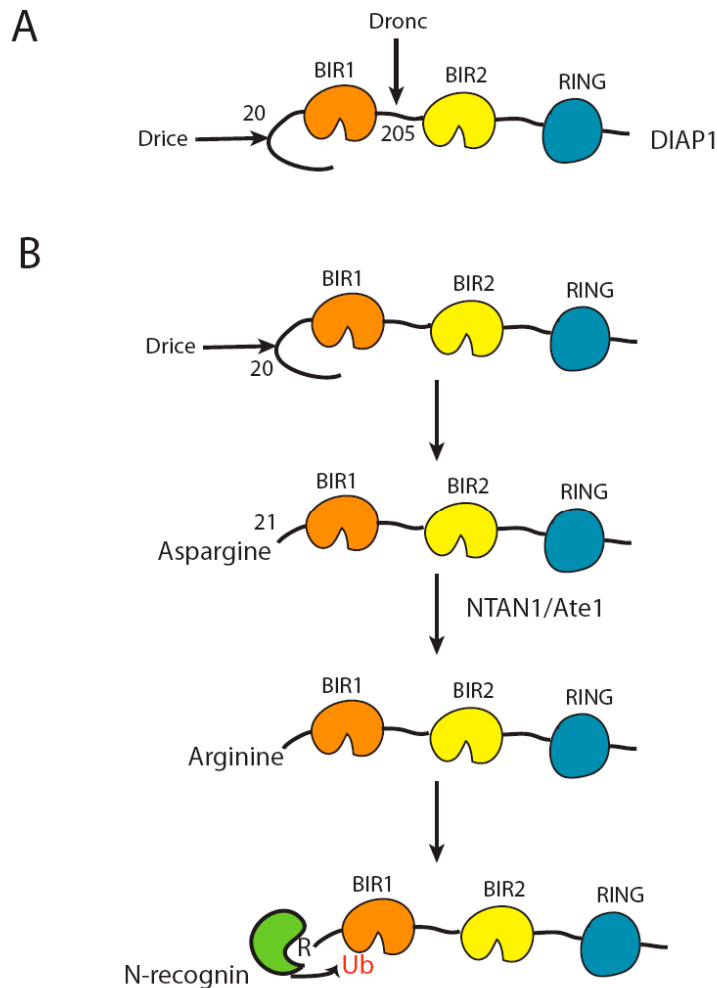


Illustration 1.8 Regulation of DIAP1 by caspases.

- (A) A schematic representing the cleavage sites of Dronc (Asp-205) and DrICE (Asp-20) in DIAP1.
- (B) A model representing the degradation of DIAP1 by the NERD pathway. As a consequence of DrICE cleavage, a tertiary destabilizing residue (Asn) is generated at the neo N-terminus of DIAP1. By sequential action of NTAN1 and Ate1, the N-terminal Asn is attached to a primary destabilizing residue, Arg. The E3 ligase implicated in the NERD pathway, Ubr1 (N-recognin), recognizes the Arg and subsequently leads to the degradation of DIAP1.

residues Asp and Glu respectively (Illustration 1.9). The N-terminal secondary destabilizing residues (Asp and Glu) are further conjugated to an Arg by an enzyme Arg-tRNA protein transferase (Ate1) thus converting it into a primary destabilizing residue. Once the protein becomes an N-degron with an N-terminal primary destabilizing residue, an internal lysine if present is recognized by the N-recognin and further subjected to polyubiquitination (Illustration 1.9). In *S. cerevisiae*, an E3 ligase known as Ubr1, in conjugation with the ubiquitin-conjugating (E2) enzyme, Ubc2p (RAD6), catalyze the addition of ubiquitin to the internal lysine residue of the N-degron, thus promoting its proteasome-dependent degradation (Varshavsky, 1996; Varshavsky, 2003). The classification of amino acids into primary, secondary, or tertiary destabilizing residues varies from each organism. For instance, unlike in *S.cerevisiae*, Cys is considered as a tertiary destabilizing residue in mammals, and it is converted to secondary and primary destabilizing residue by a series of oxidation and arginylation reactions respectively. The NERD pathway has been shown to play an important role in peptide import and chromosome stability in yeast and for cardiovascular development in mammals (Varshavsky, 2003).

In the case of DIAP1, DrICE cleavage of the full-length DIAP1 (pre-N-degron) exposes an N-terminal tertiary destabilizing Asn residue. Sequential action of Ate1 and NTAN1 enzymes is required to make DIAP1 into an N-degron, which is presumably degraded in an Ubr1-dependent manner (Illustration 1.8). In *Drosophila* S2 cells, RNAi of Ate1 and NTAN1 increases the stability of the cleaved form of DIAP1, indicating a requirement of NERD pathway for degradation. Intriguingly, the decrease in stability of

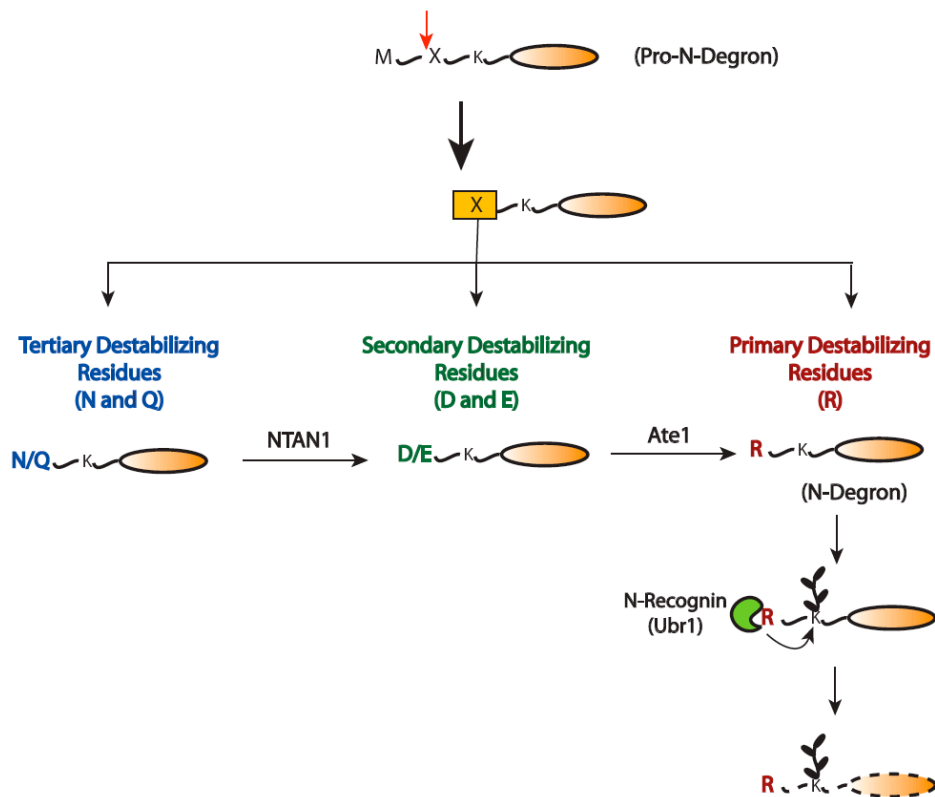


Illustration 1.9 A simplified overview of the NERD pathway.

The NERD pathway involves degradation of proteins based on the identity of the N-terminal amino acid (stable or unstable residues). In general, proteins are not synthesized with a N-terminal destabilizing residue. However, a cleavage process exposes the destabilizing residues, which can be further classified as primary, secondary, or tertiary. If the N-terminus of the protein is either a tertiary or secondary destabilizing residue, it is modified by the action of the enzymes NTAN1 and Ate1 and thereby converted to a primary destabilizing residue. Once the N-terminus has a primary destabilizing residue (N-degroun), it is recognized by the E3 ligase (N-recognin) and is degraded in a proteasome-dependent manner.

the cleaved form of DIAP1 by N-end rule pathway is associated with an increase in the anti-apoptotic ability of DIAP1. Expression of the N-degron form of DIAP1 in S2 cells offers more protection compared with the wild-type DIAP1 (or a stable form), especially against Rpr-induced cell death (Ditzel et al., 2003). These data suggests that the degradation of DIAP1 through the N-end rule pathway is required for its anti-apoptotic function, possibly by aiding in decreasing the activity of pro-apoptotic proteins. In addition, the NERD pathway has differential effects on Hid and Rpr-induced cell death. Mutations in the enzymes NTAN1 and Ate1 that disrupt the N-end rule pathway act as enhancers and suppressors of Rpr and Hid-induced cell death, respectively (Ditzel et al., 2003). However, the mechanisms that contribute to the differential effects of NERD-dependent DIAP1 degradation on Rpr and Hid-induced apoptosis are not completely understood and it is possible that mutations in NTAN1 and ATE1 may effect other modifiers of Rpr and Hid besides DIAP1.

1.4.4 Role of mitochondria in *Drosophila* apoptosis

Although the key players of apoptosis are conserved between *Drosophila* and mammals, controversy exists regarding the role of mitochondria in fly apoptosis, especially with respect to the activation of initiator caspases (Kornbluth and White, 2005). As mentioned previously, Dark is required for Dronc activation (Rodriguez et al., 2002; Zimmermann et al., 2002). Analogous to its mammalian counterpart, Dark has a CARD domain, required for homotypic interactions, a NBD and a series of WD-40 repeats that are capable of interacting with cytochrome c (Dorstyn et al., 2002; Kanuka et

al., 1999b). Despite the structural similarity, it has been argued that the activation of caspases within the *Drosophila* apoptosome does not require cytochrome c. Some of the evidence that points to the lack of mitochondria involvement in *Drosophila* apoptosis includes the absence of MOMP prior to initiator caspase activation (Zimmermann et al., 2002). Also, the addition of exogenous or recombinant cytochrome c to *Drosophila* S2 cell extracts does not lead to robust caspase activation as seen in the case of mammalian extracts (Dorstyn et al., 2004; Means et al., 2006). Similarly, RNAi of the two forms of cytochrome c, cyt-c-p and cyt-c-d, in *Drosophila* S2 cells does not inhibit apoptosis (Dorstyn et al., 2004). This controversy is further strengthened by the recent structural data of the *Drosophila* apoptosome. Unlike its mammalian counterpart, the *Drosophila* apoptosome is composed of two rings of eight subunits each and does not require cytochrome c for oligomerization (Yu et al., 2006). This has led to a hypothesis that an activating factor other than cytochrome c is required for apoptosome formation in flies (Kornbluth and White, 2005). In addition, there are reports suggesting that the *Drosophila* apoptosome is constitutively active prior to MOMP. This hypothesis is based on the observation that down-regulation of DIAP1 causes spontaneous caspase activation, suggesting that removal of inhibition over active caspases is sufficient to trigger apoptosis, thus placing IAPs upstream of caspases in the apoptotic pathway (Yoo et al., 2002; Zimmermann et al., 2002). Also, overexpression of IAP antagonists, such as Rpr, Hid, Grim, triggers massive apoptosis, suggesting that IAPs regulate apoptosis upstream of caspases (Goyal et al., 2000; Lisi et al., 2000). This is in contrast to the mammalian pathway, where the activation of caspases is upstream to IAP regulation (Salvesen and

Duckett, 2002). In addition, it is argued that all of the *Drosophila* IAP antagonists, with the exception of Jafrac2, are cytosolic, again undermining the role of mitochondria in *Drosophila* apoptosis (Hay and Guo, 2006).

However, a body of work suggests that mitochondria play an important role in *Drosophila* apoptosis. One of the *cytochrome c* genes expressed exclusively in the male germ line, *cyt-c-d*, has been implicated in spermatid individualization process (Arama et al., 2003; Arama et al., 2006). Similar to the mammalian apoptosis, this process requires caspase activation and is also regulated by the IAPs. Animals lacking *cyt-c-d* are defective in DrICE activation, implying a role of cytochrome c in caspase activation. This work also suggests that Dronc and Dark may localize near the mitochondria thus gaining access to cytochrome c without the requirement of complete release (Arama et al., 2003). In addition, Rpr and Grim localize to mitochondria through their GH3 domains and have been suggested to play an important role in mitochondrial permeabilization (Abdelwahid et al., 2007). Based on these observations it can be inferred that the RHG proteins may play an important role in apoptosis, not only by antagonizing IAPs but also by causing mitochondrial permeabilization. Whether this leads to release of pro-apoptotic factors from mitochondria, however, remains unclear.

In addition to the above controversies, lack of understanding of the exact role of *Drosophila* Bcl-2 family members in the regulation of mitochondrial MOMP further complicates the debate. As mentioned previously, mammalian Bcl-2 family members have been implicated in apoptosis due to their role in modulating MOMP (Danial and Korsmeyer, 2004). Similar to mammals, *Drosophila* pro- and anti-apoptotic Bcl-2

homologs, Debcl (Death executioner for Bcl-2 homolog) and Buffy, respectively, have been implicated in cell death mechanisms (Brachmann et al., 2000; Colussi et al., 2000; Igaki et al., 2000; Quinn et al., 2003). Debcl, a *Drosophila* member of the multi-domain pro-apoptotic Bax sub family, enhances apoptosis when over expressed in embryo and larvae (Igaki et al., 2000). Similarly, transgenic expression of Debcl in the eye produces a rough eye phenotype, suggesting a perturbation in the cell death mechanism (Brachmann et al., 2000). When co-expressed with P35, a caspase inhibitor, there is only a partial reduction in the rough eye phenotype caused by Debcl, implying its involvement in both caspase-dependent and -independent cell death mechanisms (Colussi et al., 2000). The anti-apoptotic Bcl-2 family member, Buffy, decreases the cell death caused by Debcl (Quinn et al., 2003). Although the BH4 domain, characteristic of antiapoptotic Bcl-2 family members, is absent in Buffy, it is replaced by two alpha helical domains and is required for prevention of cell death (Quinn et al., 2003). In agreement with its anti-apoptotic nature, RNAi of Buffy in embryos increases cell death (Quinn et al., 2003). Despite the conserved role of *Drosophila* Bcl-2 family members in apoptosis, their role in MOMP is not characterized yet. A clear understanding of the role of Debcl and Buffy in the regulation of MOMP, will help in further clarifying the role of mitochondria in *Drosophila* apoptosis.

1.5 Significance of studying apoptosis

Deregulation of apoptosis has been implicated in several pathologies like cancer, neurodegenerative disorders, AIDS, autoimmune disease, and viral infections

(Thompson, 1995). Several kinds of cancers are associated with mutations in genes that regulate cell death pathways. Mutations in these genes are associated with increased resistance to apoptosis, thereby participating in the conversion of normal cells into cancer cells. In addition to tumorigenesis, these cancerous cells are also refractory to apoptotic stimuli and exhibit resistance to conventional chemotherapeutic drugs and irradiation. For instance, mutations in the tumor suppressor gene p53 have been linked to several kinds of cancer. p53 acts as a tumor suppressor gene by upregulating the expression of several pro-apoptotic genes in response to genotoxic stress. Some of the genes that are under the transcriptional control of p53 include pro-apoptotic Bcl-2 family members (*bax*, *bid*, and *puma*), *apaf-1*, and *caspase-9*, which play an important role in promoting apoptosis. Therefore, a number of mutations in the p53 gene lead to disruption of apoptosis and hence cancer (Fadeel and Orrenius, 2005).

Several cancers are characterized either by increased or decreased expression of anti-and proapoptotic proteins, respectively. For instance, Livin (ML-IAP) expression is detected in tumor cells and fetal tissues but not adult tissues (Vucic et al., 2000). Increased levels of XIAP and cIAP1 have been associated with bad prognosis for acute myelogenous leukaemia and prostate cancer, respectively (Krajewska et al., 2003; Tamm et al., 2004). Increased expression of the Bcl-2 protein has been implicated in non-Hodgkin's lymphomas (Weiss et al., 1987). In case of metastatic melanomas, *Apaf-1* expression is lost due to methylation, thereby leading to defects in the execution of apoptosis (Soengas et al., 2001). Furthermore, mutations that inactivate the pro-apoptotic *BAX* gene have been implicated in solid tumors and hematopoietic malignancies

(Brimmell et al., 1998). Therefore, additional insights into the roles of apoptosis in several types of cancers are beneficial not only for identifying therapeutic targets but also in developing prognostic markers (Fadeel and Orrenius, 2005).

Apoptosis plays a critical role in the development of the nervous system (Mattson, 2000). Many neurons that do not receive survival signals *via* neurotrophic factors die by apoptosis. Consistent with this role, mice deficient in caspase-3, caspase-9, or Apaf-1 show prominent neuronal defects. Apart from its role in sculpting of the nervous system, excessive apoptosis has also been implicated in neurodegenerative diseases. For instance, Spinal muscular atrophy, an inherited motor neuron disease, is characterized by the loss of anti-apoptotic IAP family member, NAIP (Roy et al., 1995). Excessive caspase activation has also been implicated in several neurodegenerative disorders such as Alzheimer's disease, Huntington's disease, and Amyotrophic lateral sclerosis (Mattson, 2000).

Apoptosis is essential for immune homeostasis and maintenance of immune tolerance. Deregulation of apoptosis is associated with defective elimination of autoreactive T or B cells, thereby resulting in tissue destruction, a characteristic of autoimmune disorders (Lauber et al., 2004). Apoptosis also plays an important role in the clearance of neutrophils (Brach et al., 1992). These short-lived cells of the immune system that contain proteolytic enzymes, produce reactive oxygen species, and are essential for fighting off bacterial infections. Disruption of this apoptotic process leads to defects in neutrophil clearance, leading to release of noxious contents into the extracellular space, tissue injury and development of an inflammatory response (Colotta

et al., 1992). Therefore, a better understanding of the apoptotic process could help us in identifying targets for several human pathologies (Fadeel and Orrenius, 2005).

1.6 Significance of studying apoptosis in *Drosophila*

As a model system, the fly offers several advantages for studying apoptosis. As a genetic tool, it can be used to identify regulators and effectors of apoptosis (Hay and Guo, 2006). It offers the advantage of understanding the role of apoptosis during development as well as in differentiated adult tissues (Gorski and Marra, 2002). When compared to other genetic model systems, such as *C.elegans* and yeast, *Drosophila* also has the advantage of having complexity similar to humans. This is evident from the conservation of key regulatory molecules involved in apoptosis. Therefore, studying cell death mechanisms in *Drosophila* can further our understanding of apoptosis in humans (Ryoo et al., 2007). This model system allows us to identify new pathways and regulatory mechanisms and at the same time enhances our knowledge of the evolutionary nature of the process.

1.7 Dissertation Objectives

The primary focus of my work was to understand the apoptotic mechanisms in *Drosophila* in order to gain a greater understanding of the human cell death pathways. The first main objective of my dissertation was to understand the role of dOmi, the fly homolog of mammalian Omi/HtrA2, in *Drosophila* apoptosis. I pursued this objective to gain a better understanding of the role of mitochondria in *Drosophila* apoptosis. I have

shown that dOmi, similar to its mammalian counterpart, has an N-terminal MTS, a central catalytic domain and a C-terminal PDZ domain. With the help of the N-terminal MTS, dOmi is translocated to mitochondria where subsequent processing results in generation of two mature forms. The N-termini of the two mature forms ($\Delta 79$ - and $\Delta 92$ -dOmi) are IBMs, which are required for their interactions with DIAP1. By treating *Drosophila* S2 cells with various apoptotic stimuli, I have demonstrated that mature dOmi, along with cytochrome c, are released into the cytosol as a consequence of MOMP. Interestingly, my data suggest that MOMP (and therefore the release of dOmi and cytochrome c) occurs through both caspase-dependent and -independent mechanisms, depending upon the nature of the apoptotic stimulus. I further proceeded to characterize the role of dOmi in *Drosophila* apoptosis. I approached this question using both over expression and RNAi methodologies, the results of which suggest that dOmi plays an important role in caspase activation. This work provides compelling evidence for a conserved role for mitochondria in *Drosophila* apoptosis. I have also identified the first *Drosophila* mitochondrial IAP antagonist and characterized the mechanisms through which it can potentiate apoptosis.

The second part of my work focused on the role of the NERD pathway in the regulation of DIAP1's function. As mentioned previously, the NERD pathway regulates the stability of DIAP1 as a consequence of DrICE cleavage at Asp-20. Although the NERD pathway decreases the stability of DIAP1, it also causes a concomitant increase in its anti-apoptotic function with respect to Rpr-induced cell death (Ditzel et al., 2003). However, the mechanism by which the NERD pathway enhances the anti-apoptotic

function of DIAP1 is not well understood. I therefore hypothesized that the NERD pathway degrades pro-apoptotic proteins in parallel to DIAP1, thereby leading to decreased cell death. Previous work suggests that NERD pathway has a differential effect on Rpr- and Hid-induced cell death. Therefore, I also hypothesized that this variation might be attributed to the differential binding affinity of the RHG proteins to DIAP1. Using a *S. cerevisiae* model, I have demonstrated that Grim can undergo degradation in an N-end rule-dependent manner as described in chapter 4. This work suggests that other pro-apoptotic proteins, which bind to BIR1 domain of DIAP1, can be similarly targeted for degradation through an N-end rule pathway. Indeed, this work demonstrates for the first time that a protein can be *trans*-ubiquitinated when bound to an N-degron. As a whole, this body of work enhances our understanding of the mechanisms that regulate apoptosis in the fly.

Chapter 2: Methods and materials

2.1 Methods and materials for chapter 3

2.1.1 Bacterial and fly expression constructs

Full-length and truncated dOmi constructs were PCR-amplified from an EST (AT14262; BDGP), using *Pfu* polymerase (Stratagene), and cloned into pRmHa3-myc (*EcoRI-BamHI*), pUAS (*EcoRI-XhoI*), or pET21b (*NdeI-XhoI*; Novagen) vectors for expression in *Drosophila* S2 cells, flies, and *E. coli* strain BL21(DE3), respectively. Active-site (S266A), IBM, and cleavage-site mutations were introduced by site-directed mutagenesis (QuikChange[®]; Stratagene). Similarly, the fly caspases, DRONC (residues 1-139) and full-length DrICE, were PCR amplified from ESTs (LD28292 and GH24292; BDGP) and cloned into the *NdeI-XhoI* and *NcoI-XhoI* sites of pET21b and pET28b, respectively. Full-length DIAP1 was generated by SOE-PCR using an EST (L49440) and a *thread* construct (kindly provided by Dr. Colin S. Duckett). For generating DIAP1-BIR1 (residues 1-205), BIR2 (residues 205-341), and BIR1-BIR2 (residues 1-341) and site-directed mutagenesis was utilized to introduce stop codons in pGEX-4T-1-DIAP1 and BIR2-RING. DIAP1 and various truncations were then PCR-amplified and cloned into pIE1-HA (*BamHI-NotI*; Novagen) or pGEX-4T-1 (*EcoRI-NotI*; Pharmacia) vectors for expression in S2 cells and *E. coli*, respectively.

2.1.2 Cell culture and transfections

Drosophila S2 cells were cultured in HyQ SFX-Insect medium (Hyclone) supplemented with 20 mM glutamax at 28°C and were passaged every 3 days at 1:10 dilution to maintain exponential growth. For transfections, 3×10^6 cells were plated per well of a multiwell-6 plate. Transfections were performed using Cellfectin reagent (Invitrogen) 24 hours after plating. For transfections, 2 µg of total DNA was resuspended in 100 µl of the medium, and was then mixed with 10 µl of cellfectin resuspended in 90 µl of the medium. After 20 minutes incubation, the mixture was added to the cells along with 2 ml of fresh medium. For preparing the lysates, S2 cells were incubated with NP-40 lysis buffer with protease inhibitors (50 mM Tris-HCl (pH 8.0), 150 mM NaCl, 1% NP-40, 1 mM PMSF, 2 µg/ml of aprotinin, 2 µg/ml of leupeptin, and 2 µg/ml of pepstatin) for 1 hour at 4°C. The cells were centrifuged at 15,000 x g for 10 minutes and the supernatant was collected and used for further analysis.

2.1.3 Cell death assays

For cell death experiments, cells were transfected with pRmHa3-myc constructs encoding various dOmi proteins (1.5 µg) along with pPAC-3-GFP (0.5 µg) and then split 24 h post-transfection into multiwell-12 plates. Protein expression was then induced with CuSO₄ (0.7 mM), in the presence or absence of Z-VAD-fmk (50 µM; Biomol). Cell death was assessed by flow cytometry (Beckman-Coulter FC500; $\lambda_{\text{ex}}/\lambda_{\text{em}} = 488/525$ nm) at various time points by quantifying the percentage of intact GFP⁺ cells in the induced versus uninduced cell populations (*i.e.* $[1 - (\text{GFP}^+_{\text{induced}}/\text{GFP}^+_{\text{uninduced}})] \times 100$). The

expression levels of dOmi and the various mutants were confirmed by western blotting with a mouse anti-myc antibody (9B11, Cell Signaling).

2.1.4 *Drosophila* genetics

Transgenic flies were generated by the Transgenic Fly Core Facility of the Cutaneous Biology Research Center at Massachusetts General Hospital. Seven lines for UAS- $\Delta 79$ -dOmi and nine lines for UAS- $\Delta 92$ -dOmi were crossed to GMR-gal4 and scored for lethality and eye phenotypes at 25°C. To score for suppression by p35, flies of the genotype *UAS-p35/GMR-gal4; UAS-dOmi/TM6B* were compared to *SM1/GMR-gal4; UAS-dOmi/TM6B*.

2.1.5 Developmental expression of dOmi

RT-PCR was performed on total RNA isolated from embryos (12 h), larvae (2nd-instar), pupae, adults, and S2 cells, using the RNeasy and One-step RT-PCR kits (Qiagen) and the following specific primers for *domi* (ggctttgcgcggttccac and caccggatagccagtctttagg) and *actin* (tgaagatcctcaccgagcgcggcta and gaccggactcgtcactcctgcttg). Protein lysates from these tissues were also utilized for pulldown assays using excess GST-DIAP1. Endogenous dOmi (bound to GST-DIAP1) was then immunoblotted with a rabbit polyclonal antibody raised against recombinant $\Delta 79$ -dOmi^{S266A}. As a loading control, lysates were also immunoblotted for actin (Santa Cruz, I-19).

2.1.6 RNA interference of dOmi

For dsRNA synthesis, the template was PCR amplified using primers containing the 5' T7 polymerase binding site (GAATTAATACGACTCACTATAGGGAGA). The sequence specific primers used for dOmi and control (human TNF) are TTACACAGTCATGCAGCCAATCGG (dOmi forward primer), GATGTCTGATCCACGTCCTCGATG (dOmi reverse primer), CCCAGGGACCTCTCTCTAATCAGC (control forward primer), and GCAATGATCCCAAAGTAGACCTGC (control reverse primer). The PCR products were purified (Genelute™ Gel Extraction Kit, Sigma) and used as templates for dsRNA synthesis (MEGAscript T7 Transcription Kit, Ambion). The dsRNA products were ethanol precipitated and resuspended in water. S2 cells (0.3×10^6) were pretreated with 40 nM dsRNA for 3 days and then exposed to STS (1 μ M) for 4-12 h. Effector caspase (DrICE) DEVDase assays were performed at several time points as described.

2.1.7 Subcellular fractionation of *Drosophila* embryos

Subcellular fractionation of *Drosophila* embryos was performed, as previously described (Wernette and Kaguni, 1986). Briefly, 6-hour old pre-cellularized embryos of *D.melanogaster* were collected and dechorionated in 50% bleach. The dechorionated embryos were resuspended in homogenization buffer (HB) (15 mM HEPES, pH 8.0, 5 mM KCl, 2 mM CaCl_2 , 0.5 mM EDTA, 0.5 mM DTT, 0.27 M sucrose, 1 mM PMSF, 2 μ g/ml of aprotinin, 2 μ g/ml of leupeptin, and 2 μ g/ml of pepstatin) at a ratio of 4 ml/ g wet weight of embryos. The resuspended embryos were homogenized by three strokes of

a glass homogenizer (Wheaton). The homogenate was passed through a 40 μ m nylon cell strainer (BD Falcon) and the retentate was homogenized in HB at a ratio of 1 ml/ g wet weight and filtered through the cell strainer. The filtrates obtained were combined and centrifuged at 1,000 x g for 10 minutes and the pellet was designated as nuclear fraction. The supernatant was further centrifuged at 15,000 x g for collecting the mitochondrial fraction. The resulting supernatant was further fractionated into pellet enriched with endoplasmic reticulum (ER) and the supernatant consisting of cytosolic fraction by centrifuging at 100,000 x g. Equal amounts of the fractions were then subjected to SDS-PAGE and immunoblotted with rabbit anti-Lamin A/C (Cell Signaling), mouse anti-cytochrome c (Clone 7H8.2C12; BD Pharmingen), rabbit anti-BiP (a kind gift from Dr. J. Sisson, University of Texas, Austin), and mouse anti- α -tubulin (clone TU-01; Biovenders Laboratory Medicine) antibodies. Endogenous dOmi was also isolated from each subcellular fraction using a GST-DIAP1 pulldown procedure (detailed below) and immunoblotted using a polyclonal rabbit anti-dOmi antibody.

2.1.8 Subcellular localization of dOmi by immunofluorescence

For immunofluorescence experiments, S2 cells were transfected with pRmHa3-myc constructs for full-length dOmi, Δ 79-dOmi, or Δ 92-dOmi (2 μ g) and then replated (1×10^6) onto polylysine-coated coverslips in a multiwell-12 plate. dOmi-myc expression was induced with CuSO₄ (0.7 mM), and after 24 h, the cells were washed twice with PBS, incubated with MitoTracker[®] Red (300 nM; Molecular Probes), fixed with 4% paraformaldehyde in PBS, permeabilized with 0.1% Triton X-100, and further incubated

with 3% BSA. Each step was performed for 10 min at 25°C. Finally, the permeabilized cells were incubated with a mouse anti-myc monoclonal antibody (1:1000, clone 9E10; Sigma) for 2 h at 25°C, followed by incubation with a secondary goat anti-mouse IgG antibody, conjugated to Alexa Fluor 488 (Molecular probes) for 1 h at 25°C. Coverslips were mounted onto slides in Vectashield (Vector Laboratories) and visualized with a Nikon Eclipse TE2000S fluorescence microscope. For cytochrome c labeling, the cells were initially stained with a mouse anti-cytochrome c antibody (clone 6H2.B4; BD Pharmingen), followed by secondary staining with the goat anti-mouse IgG-Alexa Fluor 488 antibody.

2.1.9 Mitochondrial release of cytochrome c and dOmi

S2 cells (4×10^6) were exposed to STS (1 μ M) or UVB irradiation (5 min on a UV illuminator), washed with PBS, and resuspended in 100 μ L of digitonin lysis buffer (75 mM KCl, 1 mM NaH_2PO_4 , 8 mM Na_2HPO_4 , 250 mM sucrose, 50 μ g/mL of digitonin) for 10 min on ice. Cytosolic fractions were then collected by centrifugation (15,000 $\times g$; 10 min) and immunoblotted with a mouse anti-cytochrome c antibody (clone 6H2.B4, Pharmingen). S2 cells were also transfected with empty vector or pRmHa3-dOmi-myc (2 μ g), and exposed to CuSO_4 (0.7 mM) for 24 h, in order to induce the expression of full-length, mitochondrial-localized dOmi. The transfected cells were then treated with or without STS or UVB, and the resulting cytosolic fractions immunoblotted for dOmi-myc using an anti-myc antibody (9B11, Cell Signaling).

2.1.10 GST-DIAP1 pulldown assays

For the detection of endogenous dOmi, full-length GST-DIAP1 (500 nM) was incubated with GSH-sepharose beads (30 μ L; Amersham) in 300 μ L of GST-PBS buffer (140 mM NaCl, 2.7 mM KCl, 10 mM Na₂HPO₄, 10 mM KH₂PO₄, pH 7.4) for 1 h at 25°C. The DIAP1-bound beads were then washed three times and incubated further with S2 cell lysates (100 μ g in a total volume of 300 μ L) for 3 h at 4°C. The beads were washed extensively with GST-PBS buffer to remove any non-specific proteins, boiled in 2X-SDS loading buffer, and subjected to SDS-PAGE and immunoblotting, using a rabbit polyclonal antibody (1:500). To determine the domains in DIAP1 that were responsible for binding to dOmi, identical experiments were carried out using various truncated GST-DIAP1 proteins (Fig. 3.15A).

Similar experiments were also conducted to determine the residues in dOmi that were necessary for binding to DIAP1. Briefly, GST-DIAP1 (1 μ M) was incubated with GSH-sepharose beads (200 μ L) in 5 mL of GST-PBS buffer for 1 h at 25°C. GST-DIAP1-bound beads were then washed and incubated with recombinant Δ 79-dOmi, Δ 92-dOmi, or their corresponding IBM mutants or truncations (3.2 μ M) in 5 mL of GST-PBS buffer for 2 h at 25°C. The beads were then washed extensively with wash buffer (25 mM Tris, pH 8.0, 150 mM NaCl, 2 mM DTT), and the bound proteins were eluted with wash buffer containing GSH (5 mM), and subjected to SDS-PAGE. In order to visualize all proteins, gels were stained with Coomassie Blue.

2.1.11 Displacement of DrICE and DRONC from DIAP1

To assess the potential of dOmi to antagonize BIR1-dependent inhibition of DrICE, recombinant DrICE (175 nM) was first preincubated with GST-BIR1 (3.5 μ M) for 30 min at 25°C in assay buffer (20 mM HEPES, pH7.4, 100 mM NaCl, 0.05% NP40, 5 mM MgCl₂). Recombinant Δ 79-dOmi, Δ 92-dOmi, or their IBM truncation mutant proteins (4.5 μ M), were then added, along with recombinant human PARP (5.75 μ M), in a final volume of 30 μ L. Each sample was then incubated for 60 min at 25°C, and the amount of PARP cleaved was visualized by SDS-PAGE/Coomassie Blue staining. Identical experiments were also carried out using Δ 79-IBM, Rpr-IBM, and control peptides (5 μ g) in separate incubations.

For DRONC displacement assays, GST-BIR2-RING (3 μ M) was incubated with GSH-sepharose beads (30 μ L) in a total volume of 300 μ L of GST-PBS for 1 h at 25°C. After washing thrice with GST-PBS, the beads were incubated with excess DRONC fragment (6 μ M), in the absence or presence of increasing concentrations of dOmi proteins (2-16 μ M) or Rpr-IBM peptide (0.25-4 μ M) for 1 h at 25°C. The amount of DRONC (1-139) displaced was visualized by SDS-PAGE/Coomassie Blue staining. Band densities for both DRONC and GST-BIR2-RING were determined using ImageJ software, and bound DRONC (normalized to the amount of precipitated GST-BIR2-RING) was then plotted versus dOmi or Rpr-IBM using DeltaGraph. EC_{50} values for dOmi and Rpr-IBM were determined by nonlinear regression and subsequently applied to the Cheng-Prusoff equation: $K_d = EC_{50} / (1 + [\text{ligand}] / K_d^*)$, in order to determine their dissociation constants (K_d). In our assays, the ligand concentration (DRONC, 6 μ M) was

known, and its dissociation constant, K_d^* (DRONC, 0.8 μ M), was previously determined (Chai et al., 2003b).

2.1.12 Effector caspase (DEVDase) activity assays

Effector caspase (*i.e.* DrICE and DCP-1) activities were determined, as previously described (Kanuka et al., 1999a). Briefly, S2 cells (1×10^6) were treated with STS (1 μ M) or UVB irradiation (5 min on a transilluminator) and collected at the indicated time points. The cells were washed twice with PBS, resuspended in lysis buffer (50 mM Tris, pH7.5, 1 mM EDTA, 10 mM EGTA, 10 μ M digitonin), and incubated at 37°C for 10 min. Cytosolic fractions were subsequently collected by centrifugation (15,000 x g , 10 min) and incubated (37°C for 30 min) with an equal volume of assay buffer (20 mM HEPES, pH 7.4, 100 mM NaCl, 0.05% NP40, 5 mM MgCl₂), containing the fluorescent substrate, Ac-DEVD-AMC (20 μ M; Biomol). DEVDase activities were then measured ($\lambda_{ex}/\lambda_{em}$ = 360/450 nm) in a 96-well plate format using a Wallac Victor³ 1420 Multilabel counter.

2.1.13 $\Delta\psi_m$ measurements

S2 cells (1×10^6) treated with STS or UVB were incubated with 5,5',6,6'-tetrachloro-1,1',3,3'-tetraethylbenzimidazolyl-carbocyanine iodide (5 μ g/mL, JC-1; Molecular Probes) for 10 min at 25°C. Cells exhibiting red ($\lambda_{ex}/\lambda_{em}$ = 488/ 620 nm) or green ($\lambda_{ex}/\lambda_{em}$ = 488/525 nm) fluorescence—corresponding to high or low $\Delta\psi_m$, respectively—were assayed by flow cytometry (Beckman-Coulter FC500).

2.1.14 DNA fragmentation assay

In some experiments, apoptosis was measured by quantifying the percentage of cells, exhibiting a sub-diploid DNA (*i.e.* sub-G1) peak. Briefly, S2 cells (2×10^6) were treated with STS or UVB, as described above. At the indicated time points, the cells were collected, washed, and resuspended in ice-cold PBS (500 μ l). Using intermittent vortexing, the cells were then slowly mixed with ice-cold 70% ethanol (4 mL), and after 2 h on ice, the fixed cells were harvested, washed with PBS, and stained with propidium iodide (40 μ g/mL propidium iodide and 100 μ g/mL RNase A in PBS) for 30 min at 37°C. Stained nuclei were analyzed by flow cytometry (Beckman-Coulter FC500; $\lambda_{\text{ex}}/\lambda_{\text{em}} = 488/620$ nm).

2.1.15 Recombinant protein expression

All proteins were overexpressed in *E. coli* strain BL21(DE3), either as C-terminal His₆-tagged proteins or as GST fusion proteins. For purification of dOmi proteins, 1 mL of an overnight culture was transferred to 400 mL of LB broth and grown at 37°C to an O.D.₆₀₀ of ~ 0.4-0.5. Protein expression was then induced with 0.1 mM isopropyl-1-thio- β -D-galactoside (IPTG) for 16 h at 16°C. Bacteria were collected by centrifugation, resuspended in 40 mL of lysis buffer with protease inhibitors [50 mM NaH₂PO₄, 30 mM NaCl, 10 mM Imidazole, 1 mM PMSF, 2 μ g/mL of aprotinin, 2 μ g/mL of leupeptin, 2 μ g/mL of pepstatin, pH 7.0], lysed by sonication, and the lysates collected by centrifugation at 20,000 x *g* for 30 min. For DRONC (1-139) and DrICE, protein expression was induced with 1 mM IPTG for 3 h at 37°C. All His₆-tagged proteins were

purified on a column packed with Ni²⁺-nitrilotriacetic acid (Ni-NTA, Novagen) resin and eluted using an imidazole gradient (0-250 mM). Similarly, bacteria expressing GST fusion proteins were resuspended in GST lysis buffer [140 mM NaCl, 2.7 mM KCl, 10 mM Na₂HPO₄, 10 mM KH₂PO₄, 1% Triton X-100, pH 7.4], and GST fusion proteins were purified on a column packed with GST-Bind resin (Novagen). Recombinant PARP was a kind gift from Zhihua Tao and Prof. Hung-wen Liu (The University of Texas at Austin).

2.1.16 dOmi protease assays

For *in vitro* dOmi protease assays, lysates of S2 cells transfected with pIE-HA-DIAP1 (2 µg) were immunoprecipitated with mouse anti-HA antibody (5 µg; 262K, Cell Signaling) bound to protein G sepharose beads (Amersham). Alternatively, purified GST-DIAP1 (1 mg) was labeled with D-Biotin-*N*-hydroxysuccinimide ester (Roche Molecular Biochemicals), according to the manufacturers suggested protocol. HA-DIAP1 and biotinylated GST-DIAP1 (250 ng) were then independently incubated (2 h at 37°C) with recombinant Δ79-dOmi or Δ92-dOmi (50-200 nM) in assay buffer (25 mM Tris, pH 8.0, 100 mM NaCl, and 1 mM dithiothreitol). DIAP1 cleavage was analyzed by western blotting with the anti-HA antibody or horseradish peroxidase-conjugated streptavidin (Amersham).

2.1.17 Ubiquitination assays

Ubiquitination assays were performed as described earlier with certain modifications. Briefly, peptides corresponding to IBMs of Reaper (AVAFYIPD), $\Delta 79$ -dOmi (AIIQREDL), $\Delta 92$ -dOmi (ASKMTGRR), and a control peptide (MKSDFYFQ) (GenScript corporation) at a final concentration of 1 μ M were incubated with 0.5 μ M of recombinant BIR2-RING-GST for 15 minutes at room temperature. In parallel, 1 μ l of 10 mg/ml lysate prepared from 6 hour old pre-cellularized embryos in EX buffer (20 mM Tris-HCl at pH 7.5, 100 mM sodium chloride, 5 mM ATP, 2.5 mM $MgCl_2$, 1 mM DTT and 0.25 M Sucrose) was incubated with UR buffer (25 mM Tris-HCl at pH 7.5, 0.5 mM DTT, 2 mM ATP and 5 mM $MgCl_2$) for 15 minutes. Pre-incubated embryo lysate is combined with the mixture containing peptides and BIR2-RING. Subsequently, 1 μ g of Flag-Ubiquitin (Sigma) was added to the mixture and incubated at 37°C. 15 μ l of lysate was collected at several time points and the reaction was stopped by adding SDS loading buffer. Ubiquitination of BIR2-GST was analyzed by western blotting with goat anti-GST antibody (Amersham) at 1:2,000 dilution. Similar experiments were also done using 1 μ M recombinant dOmi proteins instead of peptides.

2.1.18 Structural modeling

The predicted tertiary structure of dOmi was obtained by threading the dOmi sequence onto the hOmi structure (PDB code: 1LCY) using the program 3D-JIGSAW (Bates et al., 2001).

2.2 Methods and materials for chapter 4

2.2.1 Strains and culture media

Saccharomyces cerevisiae strains used in this study include JD53 (*MAT α trp1- Δ 63 ura3-52 his3- Δ 200 leu2-3, 112 lys2-801*) and JD83-1A (*MAT α ubr1 Δ ::HIS3 trp1- Δ 63 ura3-52 his3- Δ 200 leu2-3, 112 lys2-801*) (Suzuki and Varshavsky, 1999). The strains were grown either in rich (YPD) medium containing 2% peptone (Difco), 1% yeast extract (Sigma), and 2% glucose (Sigma) or in synthetic yeast medium (SD medium) containing 0.67% yeast nitrogen base without aminoacids (Difco) enriched with auxotrophic nutrients (Qbiogene) and 2% sugars (galactose (USBiological), raffinose (MP Biomedical), and glucose) as required. For induction of the P_{GALI} promoter, the cells were grown in SD-raffinose medium to the required density and pelleted and transferred to SD-galactose medium. For induction of P_{CUP1} promoter the strains were grown in SD medium with CuSO₄ added to a final concentration of 0.2 mM.

2.2.2 Plasmid construction

The ubiquitin-fusion plasmids encoding DIAP1 proteins were generated by modifying the copper-inducible P_{CUP1} promoter containing pDhaUbXK1 β gal construct. Briefly, the pDhaUbXeK1 β gal comprised of mouse DHFR gene fused to ubiquitin gene bearing arginine instead of lysine at position 48 (K48R) through a 20-residue spacer containing the hemagglutinin (HA-tag), which encodes the reference protein. Following the ubiquitin gene, sequence encoding an amino acid either Met or Arg (notated as X) is

present. The β gal gene was cloned after the X into *Bam*HI and *Xho*I sites. To generate the DIAP1 ubiquitin fusion plasmids, the β gal gene is replaced by DNA corresponding to either BIR1-GST or BIR1-BIR2-GST which were PCR amplified and subcloned into *Bam*HI and *Xho*I. The *Bam*HI site was later removed by site-directed mutagenesis. The constructs expressing Grim wild-type and GGAY mutant were generated by cloning the coding sequence into *Bam*HI and *Xho*I sites of pYES2 vector with GAL1 promoter (Invitrogen). Site-directed mutagenesis of the template pYES2-Grim was performed to generate the mutant lacking lysine (pYES2-Grim (K136A)).

2.2.3 Yeast transformation

Yeast were transformed by using YEAST-1 transformation kit (Sigma). Briefly, *S. cerevisiae* strains were inoculated in 3 ml of YPD medium cultured at 30°C. The dense cultures were diluted to an initial O.D of ~ 0.2-0.4 in 100 ml of YPD medium and were grown at 30°C until the final O.D reaches a value of ~ 1-1.2. Cells were pelleted by centrifugation for 5 minutes at 3,000 x g and washed with 50 ml of sterile water. The pelleted cells were then resuspended in 1 ml of transformation buffer. For each transformation, 500 ng of plasmid DNA and 100 μ g of salmon testes DNA were added to 100 μ l of cells resuspended in transformation buffer. The cells were vortexed and 600 μ l of plate buffer was added. The cells were vortexed again and incubated at 30°C by shaking for 30 minutes. Cells were then heat shocked for 30 minutes at 42°C. The heat shocked cells were pelleted by spinning at maximum speed for 1 minute and washed with 500 μ l of sterile water. Cells were suspended in a final volume of 500 μ l and plated on

SD-glucose agar plates with the appropriate auxotrophic nutrients. The plates with yeast were incubated for 3 days at 30°C.

2.2.4 Degradation analysis of the ubiquitin-fusion proteins

To analyze the stability of various ubiquitin-fusion proteins of DIAP1, the transformant colonies were inoculated in 2.5 ml of SD-glucose medium lacking Trp (SD-Trp (glucose)) and cultured for 1-2 days until dense cultures were obtained. Dense cultures were diluted to an initial O.D ~0.1 and allowed to grow until they reach an O.D of 0.8-1.2 (6-8 hours). Cells were pelleted and resuspended into fresh SD-Trp (glucose) medium with 0.2 mM CuSO₄ to induce the ubiquitin-fusion proteins. Cells were collected at the required time points and resuspended in 2X-SDS loading buffer and further analyzed by immunoblotting using rabbit polyclonal anti-GST (ab21070; Abcam) and mouse monoclonal anti-HA (clone 16B12; Covance) antibodies.

2.2.5 Degradation analysis of the Grim protein

To analyze the stability of Grim in the presence of various ubiquitin-fusion proteins of DIAP1, the co-transformants were inoculated in 2.5 ml of SD-raffinose medium lacking Trp (SD-Trp-Ura (raffinose)) and cultured for 1-2 days until dense cultures were obtained. Dense cultures were diluted to an initial O.D ~0.1 and allowed to grow until they reach an O.D of 0.8-1.2 (6-8 hours). Cells corresponding to 31.5 O.D units were pelleted and resuspended in 12.5 ml of fresh SD-Trp-Ura (galactose) medium and incubated for 3 hours to induce the expression of Grim protein. Then 0.2 mM CuSO₄ was added to the medium to induce the expression of ubiquitin-fusion proteins.

Thereafter, 2.5 ml of the culture was collected at various time points as indicated and the cells were resuspended in 150 μ l of 2X-SDS loading buffer. The cells were boiled for 15 minutes and spun at maximum speed for 1 min. The supernatants were further analyzed by immunoblotting using mouse anti-HSV (69171, Novagen), anti-tubulin (clone TU-01; Biovenders Laboratory Medicine), rabbit polyclonal anti-GST (ab21070; Abcam), and mouse monoclonal anti-HA (clone 16B12; Covance) antibodies.

2.2.5 Viability assays

For determining the viability of the yeast harboring the vectors expressing Grim as well as various DIAP1 proteins, the co-transformants were inoculated in 2.5 ml of SD-Trp-Ura (raffinose) medium. Cells corresponding to 0.5 O.D units were pelleted and resuspended in 1 ml of sterile water. Cells were 10-fold serially diluted and 10 μ l of each serial dilution was spotted on to the plates containing either glucose or galactose either with or without CuSO₄. Plates were incubated for 2 days at 30°C and the viability of the cells was analyzed visually.

2.2.5 Cell culture and transfections

Drosophila S2 cells were maintained and transfected as mentioned previously. For Grim expression analysis, cells were also transfected with pRmHa3-Grim-HSV (2 μ g) and then split 24 h post-transfection into multiwell-12 plates. Protein expression was then induced with CuSO₄ (0.7 mM), in the presence or absence of Z-VAD-fmk (50 μ M; Biomol). The expression levels of Grim and endogenous DIAP1 were analyzed by

western blotting with a mouse anti-HSV antibody (Novagen) and rabbit anti-DIAP1 antibody (a kind gift from Dr. Kristin White, Harvard medical school, MA).

Chapter 3: *Drosophila* Omi, a mitochondrial-localized IAP antagonist and proapoptotic serine protease

3.1 Introduction

Apoptosis, or programmed cell death, is an evolutionarily-conserved process that is required for the normal development and homeostasis of most (if not all) metazoans. Caspases are generally activated during apoptosis and are responsible for the biochemical and morphological features commonly associated with this form of cell death (Danial and Korsmeyer, 2004; Kornbluth and White, 2005). Consequently, the mechanisms that mediate the activation of caspases and/or regulate their activities are of considerable interest (Fuentes-Prior and Salvesen, 2004). In mammals, cellular stress often results in MOMP, which facilitates the release of cytochrome c from the intermembrane space into the cytosol. Cytochrome c then binds to the adapter protein, Apaf-1, and in the presence of dATP or ATP, stimulates oligomerization of Apaf-1 into a large ~700-1400 kDa apoptosome complex that sequentially recruits and activates the initiator caspase-9 and the effector caspase-3 (Cain et al., 2002).

Given the importance of MOMP for apoptosis, both proapoptotic (*e.g.* Bim, Bid, Bax, and Bak) and antiapoptotic (*e.g.* Bcl-2, Bcl-x_L, and Mcl-1) Bcl-2 family members have evolved to tightly regulate this process (Danial and Korsmeyer, 2004). Nevertheless, in the event that caspases are activated, a second layer of protection also exists, comprised of the IAP proteins (Salvesen and Duckett, 2002). Originally identified in baculoviruses, where they serve to inhibit host cell death during viral replication, IAPs

are characterized by the presence of one or more BIR domains and in some cases, a C-terminal RING domain that functions as an E3 ubiquitin ligase. XIAP, the prototypical IAP in mammals, binds to and potently inhibits the activities of caspases-9 and -3 *via* its BIR3 and linker-BIR2 domains, respectively, and may in turn catalyze the ubiquitinylation and turnover of caspases *via* the 26S proteasome (Salvesen and Duckett, 2002).

By contrast, in flies previous studies suggest that MOMP does not occur and that cytochrome c is not released into the cytosol in response to stress (Dorstyn et al., 2004; Varkey et al., 1999; Zimmermann et al., 2002), despite the existence of both proapoptotic (Debcl/dBorg-1/Drob-1/dBok) and antiapoptotic (Buffy/dBorg-2) Bcl-2 family members (Igaki and Miura, 2004). Moreover, the Apaf-1 homologue, *Drosophila* Apaf-1-related killer (DARK/Hac-1/dApaf), reportedly does not require cytochrome c for its activation and is constitutively active in cells, where it binds to and continuously processes the initiator caspase DRONC (Dorstyn et al., 2004; Muro et al., 2002; Zimmermann et al., 2002). Other reports, however, suggest that cytochrome c can bind to DARK and that it is required for DARK-dependent activation of caspases, at least during spermatid individualization and developmental apoptosis in the fly eye (Arama et al., 2003; Arama et al., 2006; Kanuka et al., 1999b; Mendes et al., 2006). Thus, in flies the specific roles that mitochondrial proteins play in apoptosis remain highly controversial (Means et al., 2006). Regardless, once formed, the DARK•DRONC apoptosome complex is held in check by DIAP1, which binds *via* its BIR2 domain to the linker region separating the prodomain and the large subunit (protease domain) of DRONC (Chai et al., 2003a; Meier

et al., 2000). Intriguingly, DIAP1 apparently does not directly inhibit DRONC activity, but instead promotes its turnover in the cell through ubiquitinylation (Chai et al., 2003a; Wilson et al., 2002).

Consistent with its central role in regulating apoptosis, mutations in DIAP1 that diminish its interaction with caspases, consequently enhance or induce apoptosis (Goyal et al., 2000; Hay et al., 1995; Lisi et al., 2000). Moreover, a number of *Drosophila* IAP antagonists have been discovered, including Rpr, Hid, Grim and Sickie, that are either transcriptionally upregulated or posttranslationally modified in response to specific developmental cues or stressful stimuli (Kornbluth and White, 2005). Each of these IAP antagonists possesses an N-terminal IAP binding motif (IBM) that displaces active caspases from DIAP1 and/or induces DIAP1 autoubiquitinylation, resulting in the induction of apoptosis (Kornbluth and White, 2005). In sharp contrast, the mammalian IAP antagonists, Smac/DIABLO and Omi/HtrA2, are constitutively expressed and sequestered to the mitochondrial intermembrane space prior to stress-induced MOMP (Du et al., 2000; Hegde et al., 2002; Martins et al., 2002; Suzuki et al., 2001a; Verhagen et al., 2000; Verhagen et al., 2002). Thus, it could be reasonably argued that MOMP may not be required for apoptosis in flies, because their IAP antagonists are not sequestered to mitochondria.

Recent studies however indicate that Rpr and Grim contain a second conserved motif, referred to as the Trp-block or GH3 domain, which mediates their relocalization to mitochondria and is required for efficient cell killing (Claveria et al., 2002; Olson et al., 2003b; Wing et al., 2001). Moreover, there is precedence for the sequestration of IAP

antagonists in the fly, as Jafrac2 is initially localized to the endoplasmic reticulum (ER), prior to its release during ER stress (Tenev et al., 2002). Thus, we sought to further investigate the putative role(s) of mitochondrial proteins in fly apoptosis and report here the identification and characterization of *Drosophila* Omi (dOmi), the first mitochondrial-sequestered dual IAP antagonist and proapoptotic serine protease in flies.

3.2 Results

3.2.1 dOmi is a *Drosophila* Omi/HtrA2 homologue. A TBLASTN search of the *Drosophila* sequence database (FlyBase) was performed using human Omi/HtrA2 (hOmi; amino acids 1-458). This resulted in identification of a putative *omi*-like homologue (gene CG8464), which mapped to region 88C3 on chromosome arm 3R and contained three exons spanning ~1.8 kilobases, including a 286-bp 5'-UTR, a 1270-bp coding region, and a 92-bp 3'-UTR (Fig. 3.1A). A full-length EST (AT14262) was subsequently obtained, and the entire open reading frame cloned into both insect and bacterial expression plasmids. Expression of *domi* confirmed that it encoded a 422 amino acid protein with a molecular mass of ~46 kDa (see below). Alignment of dOmi with several members of the HtrA family revealed significant homology, particularly within the serine protease and PDZ domains, where dOmi shares ~57% and ~45% identity with hOmi, respectively (Fig. 3.1B). Moreover, threading of the dOmi sequence onto the structure of hOmi suggested significant overall structural similarity (Figs. 3.2A and B; PDB code 1LCY)(Li et al., 2002).

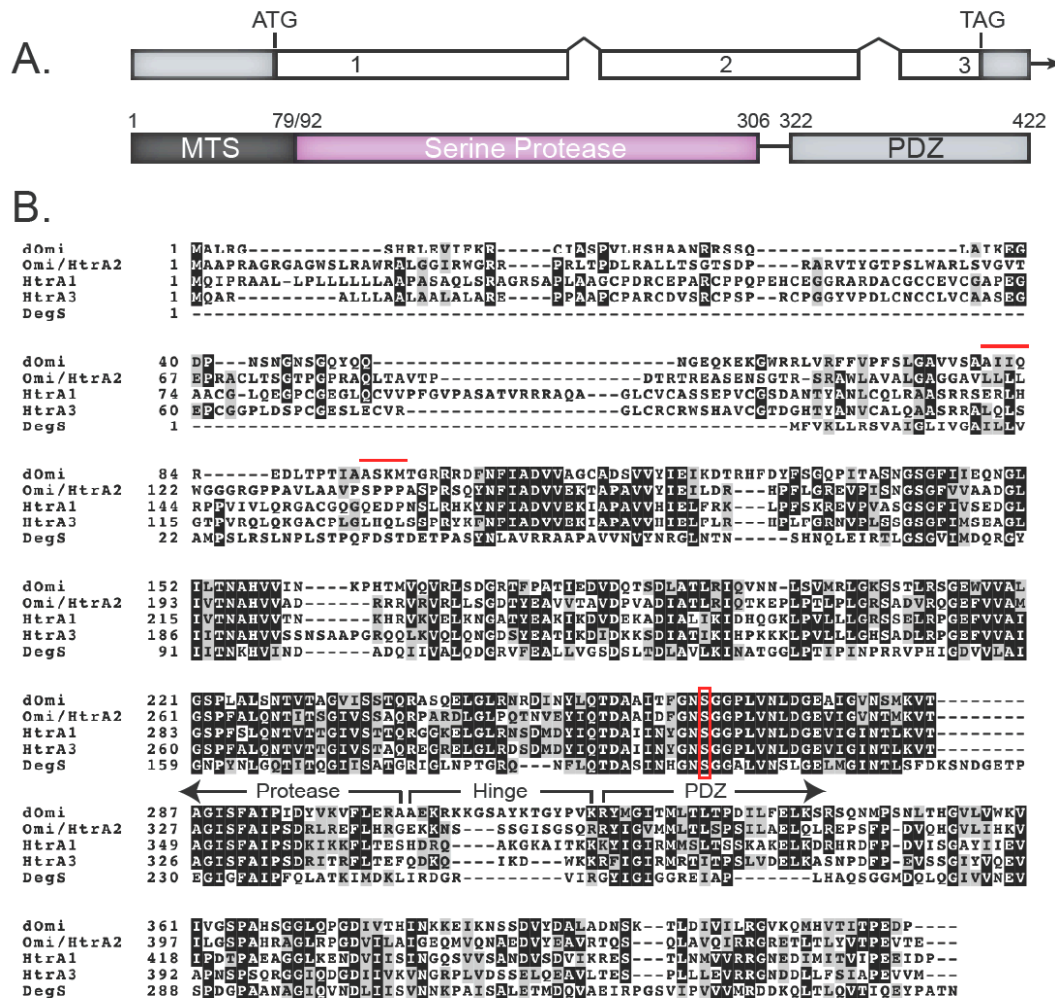


Figure 3.1 *Drosophila* Omi is a HtrA family member.

- (A) *domi* contains three exons spanning ~1.8 kilobases, including a 286-bp 5'-UTR (gray), a 1270-bp coding region, and a 92-bp 3'-UTR (gray). The protein sequence contains an N-terminal mitochondrial targeting sequence (MTS), a serine protease domain, a hinge region, and a PDZ protein interaction domain.
- (B) The coding sequence of dOmi was aligned (ClustalW) with human HtrA1, Omi/HtrA2, HtrA3, and bacterial DegS. Red bars indicate dOmi's two IBMs; the red box indicates the conserved active-site serines present in all HtrA family members.

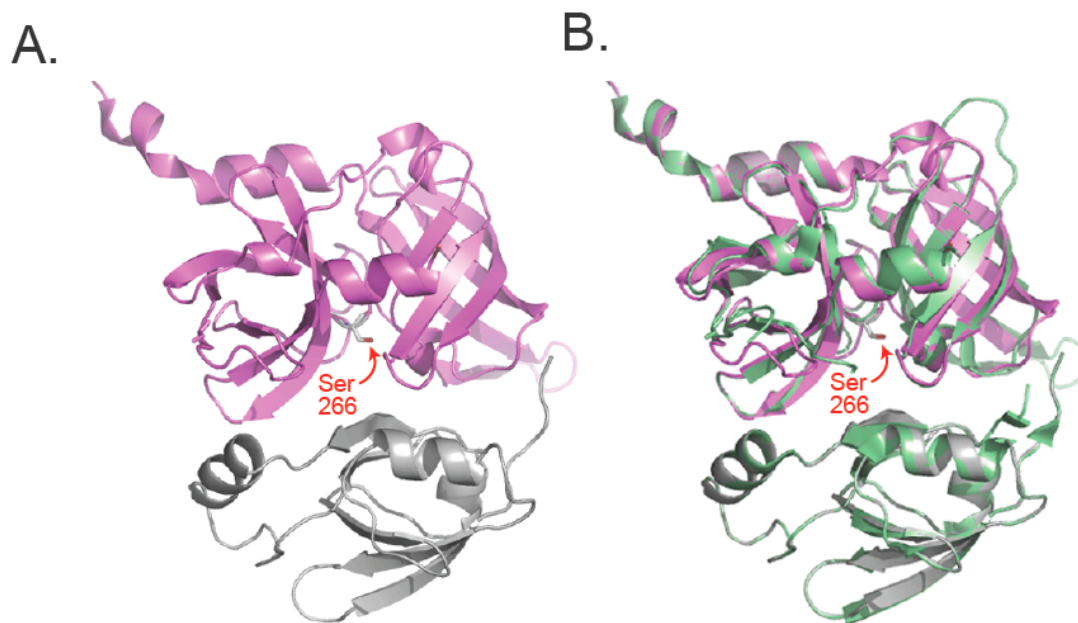


Figure 3.2 *Drosophila* and mammalian Omi are similar at tertiary structural level.

- (A) A structural model of dOmi was created by threading its primary amino acid sequence onto the solved crystal structure of human Omi. Structure showing the protease domain (*pink*) with the active site serine (*red arrow*) and the PDZ domain (*gray*).
- (B) Overlay of dOmi (*pink and gray*) with human Omi (*green*).

3.2.2 dOmi contains an N-terminal targeting sequence that is proteolytically removed during mitochondrial import. hOmi, a class I intermembrane space protein, contains a MTS that mediates its import across the outer mitochondrial membrane, as well as its insertion into the inner mitochondrial membrane (Illustration 3.1). Analysis of the dOmi sequence using the PSORTII program suggested that dOmi also possessed a putative N-terminal MTS (Fig. 3.3). Therefore, we transiently transfected *Drosophila* S2 cells with a C-terminal, myc-tagged version of dOmi and examined the cells by immunofluorescence microscopy. As predicted, both dOmi-myc and cytochrome c (positive control) were found exclusively in mitochondria, as indicated by their colocalization with Mitotracker[®] Red (Fig. 3.5). Immunoblotting of the dOmi-myc transfected cells subsequently revealed that, following its import into mitochondria, dOmi underwent N-terminal processing at two sites, resulting in the generation of two distinct dOmi fragments (~37 and ~35 kDa) (Fig. 3.4B, lane 2). A hydrophobicity plot of dOmi's N-terminus indicated the presence of a putative transmembrane domain (amino acids 63-82)—likely utilized for insertion into the inner mitochondrial membrane (Fig. 3.3)—as well as a second hydrophobic patch (amino acids 100-120) that was highly homologous to the trimerization domain previously described for hOmi (Figs. 3.1B, 3.3) (Li et al., 2002). We therefore speculated that cleavage of dOmi might occur within the region separating these two hydrophobic motifs. Further analysis using the SignalP program predicted cleavage at A⁷⁹↓AIIQ, and we noted a second di-alanine motif at A⁹²↓ASKM (Figs. 3.3, 3.4A). Since cleavage at these two sites would yield dOmi fragments of ~3

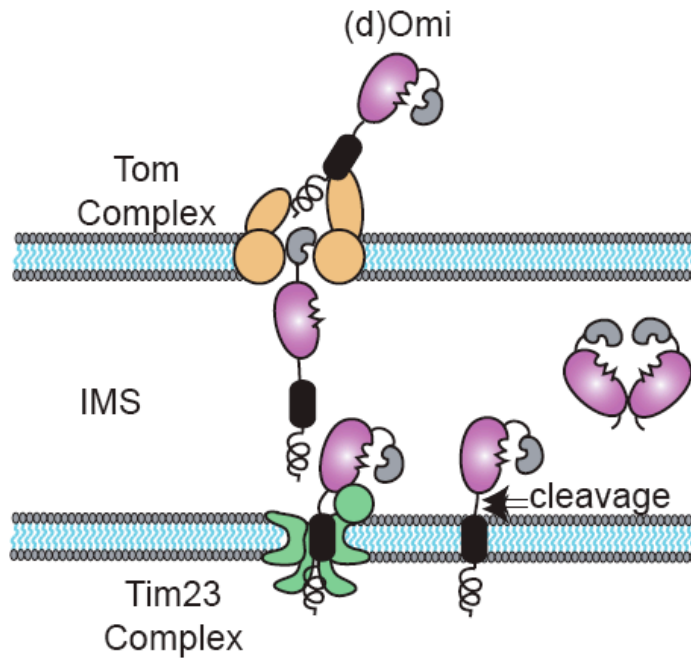


Illustration 3.1 **Model of dOmi import across the outer mitochondrial membrane and processing within the intermembrane space (IMS).**

TOM/TIM23 complexes are located on the outer and inner mitochondrial membranes, respectively. The protease (*pink*), PDZ (*gray*), and the transmembrane (*black*) domains as well as the MTS (*black spiral*) are represented. dOmi is recognized by TOM/TIM23 complexes through the MTS. After the translocation of dOmi into the inner membrane a cleavage event occurs thereby releasing mature dOmi into IMS.

61 WRRLVRFVFPFSLGAVVSAAIIQREDLTPTIAASKMTGRRRDFNFIADVAGCADSVVYIE 121

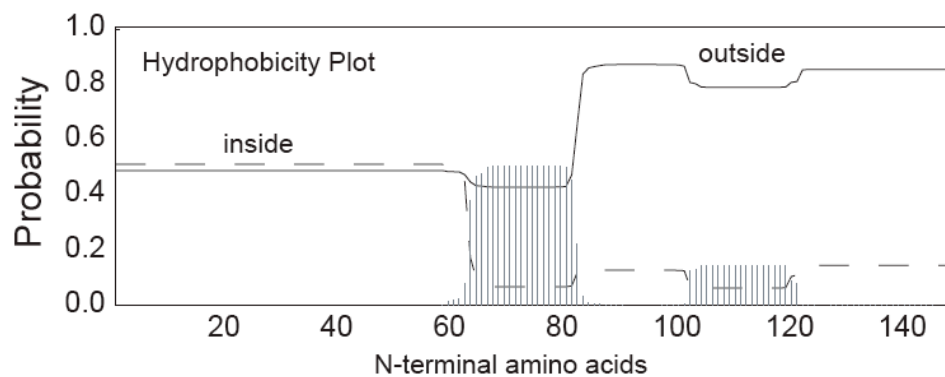


Figure 3.3 dOmi has two putative cleavage sites after the transmembrane domain.

A hydrophobicity plot of the N-terminus (residues 1-150) of dOmi was performed using the TMHMM Server v. 2.0 (CBS; Denmark). The inside/outside probability determinations indicate that residues 82-140 are located on the same side of the intermembrane, facing the IMS. Underlined amino acids represent the putative IBMs obtained as a result of the cleavage event.

and ~35 kDa, respectively, we mutated each pair of alanines to aspartic acids in an effort to inhibit proteolytic processing.

As anticipated, mutation of Ala-92 and Ala-93 to aspartic acids almost entirely prevented formation of the 35-kDa dOmi fragment (Fig. 3.4B; lane 4). Similarly, mutation of Ala-79 and Ala-80 to aspartic acids prevented formation of the 37-kDa dOmi fragment; however, the negatively-charged aspartic acid residues disrupted the adjacent transmembrane domain and brought about unnatural processing of dOmi at another site (data not shown). We therefore generated an A79W/A80W mutant, which preserved the overall hydrophobicity of the putative cleavage site but, due to the increased size of the tryptophan residues, completely prevented processing and formation of the 37 kDa dOmi fragment (Fig. 3.4B; lane 3). Interestingly, the A79W/A80W mutant also exhibited reduced processing at the A⁹²↓ASKM site, which suggested that dOmi was initially processed to the 37 kDa fragment, followed by secondary processing to the 35 kDa fragment. dOmi did not appear to undergo autocatalytic cleavage at either site, since the active-site serine mutant S266A failed to inhibit processing of the enzyme (data not shown). In any event, mutation of all four alanine residues (A79W/A80W/A92D/A93D) resulted in essentially a noncleavable mutant of dOmi (Fig. 3.4B, lane 5). The minor cleavage products that were observed likely resulted from promiscuous cleavage of dOmi by its signal peptide protease complex. Since proteolytic processing of mitochondrial proteins often results in the removal of their MTS residues, we next expressed the Δ79 and Δ92 mature forms of dOmi-myc in S2 cells (corresponding to the 37 and 35 kDa fragments, respectively) and analyzed them by fluorescence microscopy. As anticipated,

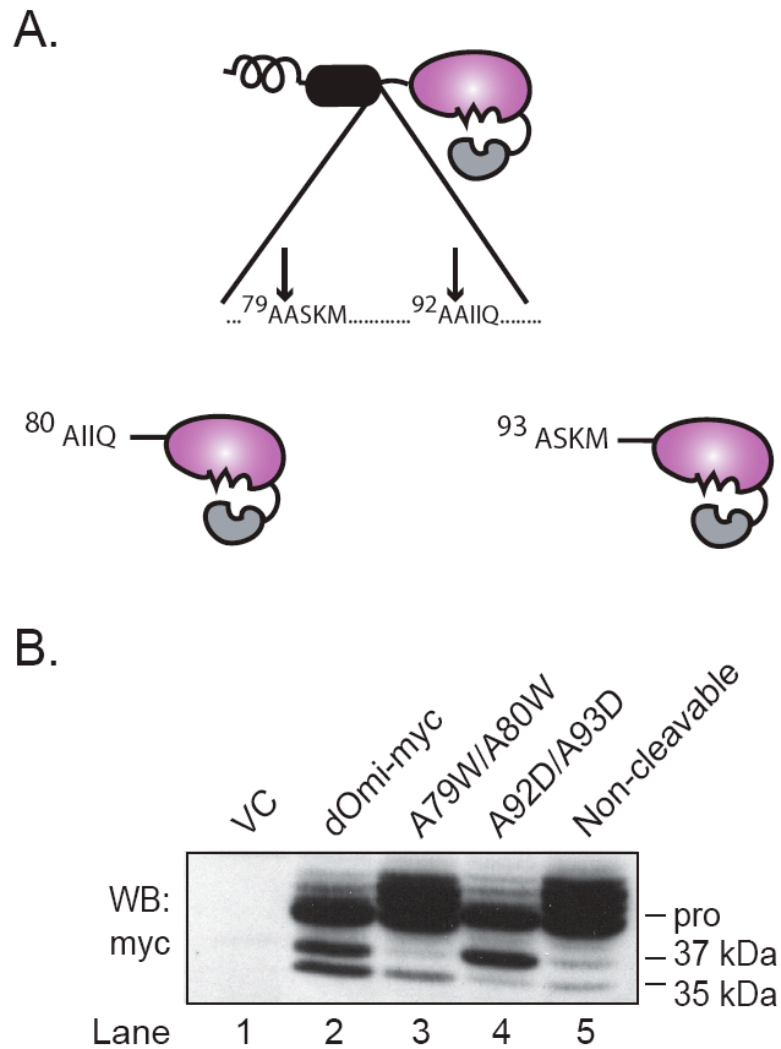


Figure 3.4 Full-length dOmi is processed into two mature forms.

- (A) A model representing the putative mature fragments obtained after the cleavage of full-length dOmi.
- (B) S2 cells were transfected with full-length wild-type dOmi-myc, or various cleavage site mutants, for 24 h and then immunoblotted using an anti-myc antibody.

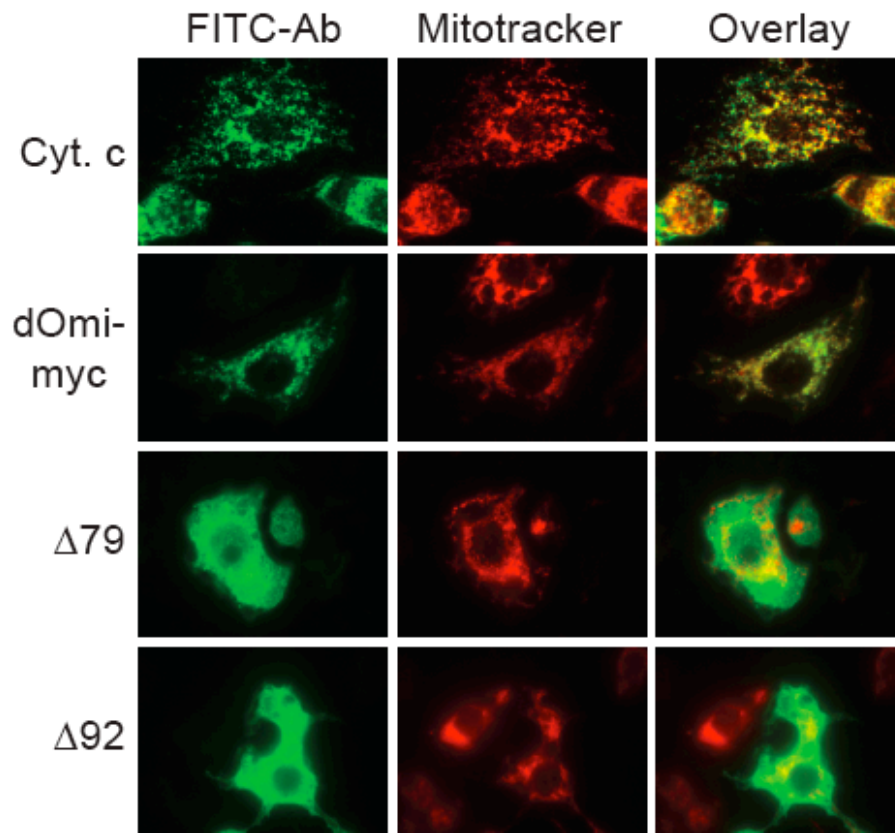


Figure 3.5 **dOmi is a mitochondrial resident protein.**

S2 cells were transiently transfected with either full-length, $\Delta 79$ or $\Delta 92$ -dOmi-myc for 24 h and stained with primary anti-myc or anti-cytochrome c (*positive control*) antibodies, followed by a secondary FITC-labeled anti-mouse antibody. Mitochondrial localization was determined by staining cells with Mitotracker[®] Red.

removal of these N-terminal residues from dOmi prevented its import into mitochondria, as dOmi no longer colocalized with Mitotracker[®] Red and instead remained present within the cytoplasm (Fig. 3.5).

3.2.3 Mature dOmi contains two IBMs and is developmentally-regulated in flies.

Proteolytic removal of the MTS from hOmi not only liberates the enzyme from its inner mitochondrial membrane anchor (Illustration 3.1), but also exposes a cryptic IBM that is required for its interaction with XIAP (Hegde et al., 2002; Martins et al., 2002; Suzuki et al., 2001a; Verhagen et al., 2002). Anecdotal reports have suggested that homologues of hOmi do not contain IBMs, primarily because the AVPS motif in hOmi is not conserved in other species, including *Drosophila* (Fig. 3.1B). However, the fact that dOmi underwent cleavage at two distinct di-alanine motifs raised the possibility that it might contain functional IBMs. Indeed, $\Delta 79$ -dOmi contained an N-terminal AIIQ motif that was similar to that observed for the known IAP antagonists Grim and Sickie, and $\Delta 92$ -dOmi contained an ASKM motif with the requisite N-terminal alanine, as well as a preferred hydrophobic residue in the P₄ position (Fig. 3.6A). We therefore performed *in vitro* pulldown assays using highly purified GST-DIAP1 and either recombinant $\Delta 79$ -dOmi or $\Delta 92$ -dOmi. As shown in Fig. 3.6B, DIAP1 bound each of the cleaved forms of dOmi (lanes 3, 5, 9, and 11), but failed to do so when the corresponding IBMs (AIIQ and ASKM) were removed (lanes 4 and 6) or when the first two amino acids were mutated to glycines (lanes 10 and 12). Thus, proteolytic removal of the MTS from dOmi resulted in

the formation of two fragments, both of which possessed N-terminal IBMs capable of binding to DIAP1.

To verify that processing of *endogenous* dOmi occurred within mitochondria and resulted in the generation of IAP antagonists in flies, we prepared lysates from wild-type embryos (12 h) and performed DIAP1 pulldown assays using various subcellular fractions. DIAP1 precipitates were then immunoblotted with a rabbit polyclonal antibody raised against recombinant $\Delta 79$ -dOmi. As expected, DIAP1-bound dOmi fragments were isolated exclusively from the mitochondrial fraction (Fig. 3.7). We then prepared lysates from embryos (12 h), larvae (2nd instar), pupae, and adult flies, as well as S2 cells, and once again performed pulldown assays using GST-DIAP1. Intriguingly, we found that the expression of dOmi fluctuated depending upon the developmental stage of the flies. dOmi expression levels were initially high in embryos, but declined during the larval and pupal stages, only to rebound in the adult flies (Fig. 3.8). The observed changes in dOmi expression could not be accounted for by differences in total mitochondrial density, as cytochrome c levels were increased only in the adult flies (Fig. 3.8). We performed RT-PCR on total RNA isolated from each tissue sample and correspondingly observed that *domi* expression was slightly reduced in both larvae and pupae (Fig. 3.8). It is currently unclear why dOmi expression levels change during development, or if additional posttranslational modifications (*e.g.* ubiquitinylation) may also enhance its turnover.

A.

Δ79 dOmi	A I I Q	RED L T P
Δ92 dOmi	A S K M	T G R R R D
Reaper	A V A F	Y I P D Q A
Grim	A I A Y	F I P D Q A
Hid	A V P F	Y L P E G G
Sickle	A I P F	F E E E H A
Jafrac2	A K P E	D N E S C Y
Δ133 Omi	A V P S	P P P A S P
Δ55 Smac	A V P I	A Q K S E P

B.

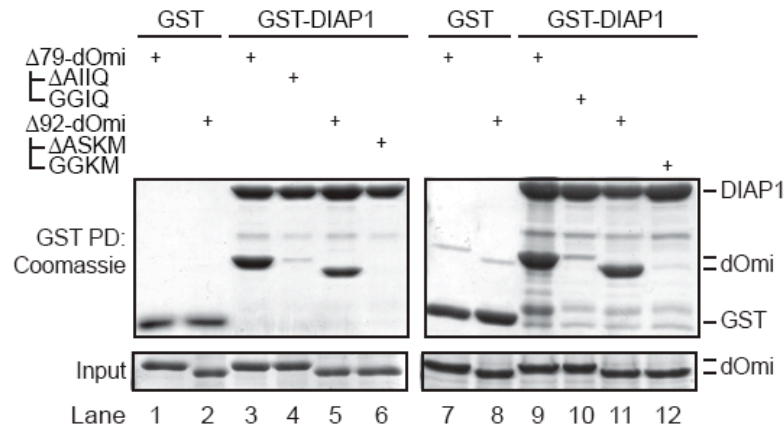


Figure 3.6 Mature dOmi binds DIAP1 via two distinct IBMs.

- (A) The IBMs in Δ79-dOmi and Δ92-dOmi were aligned with known IAP antagonists in *Drosophila* (Reaper, Grim, Hid, Sickle, Jafrac2) and humans (Δ133-hOmi, Δ55-Smac).
- (B) GST-DIAP1 pulldown assays were performed using recombinant Δ79-dOmi and Δ92-dOmi, as well as their corresponding IBM truncations (ΔAIIQ, ΔASKM) or point mutants (GGIQ, GGKM), respectively. Each of the dOmi proteins also contained an active-site mutation (S266A). Isolated protein complexes were separated by SDS-PAGE, and the gels were stained with Coomassie Blue.

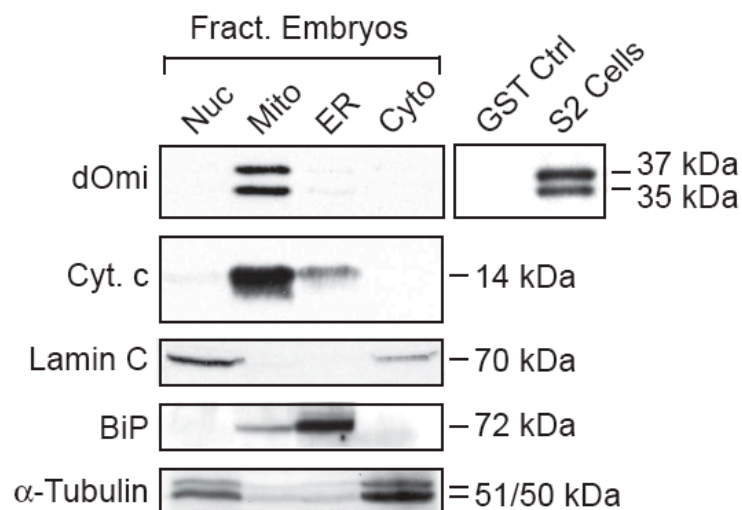


Figure 3.7 Processing of dOmi occurs in the mitochondria.

Subcellular fractions were isolated from fly embryo (12 h) lysates and incubated with GST-DIAP1. DIAP1 complexes from each fraction were then washed and immunoblotted for endogenous dOmi, using a rabbit polyclonal antibody raised against recombinant dOmi. Each fraction was also immunoblotted for cytochrome c, lamin C, BiP, and α -tubulin, in order to verify the purity of the fraction.

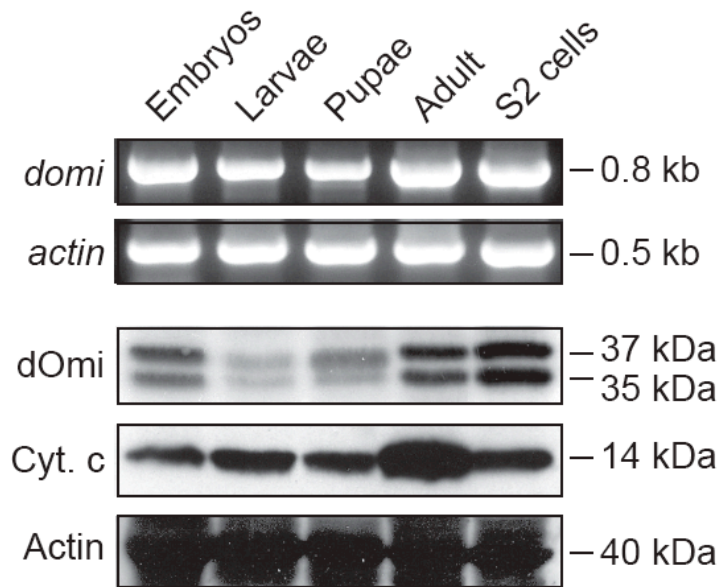


Figure 3.8 Expression of dOmi is developmentally regulated.

Lysates from embryos (12 h), larvae (2nd instar), pupae and adult flies were immunoblotted for cytochrome c and endogenous dOmi (as described in Fig. 3.6). Total RNA was also isolated at each developmental stage and subjected to RT-PCR for *domi* and *actin* (internal control).

3.2.4 Mature dOmi is released from mitochondria during apoptosis via caspase-dependent and -independent mechanisms. As previously noted, the role of mitochondria in fly apoptosis remains highly controversial, in part because some previous reports suggest that mitochondria do not undergo outer membrane permeabilization and that cytochrome c is not required for activation of the DARK•DRONC apoptosome complex (Dorstyn et al., 2004; Varkey et al., 1999; Zimmermann et al., 2002). Therefore, in order to determine if cytochrome c was released from mitochondria during apoptosis, we treated S2 cells with the general serine/threonine kinase inhibitor staurosporine (STS) or exposed them to DNA-damaging UVB irradiation. In each case, we observed the release of cytochrome c from mitochondria (Figs. 3.9G and H), a loss in mitochondrial membrane potential ($\Delta\psi_m$) (Figs. 3.9C and D), an increase in effector caspase DEVDase activity (Figs. 3.9E and F), and DNA fragmentation (SubG₁ peak) (Figs. 3.9A and B). Similarly, in cells transfected with full-length dOmi-myc, STS and UVB irradiation also stimulated the release of both $\Delta 79$ -dOmi and $\Delta 92$ -dOmi, along with cytochrome c (Fig. 3.10), and once in the cytosol, mature dOmi enhanced effector caspase DEVDase activity (Fig. 3.11). Correspondingly, in *loss-of-function* experiments, depletion of dOmi by RNA interference delayed caspase activation (Fig. 3.12).

Interestingly, pretreatment of cells with the pancaspase inhibitor Z-VAD-fmk inhibited all of the aforementioned events in UVB irradiated cells, including the release of cytochrome c and dOmi, but failed to do so in STS treated cells (Fig. 3.9, 3.10). Thus, depending upon the proapoptotic stimulus, both cytochrome c and dOmi were released from mitochondria *via* caspase-dependent and -independent mechanisms, the precise

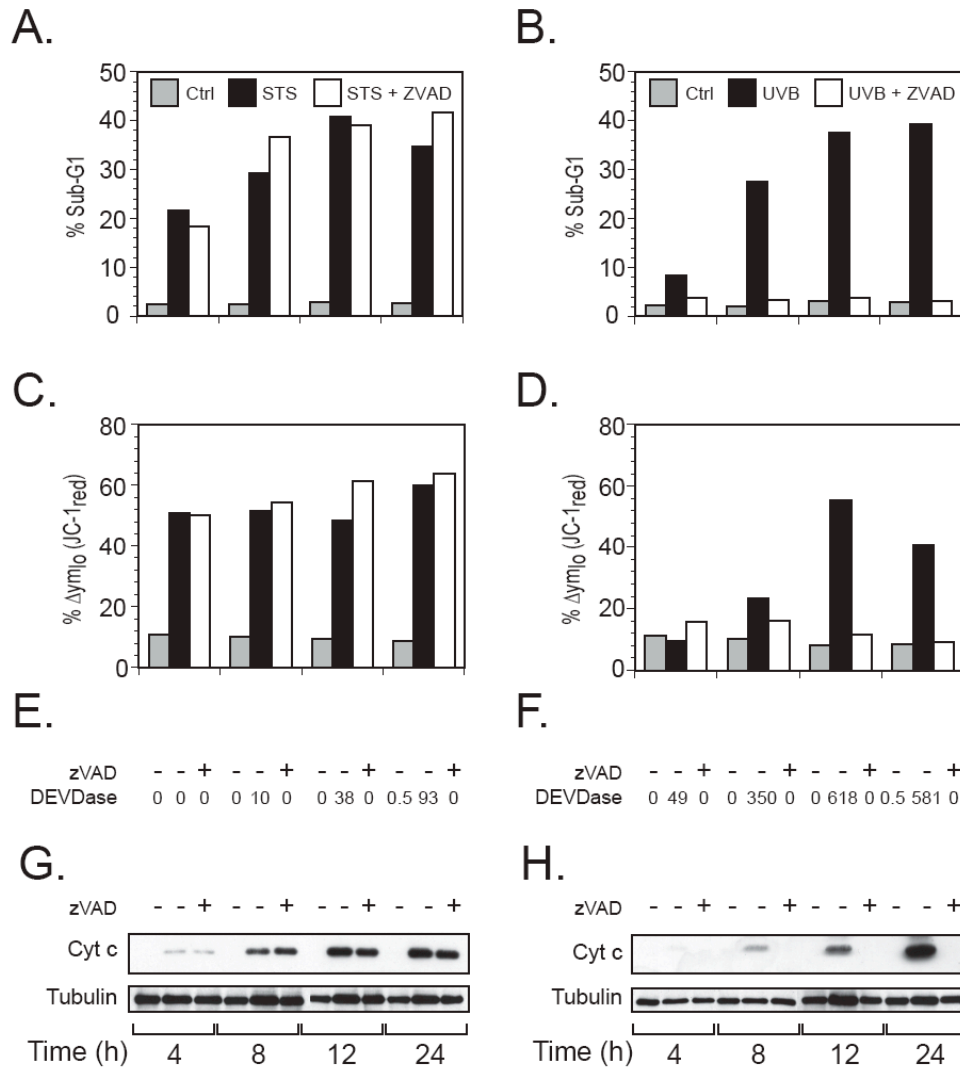


Figure 3.9 STS and UVB irradiation induce caspase-dependent and -independent MOMP in S2 cells.

S2 cells were exposed to STS (1 μ M) (A, C, E, and G) or UVB irradiation (5 min on a UV transilluminator) (B, D, F, and H), in the presence or absence of the pancaspase inhibitor Z-VADfmk (50 μ M). Cells were subsequently examined for $\Delta\Psi_m$ (JC-1 staining) (C and D) and DNA fragmentation (SubG1 peak) (A and B). In addition, cytosolic fractions were prepared and immunoblotted for cytochrome c (G and H) and assayed for effector caspase DEVDase activity (E and F).

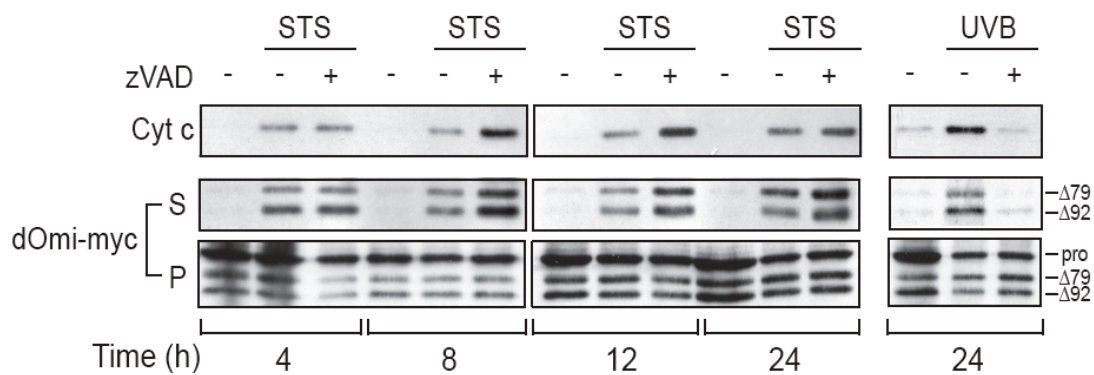


Figure 3.10 dOmi, similar to cytochrome c, is released into cytosol in a caspase-dependent and -independent manner in S2 cells.

S2 cells transfected with full-length dOmi were exposed to STS (1 μ M) or UVB irradiation (5 min on a UV transilluminator). Cells were lysed with digitonin and cytosolic fractions were isolated by differential centrifugation. We then examined for mitochondrial release of cytochrome c and dOmi into the cytosol by immunoblotting.

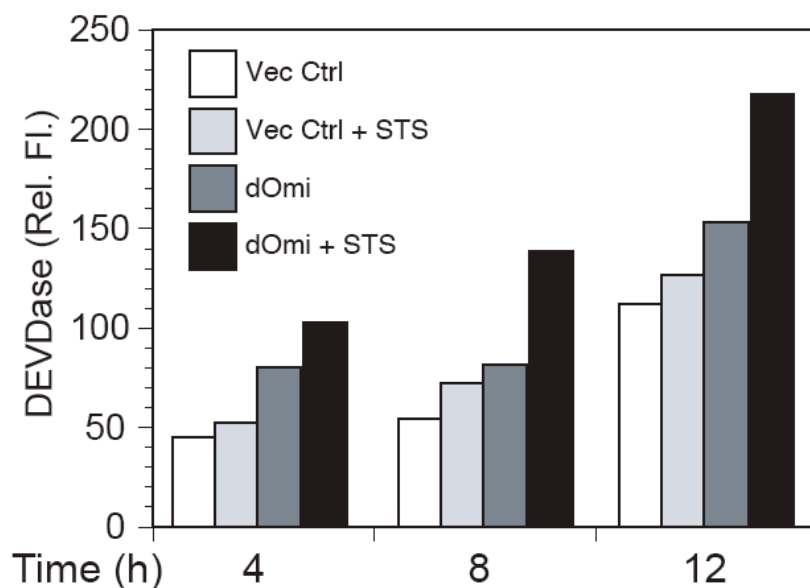


Figure 3.11 Overexpression of full-length dOmi sensitizes cells to STS treatment.

S2 cells were either transfected with a vector control or plasmid expressing full-length dOmi under the control of the metallothionein promoter. The expression of dOmi is induced by the addition of CuSO_4 (0.7 mM) to the culture medium. The cells were exposed to STS (1 μM) 24 hours after induction with CuSO_4 . Effector caspase DEVDase activity was measured at various time points as indicated by fluorometric assay.

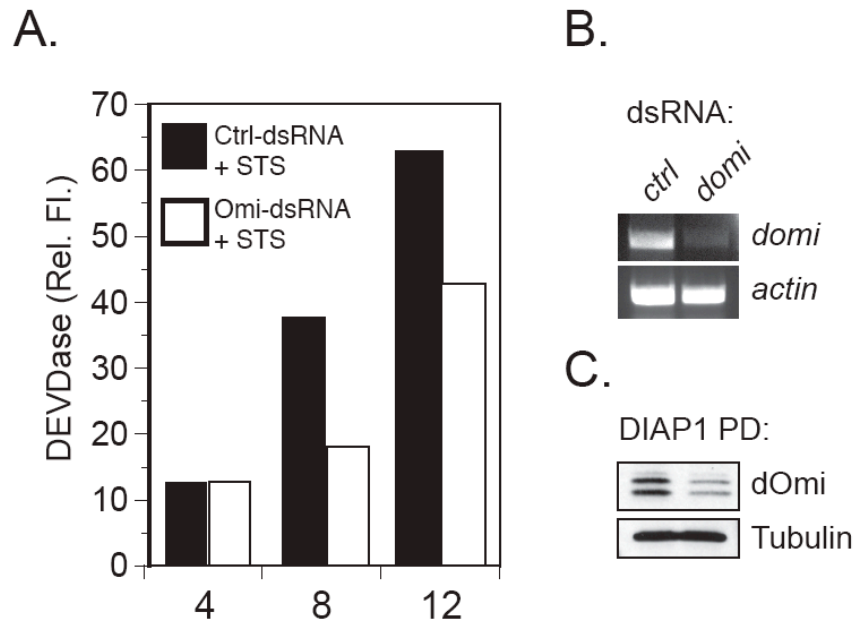


Figure 3.12 Knock down of dOmi by RNAi decreases the caspase activation after STS treatment.

- (A) S2 cells (0.3×10^6) were pretreated with control or *domi* dsRNA (40 nM) for 3 days, exposed to STS (1 μ M) for 4-12 h, and subsequently assayed for effector caspase DEVDase activity.
- (B) Levels of dOmi mRNA in control and dsRNA treated cells was measured by RT-PCR.
- (C) The effect of dsRNA on dOmi protein levels was analyzed by immunoblotting.

details of which remain to be elucidated. Notably, UVB irradiation selectively induces expression of DARK in early stage embryos (Zhou and Steller, 2003). Therefore, it is possible that DRONC, or perhaps its downstream targets, DrICE or DCP-1, may be required for MOMP in this context.

3.2.5 Mature dOmi induces cell death in S2 cells and in the developing fly eye, primarily through its serine protease activity.

Though dOmi was released from mitochondria during apoptosis, it remained unclear precisely how cytoplasmic dOmi might induce apoptosis in *Drosophila* cells. We therefore expressed mature $\Delta 79$ -dOmi or $\Delta 92$ -dOmi in the cytoplasm of S2 cells (Fig. 3.5) and found that both forms induced ~40% cell death by 48 h (Figs. 3.13A and E, WT vs. Vec Ctrl). Interestingly, however, the IBM mutants $\Delta 79$ -dOmi^{GGIQ} and $\Delta 92$ -dOmi^{GGKM} triggered similar levels of cell death compared to wild-type dOmi (Figs. 3.13A and B, WT vs. IBM Mt), despite their inability to bind DIAP1 (Fig. 3.6B). Moreover, mutation of dOmi's catalytic serine reduced cell death (Figs. 3.13A and C, WT vs. S266A), whereas removal of its regulatory PDZ domain (which provides greater access to its active-site) significantly enhanced cell death (Fig. 3.2A; Figs. 3.13A and D, WT vs. Δ PDZ). Thus, dOmi's serine protease activity appeared to be primarily responsible for inducing cell death in S2 cells. Pretreatment of cells with Z-VAD-fmk partially inhibited cell death induced by the catalytically-active forms (WT, Δ PDZ, IBM Mt) of dOmi (Figs. 3.13A, D, and B), indicating that dOmi's proteolytic activity could promote the activation of caspases and induce caspase-dependent apoptosis. However, dOmi, like its mammalian counterpart, also induced caspase-independent cell death (Hegde et al., 2002).

To determine if dOmi could induce cell death in the developing fly eye, we generated transgenic flies expressing wild-type $\Delta 79$ -dOmi (*GMR-gal4;UAS-domi $\Delta 79$ ^{wt}7B*), $\Delta 92$ -dOmi (*GMR-gal4;UAS-domi $\Delta 92$ ^{wt}5A*), or their catalytically-inactive S266A mutants (*GMR-gal4;UAS-dOmi $\Delta 79$ S266A4A* and *GMR-gal4;UAS-dOmi $\Delta 92$ S266A42A*). Interestingly, when compared to control flies, expression of $\Delta 79$ -dOmi and $\Delta 92$ -dOmi resulted in phenotypes ranging from organismal lethality at pupal stages to a rough eye (Figs. 3.14A and B). The effects of $\Delta 92$ -dOmi were consistently much stronger than $\Delta 79$ -dOmi (Fig. 3.14B), but as previously observed in S2 cells, expression of the catalytically inactive S266A dOmi mutants did not result in any phenotype (Fig. 3.14A). In contrast to the effects of Z-VAD-fmk in S2 cells, expression of the baculoviral caspase inhibitor p35 did not inhibit cell death induced by $\Delta 79$ -dOmi or $\Delta 92$ -dOmi (Fig. 3.14A; data not shown). GMR-driven expression of dOmi in the fly eye however occurred over an ~4 day period throughout pupal development, whereas the effects of dOmi expression in S2 cells were examined after 1-2 days. Thus, dOmi could promote caspase-dependent apoptosis *via* its serine protease activity, but in the long term did not require caspase activity in order to induce cell death.

3.2.6 The IBMs in dOmi interact selectively with the BIR2 domain in DIAP1 and displace the initiator caspase DRONC. Rpr, Hid, Grim, Sickie and Jafrac2 all reportedly induce apoptosis in the fly by interacting with and displacing the effector caspase DrICE from the BIR1 domain in DIAP1 and/or the initiator caspase DRONC from the BIR2 domain (Chai et al., 2003a; Yan et al., 2004b; Zachariou et al., 2003).

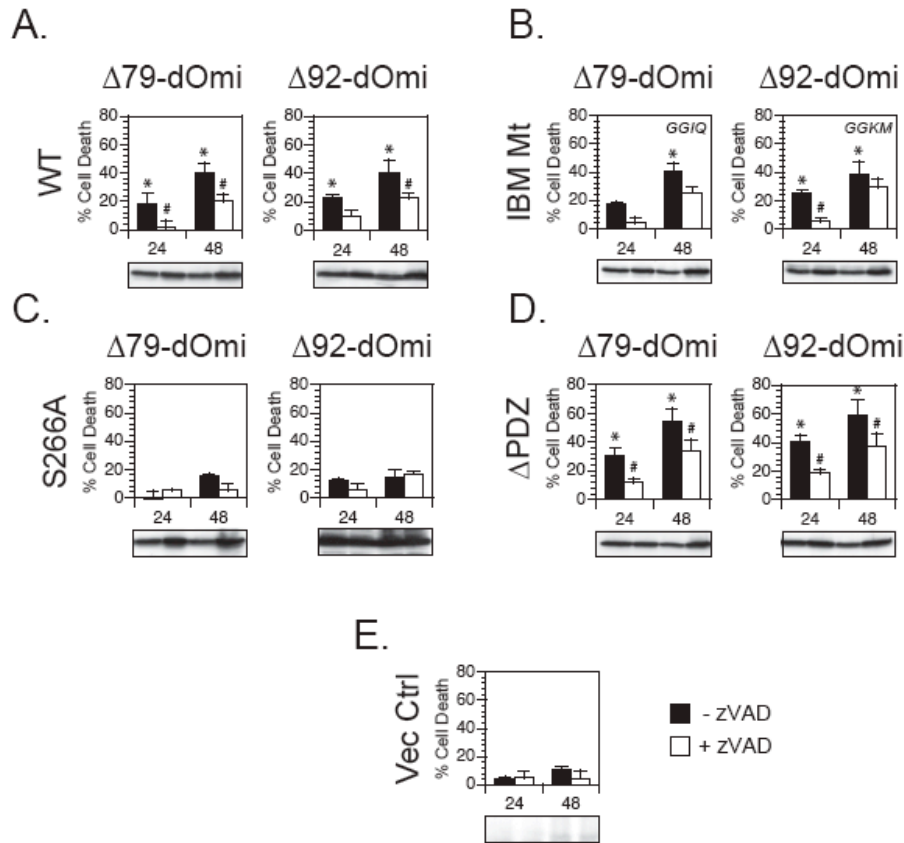
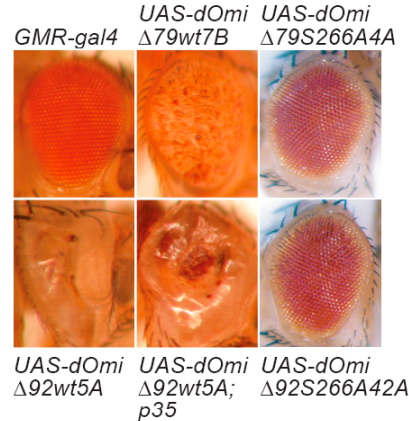


Figure 3.13 Mature dOmi induces cell death in S2 cells.

S2 cells were cotransfected with expression plasmids for EGFP and wild-type dOmi ($\Delta 79$ -dOmi, $\Delta 92$ -dOmi) (A), or various IBM mutants ($\Delta 79$ -dOmi^{GGIQ}, $\Delta 92$ -dOmi^{GGKM}) (B), catalytically-inactive mutants ($\Delta 79$ -dOmi^{S266A}, $\Delta 92$ -dOmi^{S266A}) (C), PDZ truncation mutants ($\Delta 79$ -dOmi^{APDZ}, $\Delta 92$ -dOmi^{APDZ}) (D), or vector control (E). All dOmi constructs were expressed under the control of the metallothionein promoter by adding CuSO₄ (0.7 mM) to the culture medium, in the presence and absence of Z-VAD-fmk (50 μ M). Cell death was assessed by determining the percent of GFP⁺ cells remaining at 24 and 48 h. For statistical analyses, ANOVA was performed, along with a *Student-Newman-Keuls* posthoc analysis (StatView software): *, significantly different from the Vec Ctrl (p<0.05); #, significantly different from cells not treated with Z-VAD-fmk (p<0.05).

A.



B.

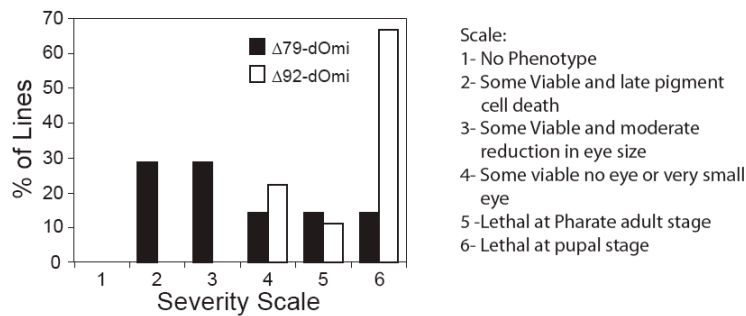


Figure 3.14 Mature dOmi causes eye ablation phenotype when expressed in *Drosophila* eye.

- (A) Expression of $\Delta 79$ -dOmi resulted in phenotypes ranging from early pupal lethality in some lines to a mild, slightly rough eye in other lines (as shown: *GMR-gal4/+; UAS- $\Delta 79$ -dOmi7B*). Expression of $\Delta 92$ -dOmi resulted in consistently stronger phenotypes, ranging from early pupal lethality in some lines to eyeless flies in other lines (as shown: *GMR-gal4/+; $\Delta 92$ -dOmi5A/+*). Co-expression of the baculoviral caspase inhibitor p35 failed to significantly inhibit cell death induced by $\Delta 79$ -dOmi or $\Delta 92$ -dOmi (as shown: *GMR-gal4/UAS-p35; $\Delta 92$ -dOmi5A/+*), and expression of the catalytically-inactive dOmi mutants failed to induce cell death (as shown: *GMR-gal4/+; UAS- $\Delta 79$ -dOmiS266A4A* and *GMR-gal4/+; UAS- $\Delta 92$ -dOmiS266A 42A*).
- (B) Transgenic lines were crossed to *GMR-gal4* and scored for phenotype based on the scale. Nine independent lines were scored for $\Delta 92$ -dOmi and seven for $\Delta 79$ -dOmi, and each line was tested at least twice and produced at least 10 flies with the same phenotype. Expression of $\Delta 92$ -dOmi consistently resulted in a more severe phenotype ($p < 0.02$, student T test).

Therefore, since dOmi clearly bound to DIAP1 in an IBM-dependent manner (Fig. 3.6B), it was surprising that this interaction alone failed to induce significant amounts of apoptosis in S2 cells or in the developing fly eye (Figs. 3.13A and E, S266 vs. Vec Ctrl; data not shown). In order to resolve this dilemma, we sought to further characterize dOmi's interaction with DIAP1, as well as its role in promoting caspase activation. We began by expressing various DIAP1 truncation mutants as GST fusion proteins and subsequently performed pulldown assays using naïve S2 cell lysates (Figs. 3.15A and B). Importantly, the BIR2 domain in DIAP1 was found to be essential for binding both processed forms of endogenous dOmi, whereas neither the BIR1 nor the RING domains were required (Fig. 3.15B).

Given that dOmi failed to bind BIR1, we predicted that it would be unable to antagonize BIR1-dependent inhibition of DrICE. To provide definitive proof, we incubated recombinant DrICE with its substrate PARP, either alone or in the presence of GST-BIR1. At its approximate IC_{50} , GST-BIR1 inhibited DrICE-mediated cleavage of PARP by ~50% (Figs. 3.17A and B, lanes 1-3). As expected, this inhibition was readily overcome by a Rpr peptide, matching its N-terminal IBM (Rpr-IBM; AVAFYIPD), but not by a control peptide (MKSDFYFQ) (Fig. 3.17B, lanes 4 and 6). More importantly, however, neither recombinant $\Delta 79$ -dOmi, $\Delta 92$ -dOmi, nor their IBM truncation mutants (Δ AIIQ or Δ ASKM) promoted DrICE-dependent cleavage of PARP (Fig. 3.17A, lanes 4-7). Moreover, unlike Rpr-IBM, the IBM peptide of $\Delta 79$ -dOmi (AIIQREDL) also failed to antagonize BIR1-dependent inhibition of DrICE (Fig. 3.17B, lanes 4-5). To determine why dOmi failed to displace DrICE, we modeled the $\Delta 79$ -IBM into the BIR1 binding

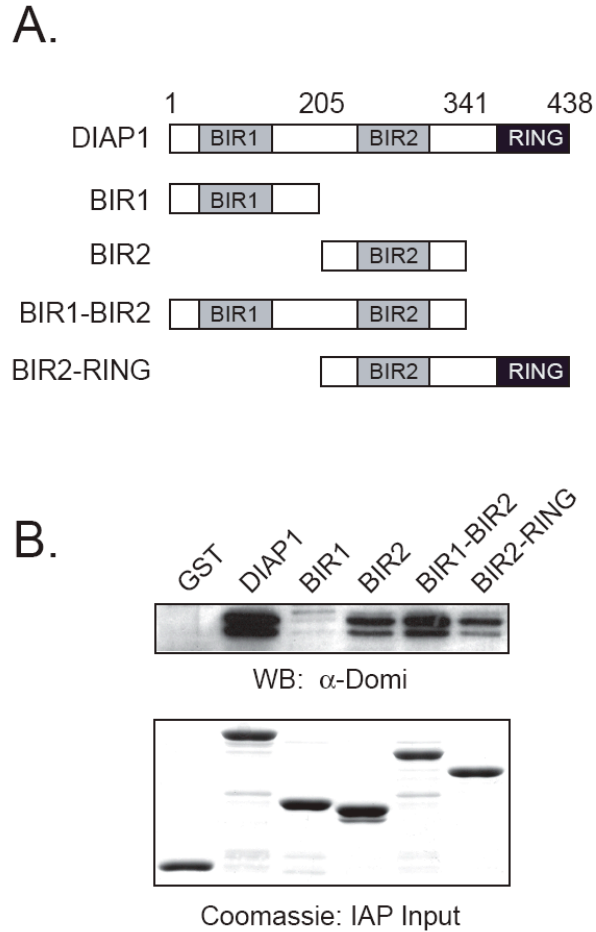
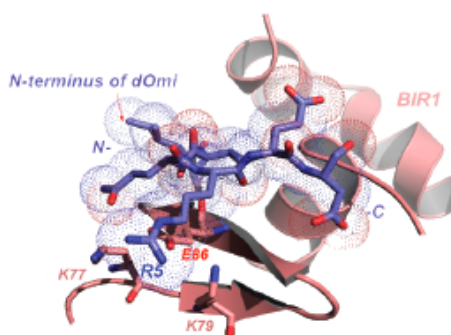


Figure 3.15 Mature dOmi binds to the BIR2 domain in DIAP1.

- (A) Schematic representing GST-DIAP1 and truncation mutants.
- (B) Proteins of GST-DIAP1 and various truncation mutants were expressed in bacteria and purified to homogeneity. The proteins (500 nM) were then captured using GSH-sepharose beads and incubated (3 h at 4°C) with naïve S2 cell lysates (100 μ g) in a final volume of 300 μ L. The bead complexes were subsequently isolated, separated by SDS-PAGE, and immunoblotted using a rabbit anti-dOmi polyclonal antibody.

A.



B.

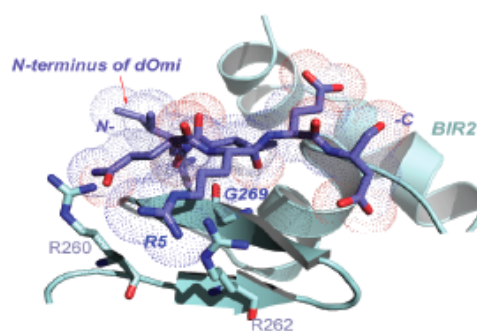
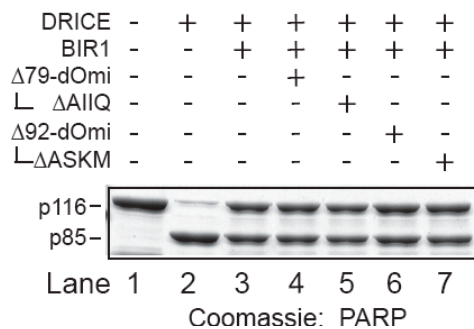


Figure 3.16 The IBM of $\Delta 79$ -dOmi shows exhibits differential binding to the BIR1 and BIR2 domains of DIAP1.

Structural modeling representing the binding of $\Delta 79$ -IBM to BIR1 (A) and BIR2 domains (B) in DIAP1 was done by using the previously solved crystal structures of BIR1:Rpr-IBM and BIR2:Hid-IBM.

A.



B.

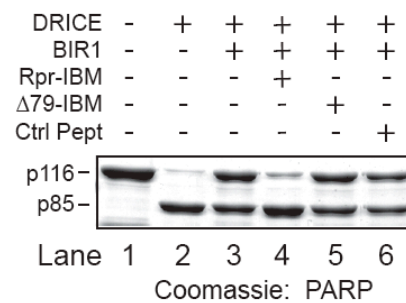


Figure 3.17 Mature dOmi cannot displace BIR1 domain bound active DrICE.

- (A) Recombinant DrICE (175 nM) was preincubated with or without GST-BIR1 (*inhibitor*; 3.5 μ M) for 30 min at 25°C. Human PARP (*substrate*, 5.75 μ M) was then added alone, or in combination with recombinant $\Delta 79$ -dOmi, $\Delta 92$ -dOmi, or the IBM truncation mutants (Δ AIHQ, Δ ASKM) (4.5 μ M), and further incubated for 60 min at 25°C. All protein complexes were separated by SDS-PAGE, and the gels stained with Coomassie Blue.
- (B) DrICE displacement was also analyzed by using $\Delta 79$ -IBM peptide and the positive control, Rpr-IBM peptide (5 μ g), in separate incubations.

pocket of DIAP1, using the previously solved crystal structure for BIR1 bound to Rpr-IBM (PDB code: 1SDZ) (Yan et al., 2004b). As shown in Fig. 3.16A, Arg5 in dOmi appeared to sterically clash with Glu86 in the bottom of the BIR1 pocket, thus preventing $\Delta 79$ -dOmi from forming a stable complex with BIR1.

Since mature dOmi bound to the BIR2 domain in DIAP1 (Fig. 3.15B), we predicted that dOmi might displace the initiator caspase DRONC from the BIR2 binding pocket. We therefore incubated GST-BIR2-RING with an N-terminal fragment of DRONC (1-139) and observed the formation of a BIR2-RING•DRONC complex (Fig. 3.18A, lanes 1 and 10), consistent with a previous report (Chai et al., 2003a). As expected, addition of $\Delta 79$ -dOmi or $\Delta 92$ -dOmi to the incubation mixture resulted in a concentration-dependent displacement of DRONC from the complex (Fig. 3.18A, lanes 2-5 and 11-14), with $\Delta 79$ -dOmi displaying a higher affinity for BIR2-RING compared to $\Delta 92$ -dOmi ($K_d \sim 0.27 \mu\text{M}$ vs. $\sim 1.18 \mu\text{M}$) (Table 3.1). By contrast, neither of the IBM truncation mutants (ΔAIIQ or ΔASKM) bound to BIR2-RING or displaced DRONC (Fig. 3.18A, lanes 6-9 and 15-18). In additional experiments, the Rpr-IBM peptide also displaced DRONC from the BIR2 binding pocket (Fig. 3.18B), with an affinity similar to that reported for the Hid-IBM ($K_d \sim 0.036 \mu\text{M}$ vs. $0.041 \mu\text{M}$) (Table 3.1). Thus, in our assays, Rpr was ~ 7 -fold more potent than $\Delta 79$ -dOmi at displacing DRONC (Table 3.1) (Wu et al., 2001). Nevertheless, the affinity of $\Delta 79$ -dOmi for DIAP1-BIR2 was ~ 3 -fold higher than that reported for DRONC (Table 3.1) (Chai et al., 2003a). Moreover, by comparison, the affinity of $\Delta 79$ -dOmi for DIAP1-BIR2 was higher than that reported for Smac with XIAP-BIR3 (Liu et al., 2000), which is compelling given that DRONC and

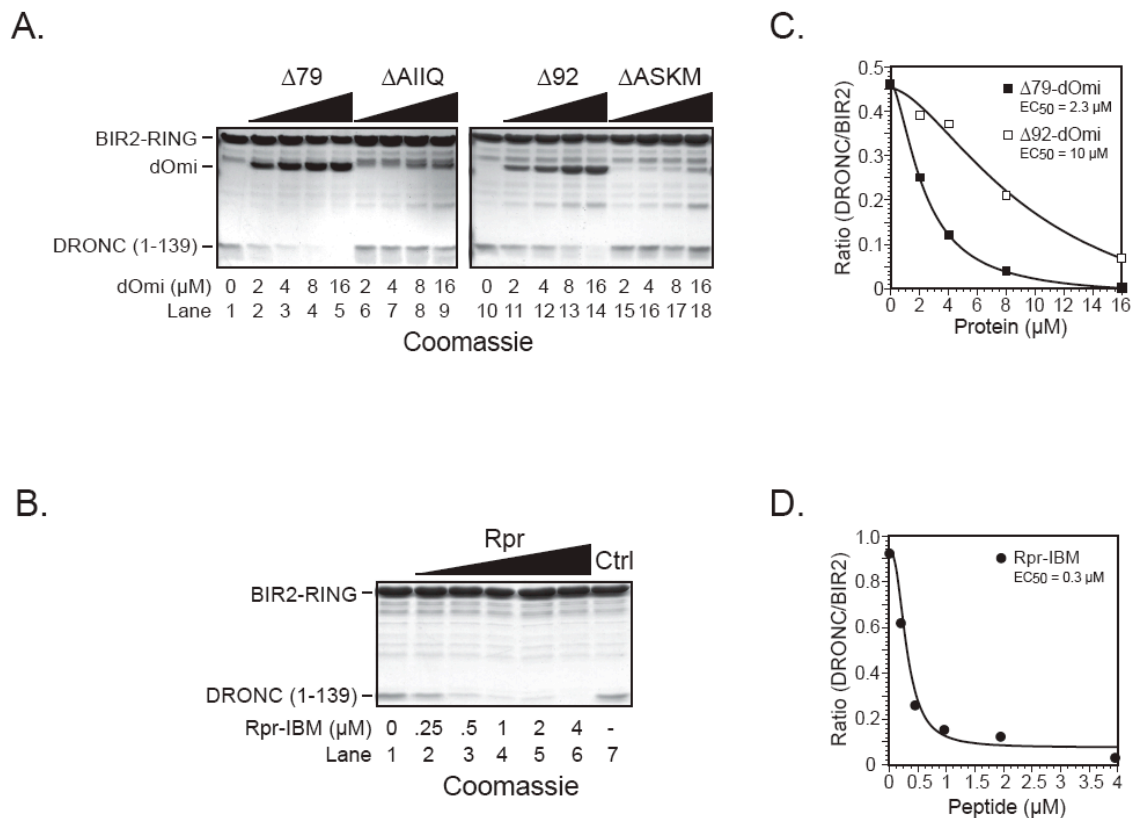


Figure 3.18 Mature dOmi displaces the BIR2 domain bound initiator caspase DRONC.

GST-BIR2-RING (3 μM) was incubated with an N-terminal fragment of DRONC (6 μM), in the absence or presence of the Rpr-IBM peptide (0-4 μM) (B), recombinant $\Delta 79$ -dOmi, $\Delta 92$ -dOmi, or their corresponding IBM mutants ($\Delta AIIQ$, $\Delta ASKM$) (A) (2-16 μM). The dOmi proteins also contained an active-site mutation (S266A) to ensure that dOmi's proteolytic activity did not interfere with the displacement of DRONC. Displacement curves were plotted to determine the EC_{50} values for each of the Rpr-IBM peptide and dOmi proteins (C and D). All protein complexes were then separated by SDS-PAGE, and the gels were stained with Coomassie Blue.

IAP antag. / Caspase	K_d (μ M)	
	DIAP1-BIR2	XIAP-BIR3
Δ 79-dOmi	0.27 ^a	
Δ 92-dOmi	1.18 ^a	
Reaper	0.036 ^a	
Hid	0.041 ^b	
DRONC	0.80 ^b	
Smac		0.42 ^c
Caspase-9		0.74 ^c

Table 3.1 The IBM of mature dOmi has less affinity towards BIR2 domain in DIAP1 relative to Rpr-IBM.

The dissociation constants for specific fly and mammalian IAP antagonists and initiator caspases with their respective IAPs were compared. The dissociation constants of Δ 79-IBM, Δ 92-IBM, and Rpr-IBM were calculated using Cheng-Prusoff equation and the EC_{50} values were obtained from Fig. 3.19C and D (a). Other K_d values were obtained from *Chai, et al.* (b) and *Liu, et al.* (c) and used for comparison.

caspase-9 exhibit virtually identical binding affinities for their respective IAPs (Table 3.1).

The reasons for the selectivity of $\Delta 79$ -dOmi for BIR2 over BIR1 were subsequently revealed through modeling studies, using the solved crystal structure of BIR2 bound to Hid-IBM (PDB code: 1JD6) (Wu et al., 2001) (Fig. 3.16B). Indeed, the steric clash observed between Arg-5 in $\Delta 79$ -dOmi and Glu-86 in BIR1 (Fig. 3.16A) did not exist in the BIR2 model, as Glu-86 is replaced by a glycine in the analogous position (Gly269) (Fig. 3.16B). Arg-5 appeared to exhibit some electro-repulsion with Arg-260 and Arg-262 in BIR2, and thus may account for the reduced affinity of $\Delta 79$ -dOmi for BIR2 compared to Rpr and Hid (Table 3.1 and Fig. 3.16B). Collectively, the biochemical and structural data indicate that $\Delta 79$ -dOmi can selectively displace DRONC from the BIR2 domain in DIAP1. However, this interaction is insufficient, on its own, to induce significant levels of cell death, perhaps because the BIR1 domain retains its ability to inhibit the effector caspase, DrICE. Indeed, we have previously shown in human cells that the linker-BIR2 domain in XIAP can inhibit the effector caspase-3 and prevent cell death, even when mutations in its BIR3 domain prevent inhibition of the initiator caspase-9 (Bratton et al., 2002).

3.2.7 dOmi alleviates DIAP1 inhibition of caspases by proteolytically degrading DIAP1. Though wild-type dOmi clearly induced cell death in both S2 cells and the developing fly eye *via* its serine protease activity, it remained unclear precisely how this led to caspase activation. hOmi proteolytically degrades certain IAPs in mammalian

cells, including cIAP1, cIAP2 and Bruce/Apollon (Jin et al., 2003; Yang et al., 2003), raising the possibility that dOmi might indirectly increase caspase activity, at least in part, by degrading DIAP1. We therefore examined the effects of dOmi on the expression levels of DIAP1 in S2 cells. As shown in Fig. 3.19A, DIAP1 was largely absent from cells when coexpressed with wild-type $\Delta 79$ -dOmi, $\Delta 92$ -dOmi, or the IBM mutants (lanes 2, 4, 5, and 7), whereas DIAP1 was readily detected in cells coexpressing the catalytically-inactive S266A mutants (lanes 3 and 6). Thus, dOmi's proteolytic activity was responsible for mediating the loss in DIAP1, independent of its IBMs. We next incubated recombinant dOmi with DIAP1 (immunoprecipitated from transfected S2 cells) and found that both $\Delta 79$ -dOmi and $\Delta 92$ -dOmi directly degraded DIAP1 in a concentration-dependent manner (Fig. 3.19B). However, it was difficult to visualize many of the DIAP1 fragments, due to proteolytic removal of the HA tag. Therefore, we repeated our *in vitro* cleavage assay by incubating recombinant dOmi with GST-DIAP1 that was first purified and then biotinylated. Under these conditions, dOmi once again proteolytically processed DIAP1 into numerous fragments that were readily visualized by blotting with streptavidin-HRP (Fig. 3.19C).

As previously noted, a number of recent studies have suggested that other IAP antagonists in the fly may stimulate DIAP1 autoubiquitinylation and target DIAP1 for destruction by the 26S proteasome (Hays et al., 2002; Holley et al., 2002; Ryoo et al., 2002; Wing et al., 2002b). dOmi, on the other hand, did not appear to induce DIAP1 autoubiquitinylation, since neither $\Delta 79$ -dOmi^{S266A} nor $\Delta 92$ -dOmi^{S266A} induced a loss in DIAP1, when coexpressed in S2 cells (Fig. 3.21A, lanes 1, 3 and 6). Furthermore, in

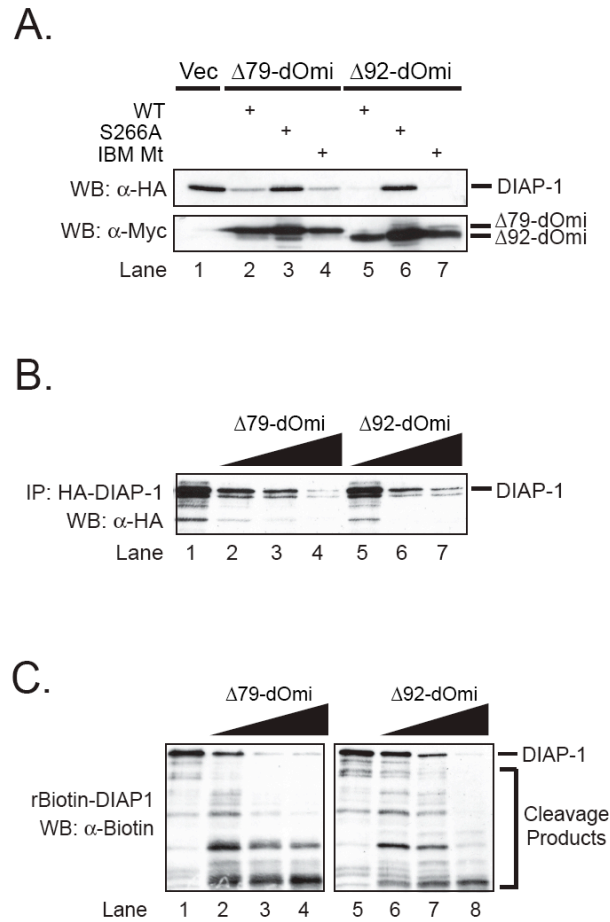


Figure 3.19 dOmi proteolytically degrades DIAP1.

- (A) S2 cells were cotransfected with pIE1-HA-DIAP1, along with pRmHa3-dOmi ($\Delta 79$ -dOmi, $\Delta 92$ -dOmi), catalytically inactive mutants of dOmi ($\Delta 79$ -dOmi^{S266A}, $\Delta 92$ -dOmi^{S266A}) or IBM mutants of dOmi ($\Delta 79$ -dOmi^{GGIQ}, $\Delta 92$ -dOmi^{GGKM}). Following the addition of CuSO₄ (0.7 mM) to induce expression of dOmi and its mutants, whole cell lysates were immunoblotted for DIAP1 and dOmi expression levels.
- (B) HA-DIAP1 was expressed in S2 cells and immunoprecipitated using an anti-HA antibody (262K, Cell Signaling). The immunoprecipitates were then incubated with wild-type $\Delta 79$ -dOmi or $\Delta 92$ -dOmi (50-200 nM) for 2 h at 37°C and subsequently immunoblotted for HA-DIAP1.
- (C) Biotinylated GST-DIAP1 (250 ng) was incubated with recombinant $\Delta 79$ -dOmi or $\Delta 92$ -dOmi (50-200 nM) for 2 h at 37°C in a total volume of 30 μ L and subsequently immunoblotted with streptavidin-HRP.

subsequent *in vitro* assays using fly embryo lysates, neither recombinant dOmi, nor the $\Delta 79$ -IBM peptide, enhanced (or suppressed) the basal level of DIAP1 autoubiquitylation (data not shown). Thus, dOmi promoted caspase activity and cell death, at least in part by ridding the cell of DIAP1. However, dOmi accomplished this feat, not by stimulating DIAP1 autoubiquitylation, but rather by directly degrading DIAP1.

3.3 Discussion

The role of mitochondria in fly apoptosis remains highly controversial, due in large part to disagreement over whether mitochondria undergo losses in $\Delta\psi_m$ and MOMP following stress (Dorstyn et al., 2004; Kanuka et al., 1999b; Senoo-Matsuda et al., 2005; Zimmermann et al., 2002). Moreover, while mitochondrial release of cytochrome c in mammalian cells initiates formation of the Apaf-1 apoptosome complex and activation of caspases (Cain et al., 2002), there is disagreement over the importance of cytochrome c for promoting cell death in flies (Arama et al., 2003; Arama et al., 2006; Dorstyn et al., 2004; Mendes et al., 2006; Zimmermann et al., 2002). The cytochrome c debate notwithstanding, there are additional mitochondrial proteins in mammals that play a role in promoting apoptosis, including the dual IAP antagonist and serine protease, Omi/HtrA2 (Hegde et al., 2002; Martins et al., 2002; Suzuki et al., 2001a; Verhagen et al., 2002). In our studies, we set out to determine if the *Drosophila* homologue of Omi might likewise participate in cell death. We found that dOmi was highly homologous to hOmi, particularly within the serine protease domain and that its expression was developmentally regulated. dOmi was imported into fly mitochondria and processed *in*

situ, resulting in the removal of its MTS and exposure of two distinct IBMs. The mature forms of dOmi were then released into the cytoplasm following stress, through both caspase-dependent and independent processes. However, once in the cytosol, dOmi induced cell death in S2 cells and in the developing fly eye, primarily through proteolytic degradation of DIAP1 and likely other substrates.

Indeed, catalytically inactive $\Delta 79$ -dOmi^{S266A} and $\Delta 92$ -dOmi^{S266A} failed to induce significant apoptosis, which was somewhat surprising given that both forms of dOmi selectively bound to the BIR2 domain in DIAP1 and displaced the initiator caspase DRONC. In particular, the affinity of $\Delta 79$ -dOmi for BIR2 ($K_d \sim 0.27 \mu\text{M}$) was lower than that observed for Rpr-IBM ($K_d \sim 0.036 \mu\text{M}$), but was slightly higher than that observed for mature Smac with XIAP-BIR3 ($K_d \sim 0.42 \mu\text{M}$) (Liu et al., 2000; Wu et al., 2001). So why did dOmi require its proteolytic activity to induce cell death, rather than inducing rapid IBM-dependent apoptosis? Notably, unlike other fly IAP antagonists, which exhibit partial preference for either the BIR1 or BIR2 domains, dOmi completely failed to bind the BIR1 domain in DIAP1 and did not displace the active effector caspase DrICE. Thus, it is possible that the continued inhibition of DrICE by DIAP1 was sufficient to inhibit cell death. There is precedence for such a scenario in mammals, as we have previously shown that XIAP mutants that fail to bind and inhibit caspase-9 can still prevent apoptosis through inhibition of caspase-3 alone (Bratton et al., 2002).

One of the primary differences between fly and mammalian IAP antagonists relates to their abilities to independently induce apoptosis. Indeed, Rpr, Hid, and Grim induce robust cell death in both cultured cells and flies (Kornbluth and White, 2005),

whereas overexpression of mature Smac in the cytoplasm of mammalian cells generally fails to induce apoptosis in the absence of an accompanying prodeath stimulus (Creagh et al., 2004; Du et al., 2000). A potential explanation for these results may involve their relative capacities to induce RING-dependent autoubiquitinylation upon binding to IAPs. Indeed, while many IAP antagonists in the fly induce DIAP1 autoubiquitinylation, Smac appears to suppress XIAP autoubiquitinylation (Creagh et al., 2004). In our studies, dOmi failed to induce or suppress DIAP1 autoubiquitinylation upon binding to its BIR2 domain. Thus, in the absence of dOmi's proteolytic activity, DIAP1 may again be free to maintain its inhibition of DrICE *via* its BIR1 domain. By contrast, given that DIAP1 can protect cells by targeting active DRONC for proteosomal degradation, it is also plausible that DIAP1 might regulate cell death in part by promoting the turnover of dOmi. Hay and colleagues have previously reported that the DIAP1-binding mutant, DRONC (F118E), induces significantly more cell death than wild-type DRONC, when expressed in the developing fly eye (Chai et al., 2003a), and correspondingly, we found that $\Delta 92$ -dOmi consistently produced a more severe phenotype than $\Delta 79$ -dOmi, in accordance with their relative affinities for DIAP1.

Others have reconciled such differences between the mammalian and fly IAP antagonists by arguing that, in contrast to the Apaf-1•caspase-9 apoptosome complex, the DARK•DRONC apoptosome complex is constitutively active. Consequently, DIAP1 is required to continuously ubiquitinylate DRONC and mediate its turnover in order to prevent cell death (Muro et al., 2002). In this model, Rpr, Hid, or Grim need only displace this active DRONC in order to promote the activation of effector caspases and

induce apoptosis. However, recent studies suggest that, at least for Rpr and Grim, the C-terminus of these IAP antagonists play important roles in promoting both mitochondrial injury and/or inhibition of protein translation (Claveria et al., 2002; Holley et al., 2002). These alternative functions for Rpr and Grim may be necessary to first initiate caspase activation, after which the IBMs serve to displace these active caspases from DIAP1. Therefore, it could be that binding of dOmi to DIAP1-BIR2 *per se* does not induce apoptosis, because in the absence of another stimulus, there may be very little active DRONC to displace. In any event, regardless of whether dOmi induces cell killing solely through its proteolytic activity, or functions as a pure IAP antagonist in certain contexts, our studies suggest that mitochondria may play a far more important role in apoptosis in the fly than previously thought.

Chapter 4: Caspase cleavage of DIAP1 promotes N-end rule-dependent *trans*-ubiquitination and degradation of the IAP antagonist Grim

4.1 Introduction

Apoptosis is an evolutionarily conserved process required during development and for maintaining normal tissue homeostasis (Budihardjo et al., 1999). A group of cysteinyl aspartate-specific proteases (caspases) are the chief executioners of apoptosis. In response to apoptotic stimuli, the initiator caspases that are distinguished by the presence of long prodomains are activated. Active initiator caspases cleave and thereby activate downstream effector caspases, which in turn cleave several cellular substrates thus leading to apoptosis (Riedl and Salvesen, 2007). IAPs are one of the key regulators of apoptosis and modulate cell death by inhibiting caspase activity. In general, IAPs are defined by the presence of one or more BIR domains, which are required for their interactions with proapoptotic proteins like caspases. Most IAPs also have a C-terminal RING-domain which functions as an E3 ligase (Salvesen and Duckett, 2002). The inhibition of caspase activity by IAPs is neutralized by IAP antagonists, which are characterized by the presence of an N-terminal tetra-peptide IAP binding motif (IBM). IAP antagonists negate the function of IAPs by binding to the BIR domains and thereby displacing the bound caspases (Vaux and Silke, 2003).

In *Drosophila*, the initiator and effector caspases, Dronc and DrICE, respectively, play important roles in regulating apoptosis (Fraser et al., 1997; Quinn et al., 2000). The *Drosophila* IAP 1(DIAP1), which contains two BIR domains and a C-terminal RING domain, regulates the activity of caspases (Kaiser et al., 1998; Meier et al.,

2000)(Illustration 1.4). Animals null for DIAP1 show increased caspase activation and exhibit embryonic lethality (Hay et al., 1995; Yoo et al., 2002). Similarly, RNAi of DIAP1 in *Drosophila* S2 cells triggers spontaneous and unrestrained caspase activation resulting in massive apoptosis (Yokokura et al., 2004; Zimmermann et al., 2002). DIAP1 binds through its BIR2 domain to Dronc and induces RING-dependent ubiquitination and degradation of Dronc (Chai et al., 2003a; Wilson et al., 2002). Consequently, cell death caused by over expression of Dronc is enhanced in a DIAP1-RING domain mutant background (Wilson et al., 2002). DIAP1 also inhibits the activity of effector caspases such as DrICE and DCP-1 by binding through its BIR1 domain (Tenev et al., 2005; Yan et al., 2004b). The pro-apoptotic IAP antagonists Reaper (Rpr), Hid, and Grim (RHG proteins) remove the inhibition of caspases by DIAP1 (Wang et al., 1999). The RHG proteins, through their N-terminal IBMs, bind to the BIR domains in DIAP1 and displace the bound caspases (Chai et al., 2003a; Tenev et al., 2005; Yan et al., 2004b; Zachariou et al., 2003). The RHG proteins can displace caspases bound to the BIR domains because they exhibit higher affinity for binding DIAP1. The RHG proteins exhibit differential interactions with the BIR1 and BIR2 domains of DIAP1 (Zachariou et al., 2003). Reaper and Grim can bind to both the BIR domains of DIAP1, whereas Hid preferentially binds to the BIR2 domain (Yan et al., 2004b; Zachariou et al., 2003) (Illustration 1.4). DIAP1 in turn regulates the function of the RHG proteins through its RING domain. When bound to DIAP1, the RHG proteins are subjected to ubiquitin-mediated degradation by the RING domain (Olson et al., 2003b).

The RING domain of DIAP1, apart from regulating the levels of RHG proteins,

also plays an important role in maintaining its own stability. Similar to other RING domain containing proteins, DIAP1 undergoes autoubiquitination in a RING domain-dependent manner (Yoo et al., 2002). The autoubiquitination rates are further enhanced upon binding of the RHG proteins to the DIAP1 (Ryoo et al., 2002; Yoo et al., 2002). In addition to autoubiquitination, DIAP1 levels are also regulated by the N-end rule-degradation (NERD) pathway (Ditzel et al., 2003). In the NERD pathway, the stability of a protein is determined, based upon the amino acid residue present at the N-terminus (Varshavsky, 2003). In case of DIAP1, effector caspase-mediated cleavage at Asp-20 leads to the exposure of an unstable residue (Asn 21) at the N-terminus, making it a substrate (N-degron) of NERD pathway (Ditzel et al., 2003). Through sequential action of N-terminal aminohydrolase (NTAN1) and Arg-RNA protein transferase (Ate1), the Asn is converted to Asp, followed by conjugation to an Arg residue. DIAP1 with the N-terminal Arg is presumably recognized by an E3 ligase, such as Ubr1 (also called N-recogin), which is required for the NERD pathway, and a proteasome-dependent degradation of the substrate (Ditzel et al., 2003; Varshavsky, 2003) (Illustration 1.6).

The NERD pathway not only reduces the stability of DIAP1 but also regulates the anti-apoptotic function of DIAP1 (Ditzel et al., 2003). Animals deficient for *NTAN1* and *Ate1*, the loci encoding the enzymes essential for the NERD pathway, show reduced cell death upon over expression of Hid under the GMR promoter. Surprisingly, disruption of the N-end rule pathway enhances the cell death caused by Rpr over expression (Ditzel et al., 2003). These data suggest that the NERD pathway enhances the anti-apoptotic function of DIAP1 with respect to Rpr-induced cell death but not in the case of Hid over

expression. This differential effect could be attributed to the binding affinities of the IAP antagonists for the BIR domains of DIAP1 as Hid preferentially binds to the BIR2 domain (Zachariou et al., 2003). We therefore hypothesized that the NERD pathway not only regulates the stability of DIAP1, but also of the IAP antagonists that can bind to the BIR1 domain of DIAP1, such as Rpr and Grim. Therefore, we sought to investigate the regulation of Grim by N-end rule-mediated degradation of DIAP1 in a tractable yeast model system. We have chosen this model system for two main reasons: (1) the mechanistic details of the N-end rule pathway are very well characterized in *S. cerevisiae* and (2) previous reports have shown that RHG proteins do not cause cell death in yeast, unlike in S2 cells, which helps in uncoupling cell death from other regulatory mechanisms (Olson et al., 2003a; Varshavsky, 2003; Wang et al., 1999). Since yeast do not have IAPs with RING domains, the effects of the NERD pathway on Grim stability can be studied without the interference of endogenous IAP-mediated degradation. In this work we have demonstrated that Grim is *trans*-ubiquitinated in an N-end rule-dependent manner when bound to the BIR1 domain of DIAP1.

4.2 Results

4.2.1 An N-degron form of DIAP1-BIR1 leads to Grim degradation. We observed that Grim, when expressed in *Drosophila* S2 cells, was rapidly degraded. However, upon pre-treatment with z-VAD-fmk (50 μ M), a pan-caspase inhibitor, Grim levels were stabilized, and this correlated well with a block in DIAP1 cleavage at Asp-20 (Fig. 4.1). Previous reports indicate that caspase-mediated cleavage of DIAP1 at Asp-20 exposes a

destabilizing N-terminal residue, Asn, resulting in formation of a N-degron (Ditzel et al., 2003). Since Grim can simultaneously bind DIAP1, we questioned if Grim might be degraded by the NERD pathway in a caspase-dependent manner. To test this hypothesis we used DIAP1 (amino acids 21-205), which corresponds to the BIR1 fragment obtained as a result of cleavage after residues 20 and 205 by DrICE and Dronc, respectively (Ditzel et al., 2003; Muro et al., 2005) (Illustration 1.8). We also reasoned that using DIAP1 (21-205), which contains the BIR1 domain only, at least in the initial experiments would help us to distinguish the effect of BIR1:Grim from BIR1-BIR2:Grim interactions. In addition, it would also allow us to study the effect of the NERD pathway on Grim stability without the influence of RING-dependent ubiquitination. We expressed DIAP1 (21-205) (henceforth referred to as BIR1) as a fusion protein DHFR-HA-Ub-X-BIR1-GST (Illustration 4.1), and we generated two versions of the fusion protein, containing either a Met (M) or Arg (R) at position X (Illustration 4.1). The fusion proteins are cleaved post-translationally after the last residue of Ub yielding equimolar amounts of an N-terminal tracer, DHFR-HA-Ub, and X-BIR1-GST. Based on the identity of the amino acid at position X, a stable M-BIR1 or an R-BIR1 (a potential N-degron) is generated (Illustration 4.1). As expected, when expressed in yeast we observed that R-BIR1 is rapidly degraded compared to M-BIR1 (Fig. 4.2, lanes 1 and 2). When expressed in a yeast strain lacking Ubr1 -the E3 ubiquitin ligase required for NERD pathway- R-BIR1 and M-BIR1 are equally stable (Fig. 4.2, lanes 3 and 4). These data clearly indicate that the NERD pathway degrades the N-degron form of DIAP1 in an Ubr1-dependent manner.

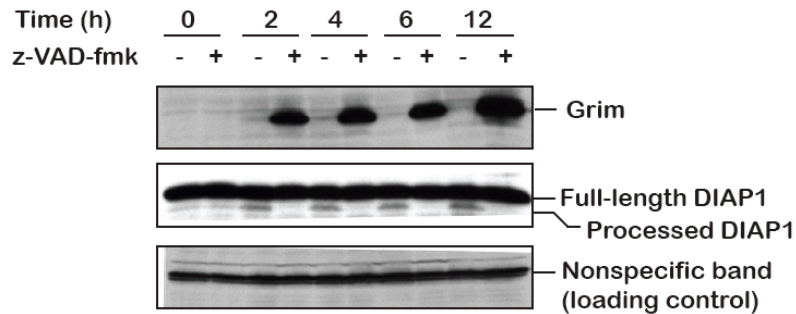


Figure 4.1 Grim stability is dependent on caspase activation.

Drosophila S2 cells were transfected with plasmid expressing C-terminally HSV-tagged Grim under a copper-inducible promoter. Grim expression was induced in cells pre-treated with either zVAD-fmk (50 μ M) or DMSO (vehicle), by adding CuSO_4 (0.7 mM). Thereafter, cells were collected at several time points as indicated above and further analyzed by immunoblotting. Expression levels of Grim (upper panel) and DIAP1 (middle panel) were analyzed by using antibodies against the HSV tag and endogenous DIAP1 respectively. A non-specific band from Grim blot was used as an internal loading control (lower panel).

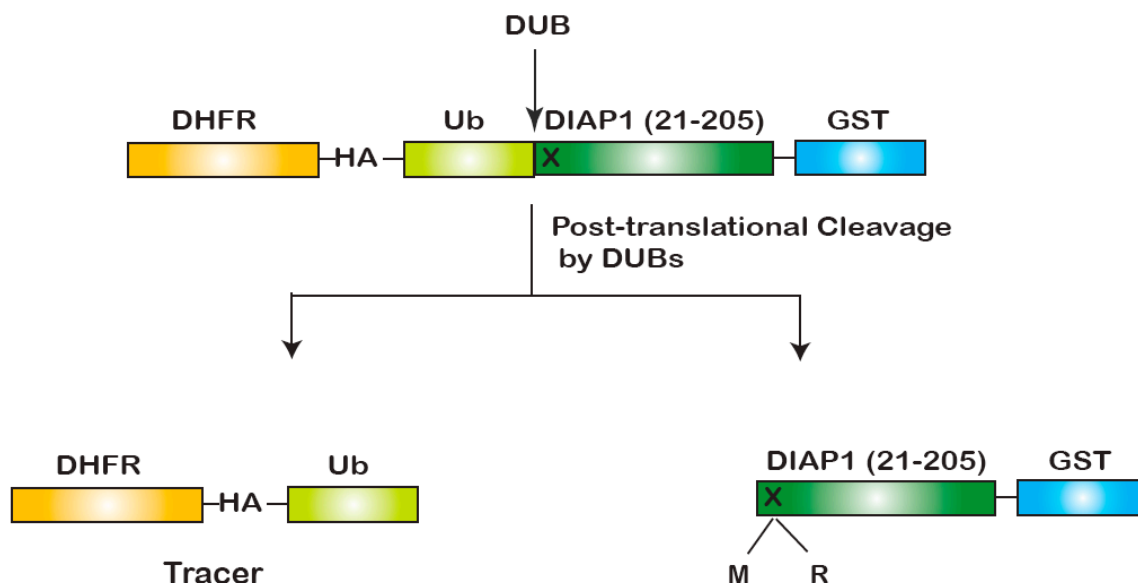


Illustration 4.1 Scheme representing the ubiquitin-fusion proteins used to generate DIAP1 proteins with either a stabilizing or destabilizing N-terminal residue.

The ubiquitin-fusion protein was comprised of an N-terminal mouse Dihydrofolate reductase (DHFR), Hemagglutinin (HA)-tag, ubiquitin (Ub) K48R, BIR1 domain of DIAP1 (21-205), and the GST tag. 'X' denotes the amino acid that is present immediately after the Ub. Once the fusion protein is translated, it undergoes processing by deubiquitinating enzymes (DUBs) after the Ub resulting in the generation of two fragments: DHFR-HA-Ub and X-DIAP1(21-205)-GST (X-BIR1-GST). Based on the identity of the amino acid 'X', DIAP1(21-205)-GST (X-BIR1-GST), with either a stable or unstable N-terminal amino acid, Met (M) or Arg (R), respectively, is generated. As the DHFR-HA-Ub is a stable protein, it is used as a tracer to analyze the levels of protein expression.

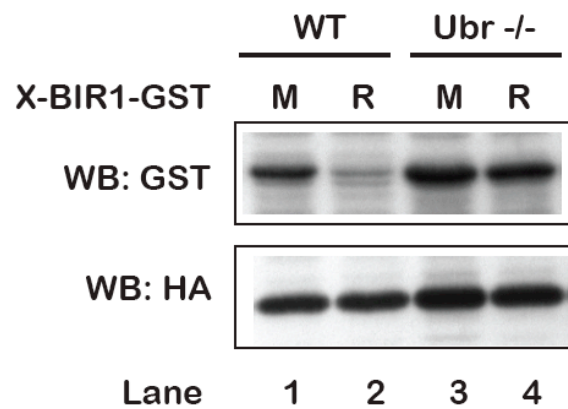


Figure 4.2 N-degron form of DIAP1 is degraded in an Ubr1-dependent manner.

S. cerevisiae strains JD53 (*UBR1*) and JD83-1A (*ubr1Δ*) carrying either pDhaUb-M-BIR1-GST or pDhaUb-R-BIR1-GST were cultured in dextrose-containing drop-out medium until mid-log phase, and thereafter expression of ubiquitin-fusion proteins was induced by adding 0.2 mM CuSO₄. The cells were collected at 3 hrs post-induction and processed for immunoblotting. The levels of the DIAP1 proteins as well as the tracer were analyzed by immunoblotting using α-GST and α-HA antibodies, respectively.

In vitro studies by Varshavsky's group have shown that within a multisubunit protein, a subunit with an N-terminal stabilizing residue can be degraded in *trans* provided that it meets the following requirements: (1) association with the N-degron subunit (a subunit that bears a destabilizing N-terminal residue and binds to the N-recognin), (2) presence of an internal lysine for the addition of polyubiquitin chains in an N-recognin-dependent manner, and (3) a correct spatial conformation of *trans*-targeted substrate relative to the N-degron subunit so that the lysine is accessible for ubiquitination (Johnson et al., 1990; Varshavsky, 1996). However, no physiological interactions are reported to undergo simultaneous *cis*- and *trans*-degradation in a N-end rule-dependent manner. So, we proceeded to test whether Grim was *trans*-ubiquitinated in a similar manner when associated with the N-degron form of DIAP1 *in vivo*. We therefore co-transformed yeast with two vectors: one expressing the Ub-fusion proteins, GST, M-BIR1-GST, or R-BIR1-GST, under a copper inducible promoter, and one expressing Grim with a C-terminal HSV tag under a GAL1 promoter. Grim expression was induced by growing cells in medium consisting of 2% galactose for three hours followed by the induction of GST, M-BIR1-GST or R-BIR1-GST with 0.2 mM CuSO₄. Thereafter, at several time points, samples were taken as indicated. In the presence of the rapidly degrading R-BIR1-GST, the levels of Grim protein declined over time (Fig. 4.3, top panels). However, in the presence of GST or M-BIR1-GST, the levels of Grim remain unchanged suggesting that R-BIR1-GST (the N-degron) was required for Grim turnover (Fig. 4.3, top panels). In the presence of Grim, R-BIR1-GST was still degraded, suggesting that *cis*-ubiquitination of the N-degron was not affected (Fig. 4.3, panels in the

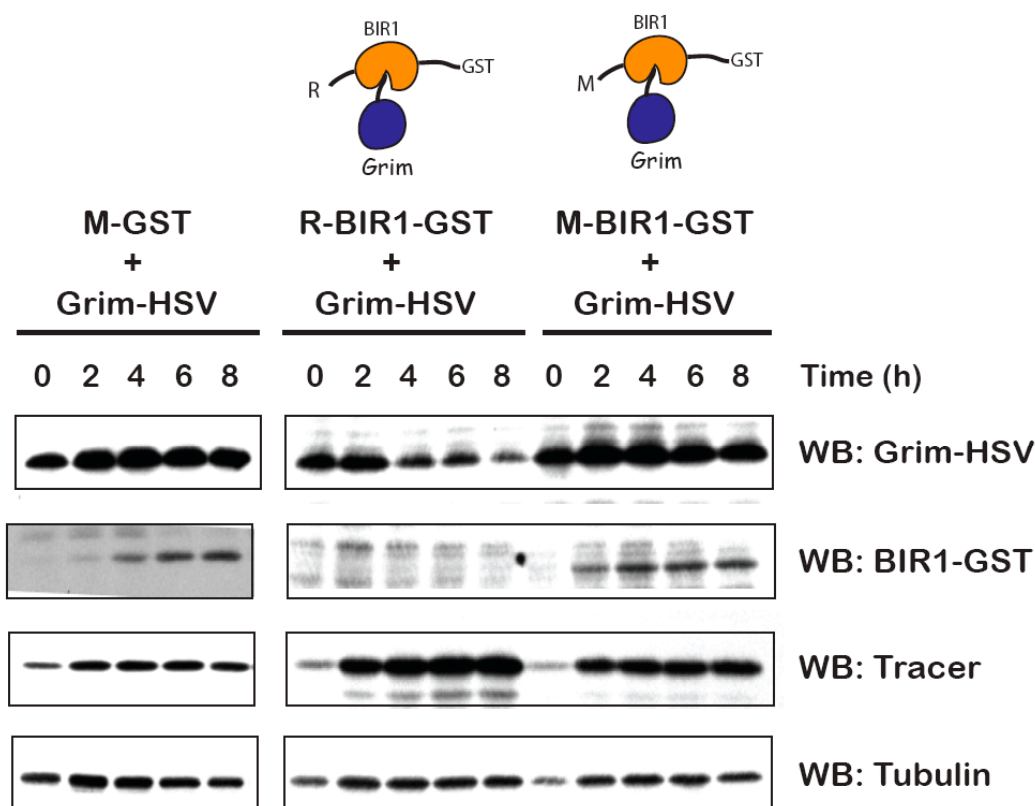


Figure 4.3 N-degron form of DIAP1 promotes *trans*-degradation of Grim.

JD47-13C (*UBR1*) strain was co-transformed with plasmids pDhaUb-GST, pDhaUb-M-BIR1-GST, or pDhaUb-R-BIR1-GST along with pYES2-Grim-HSV. Transformed cells were cultured in non-inducible raffinose-containing drop-out medium until mid-log phase and thereafter cells were transferred to galactose-containing medium to induce the expression of Grim. Three hours after Grim induction, 0.2 mM CuSO₄ was added to the galactose-containing drop-out medium to induce the expression of the ubiquitin-fusion proteins. From then on several time points were taken as indicated, and the cells were resuspended in the SDS-loading buffer. The samples were analyzed by immunoblotting for the levels of Grim (anti-HSV), ubiquitin-fusion proteins (anti-GST), tracer (anti-HA), and α -tubulin (anti- α -tubulin).

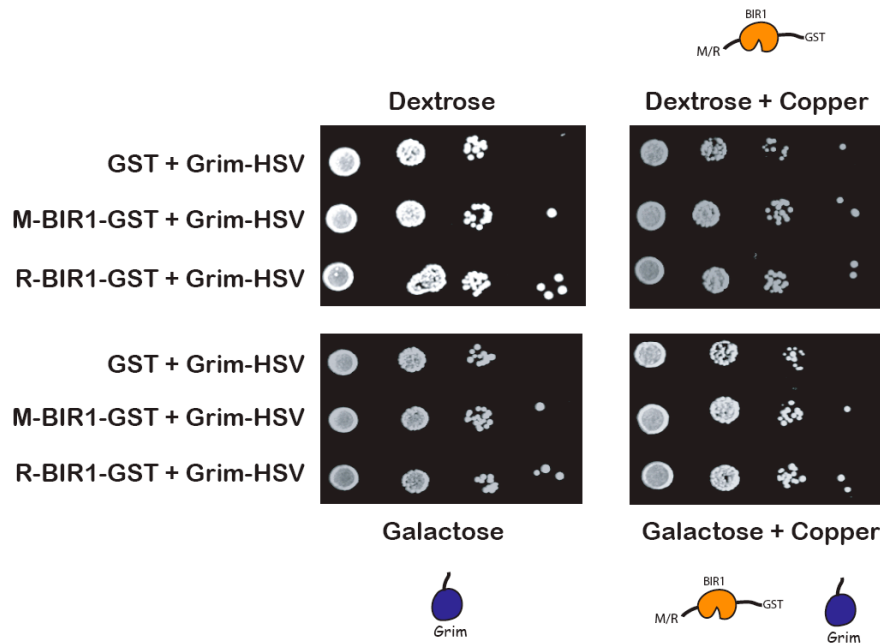


Figure 4.4 Difference in the Grim levels are not a consequence of cell death.

JD47-13C (*UBR1*) strain was co-transformed with plasmids pDhaUb-GST, pDhaUb-M-BIR1-GST, or pDhaUb-R-BIR1-GST along with pYES2-Grim-HSV. The transformants were cultured in non-inducible dextrose-containing drop-out medium to saturation. Cells were serially-diluted and spotted on to the drop-out plates containing either dextrose or galactose in the presence and absence of 0.2 mM CuSO₄. The plates were incubated at 30°C for 1-2 days and analyzed for viability.

second row). These observed differences in Grim levels could not be attributed to the variation in the expression of the ubiquitin-fusion proteins, as the levels of the tracer (DHFR-HA-Ub) were similar in each treatment (Fig. 4.3, panels in the third row).

Expression of the RHG proteins in S2 cells as well as in the fly eye has been reported to cause extensive cell death (White et al., 1994; Yokokura et al., 2004). To rule out that differences in grim expression, in the presence of M- and R-BIR1-GST proteins, was not due to cell death, we analyzed the viability of each transformant. The viability assays were performed by spotting serially diluted cells onto plates containing either glucose or galactose with or without CuSO₄. Under these conditions, where Grim was expressed alone (galactose) or in combination with the BIR1 proteins (galactose + CuSO₄) there was no difference in cell death, indicating that Grim expression does not affect the viability of yeast (Fig. 4.4). Thus, we concluded that the differences in Grim expression levels were not a result of cell death, but rather were a consequence of being degraded along with DIAP1-BIR1.

4.2.2 Grim is *trans*-ubiquitinated by Ubr1 on a critical lysine following their association with DIAP1-BIR1. To verify if the degradation of Grim was dependent on its interaction with the BIR1 domain of DIAP1 we analyzed the stability of a Grim mutant lacking its functional IBM (GGAY-Grim) (Ala2Gly, Ile3Gly) (Fig. 4.5). The levels of GGAY-Grim are equal in the presence of both M-BIR1-GST and R-BIR1-GST suggesting that the interaction of Grim with BIR1 is necessary for its degradation by NERD pathway. As mentioned earlier, one of the major requirements of the *trans*-

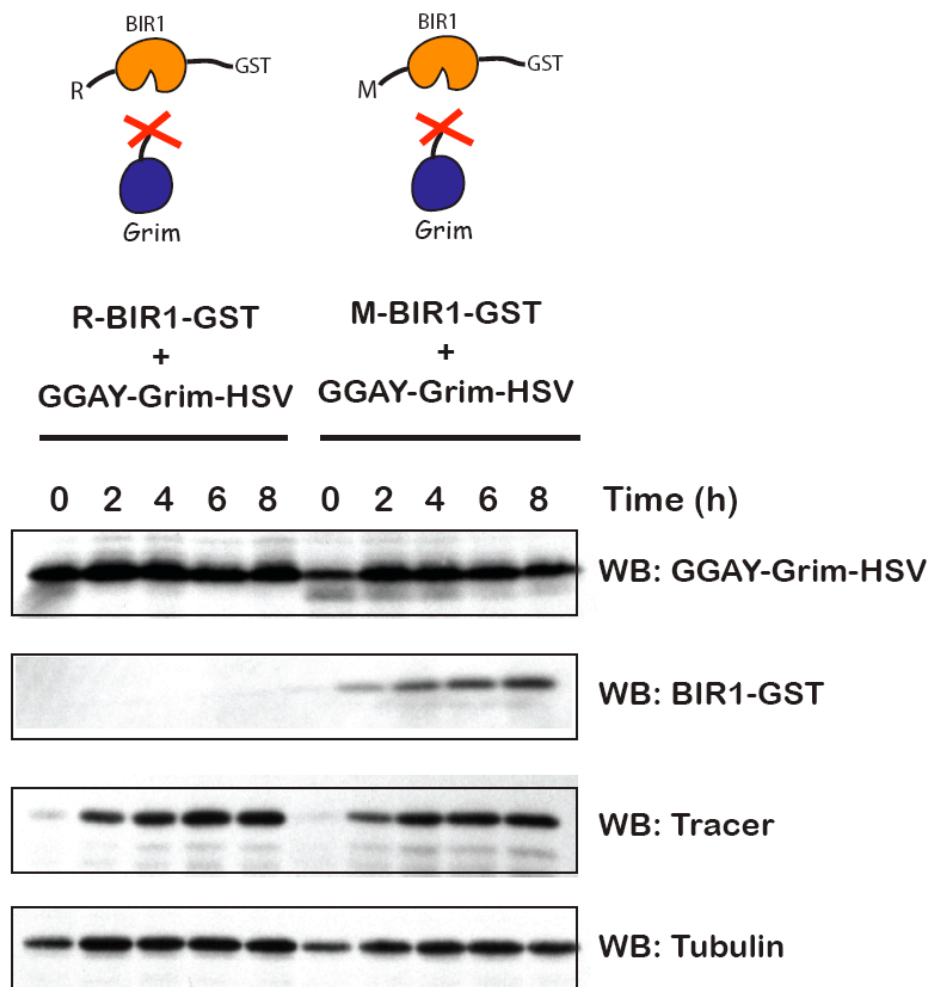


Figure 4.5 *Trans*-degradation of Grim requires its interaction with the BIR1 domain of DIAP1.

JD47-13C (*UBR1*) strain was co-transformed with plasmids pDhaUb-M-BIR1-GST or pDhaUb-R-BIR1-GST along with pYES2-GGAY-Grim-HSV. Transformed cells were further analyzed for the expression levels of Grim (anti-HSV), ubiquitin-fusion proteins (anti-GST), tracer (anti-HA), and α -tubulin (anti- α -tubulin) as described in the Fig. 4.3.

targeted protein is the presence of an internal lysine residue, which can be polyubiquitinated (Johnson et al., 1990). To check if the *trans*-degradation of Grim requires an intact lysine, we analyzed the stability of Grim by mutating the only lysine at position 136 to an alanine (Grim-K136A). Upon co-transformation with R-BIR1-GST, Grim-K136A was very stable relative to its wild-type version (Fig. 4.7). This result suggests that the degradation of Grim requires an internal lysine and is degraded presumably in a proteasome-dependent manner.

To further ascertain whether the degradation of Grim was dependent on the N-end rule pathway, we analyzed the loss of Grim in yeast lacking the N-recognin, *Ubr1*. In the *Ubr1*^{-/-} strain, R-BIR1-GST was stable and correspondingly Grim was not degraded (Fig. 4.6). This result suggests that both Ubr1 and the BIR1 domain of DIAP1 (in its N-degron form) are required for *trans*-degradation.

4.2.3 Cleavage of DIAP1 by Dronc generated a BIR1 fragment that more readily promotes *trans*-ubiquitination of Grim. As mentioned previously, the initiator caspase Dronc, cleaves DIAP1 after Asp-205 and this cleavage increases the anti-apoptotic activity of DIAP1 (Muro et al., 2005) (Illustrations 1.8 and 4.2). To further understand the significance of the Dronc-mediated DIAP1 cleavage on Grim degradation *via* the NERD pathway, we have generated a fusion protein of DIAP1 comprising both the BIR1 and BIR2 domains (amino acids 21-336), DHFR-HA-Ub-X-BIR1-BIR2-GST. As yeast do not have homologs of Dronc, DIAP1 is not cleaved at Asp-205, X-BIR1-BIR2-GST was expressed in its intact form. Upon expression in yeast similar to the BIR1 domain

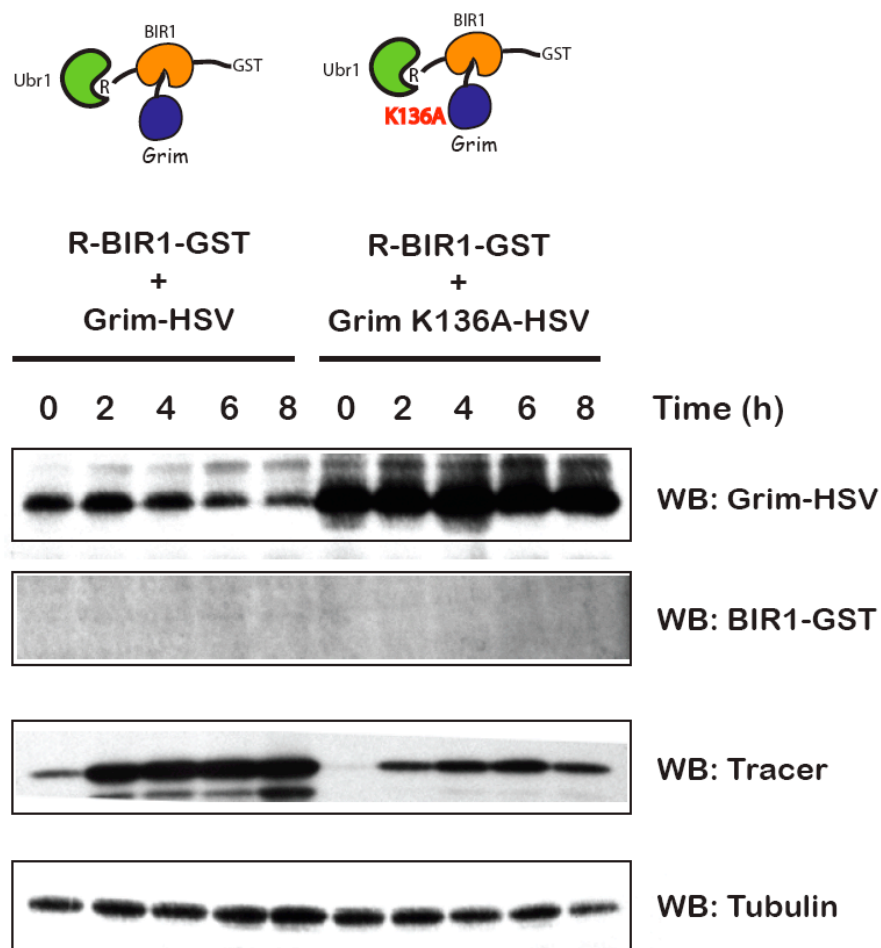


Figure 4.6 *Trans-degradation of Grim requires an intact lysine at position 136.*

JD47-13C (*UBR1*) strain was co-transformed with the pYES2-Grim-HSV or pYES2-Grim-K136A-HSV plasmids along with pDhaUb-R-BIR1-GST. Transformed cells were analyzed for the expression levels of Grim (anti-HSV), ubiquitin-fusion proteins (anti-GST), tracer (anti-HA), and α -tubulin (anti- α -tubulin) as described in the Fig. 4.3.

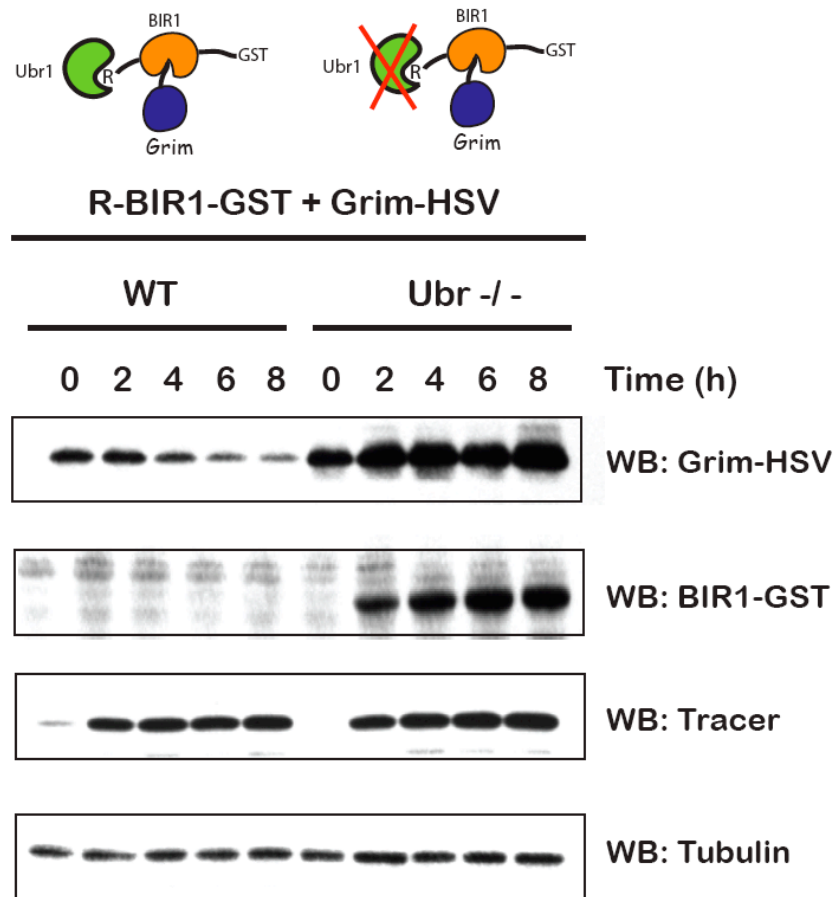


Figure 4.7 *Trans*-degradation of Grim occurs in an Ubr1-dependent manner.

JD53 (*UBR1*) and JD83-1A (*ubr1Δ*) were co-transformed with the pDhaUb-R-BIR1-GST and pYES2-Grim-HSV plasmids. Transformed cells were analyzed for the expression levels of Grim (anti-HSV), ubiquitin-fusion proteins (anti-GST), tracer (anti-HA), and α -tubulin (anti- α -tubulin) as described in the Fig. 4.3.

in its N-degron form, R-BIR1-BIR2-GST was rapidly degraded in an Ubr1-dependent manner by the NERD pathway (data not shown). We then analyzed for the stability of Grim in the presence of DIAP1 with BIR1 or both BIR1 and BIR2 domains (R-BIR1-GST and R-BIR1-BIR2-GST). To our surprise, in contrast to R-BIR1-GST, Grim was not degraded in the presence of R-BIR1-BIR2-GST (Fig. 4.8). We reasoned that the inability of Grim to be *trans*-ubiquitinated in the presence of DIAP1, containing both its BIR domains, could be due to its distributed binding to both BIR1 and BIR2 domains. To test this hypothesis, we generated a mutant form of R-BIR1-BIR2-GST (G269S), which impairs proper binding of the IAP antagonists to the BIR2 domain thus forcing most of the Grim to bind to the BIR1 domain. However, even in the presence of the G269S mutation Grim was not degraded (McGonigal, *thesis in preparation*). These data suggests that Grim, can only be degraded by DIAP1 following cleavage as Asp-20 and Asp-205 by Drice and Dronc, respectively. Presumably, binding of Grim to DIAP1-BIR1 domain, obtained as a result of Dronc cleavage, may make Grim accessible for ubiquitination in an Ubr1-dependent manner.

4.3 Discussion

It has previously been reported that the caspase-mediated cleavage of DIAP1 at its N-terminus makes it a target for the NERD pathway. Surprisingly the degradation of DIAP1 through the NERD pathway enhances its anti-apoptotic activity, despite the decrease in its stability, with respect to Rpr-induced cell death (Ditzel et al., 2003). We

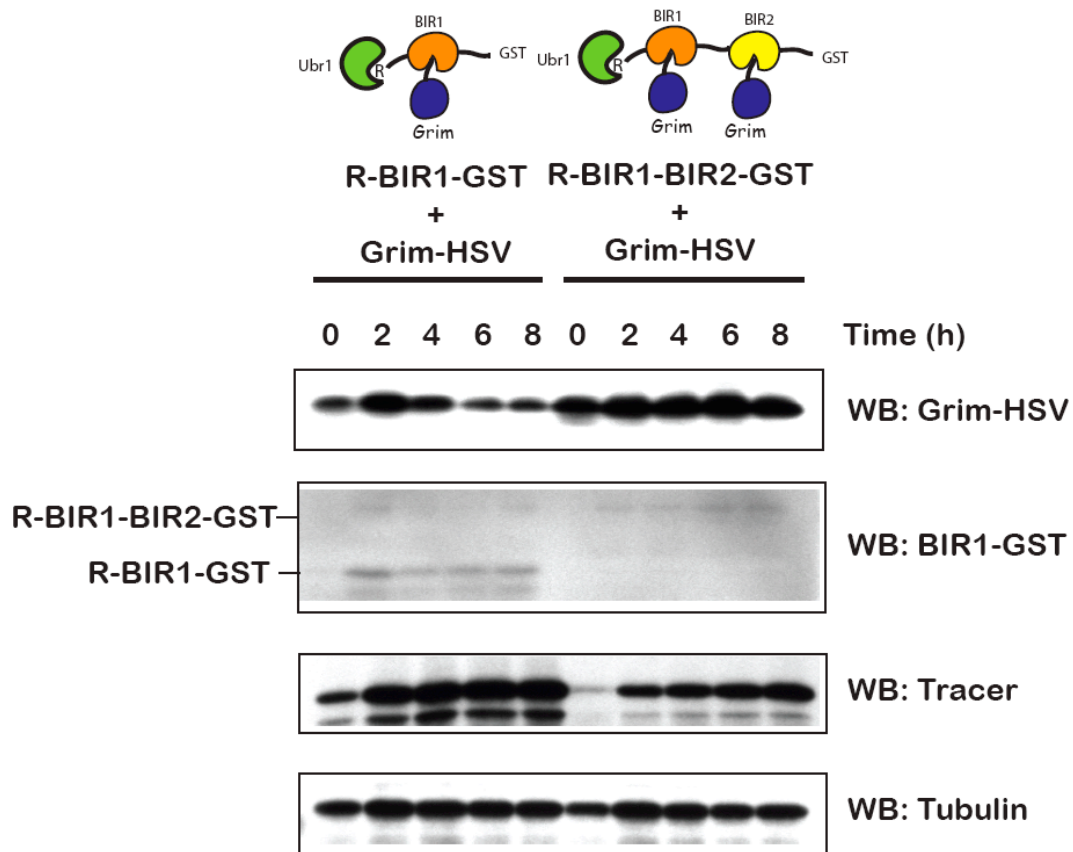


Figure 4.8 *Trans*-degradation of Grim requires binding to BIR1 domain of DIAP1 only.

JD47-13C (*UBR1*) strain was co-transformed with plasmids pDhaUb-R-BIR1-GST or pDhaUb-R-BIR1-BIR2-GST along with pYES2-Grim-HSV. Transformed cells were further analyzed for the expression levels of Grim (anti-HSV), ubiquitin-fusion proteins (anti-GST), tracer (anti-HA), and α -tubulin (anti- α -tubulin) as described in the

hypothesized that one of the possible mechanisms by which the NERD pathway enhanced the anti-apoptotic function of DIAP1 was by promoting the degradation of pro-apoptotic proteins bound to it (Illustration 4.2). In contrast to Rpr-induced cell death, the NERD pathway enhances the cell death caused by expression of Hid (Ditzel et al., 2003). These observations led us to speculate that the disparate effects of the NERD pathway on Reaper and Hid-induced cell death could be based on their differential binding affinities for the BIR1 and BIR2 domains and that only the pro-apoptotic proteins that bound to the BIR1 domain could be regulated by the NERD pathway (Illustration 4.2). To test this possibility, we studied the effects of the NERD pathway on Grim, a pro-apoptotic IAP antagonist that can bind to both the BIR1 and BIR2 domains.

In our study, using yeast, we have shown that Grim, when bound to the BIR1 domain of DIAP1, is *trans*-ubiquitinated by Ubr1 and degraded by the NERD pathway (Figs. 4.3 and 4.5). The degradation of Grim requires an intact lysine, which is required for polyubiquitination in an Ubr1-dependent manner (Figs. 4.6 and 4.7). Thus, we have demonstrated for the first time *in vivo* that a protein with a stable N-terminal residue can indeed be *trans*-targeted provided that it is in complex with an N-degron (Illustration 4.2). Our data also sheds significant light on the underlying contribution of the NERD pathway to the anti-apoptotic function of DIAP1. Despite its degradation by the N-end rule pathway, DIAP1 still maintains its anti-apoptotic activity by facilitating the degradation of Grim. Based on our data, we speculate that the NERD pathway may degrade other pro-apoptotic proteins, such as Reaper and DrICE that bind to the BIR1 domain of DIAP1 (Illustration 4.2).

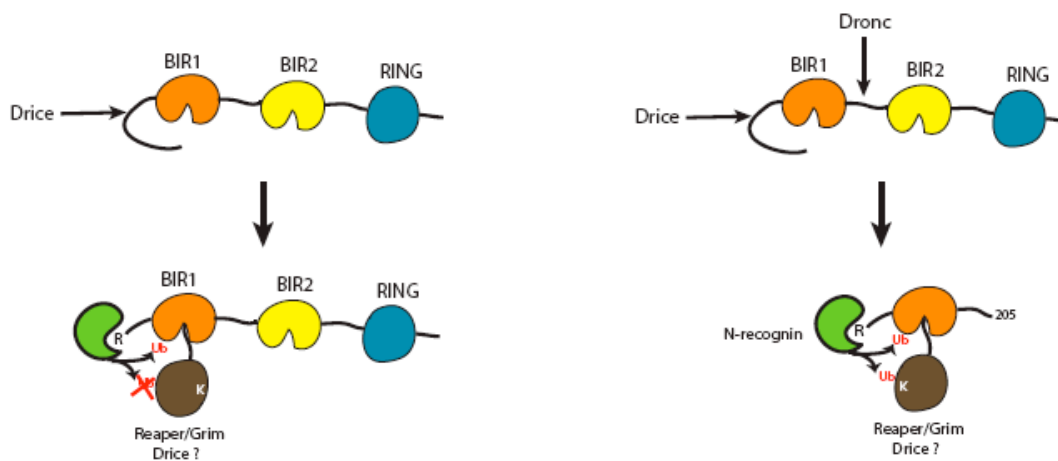


Illustration 4.2 Model depicting the mechanisms involved in the ubiquitin-mediated degradation of the pro-apoptotic proteins by DIAP1.

DIAP1 acts as a substrate for both the initiator and effector caspases, Dronc and DrICE, respectively. Cleavage by DrICE alone leads to the removal of N-terminal twenty amino acids ($\Delta 20$ -DIAP1) (left scheme). On the other hand, cleavage by both the caspases leads to generation of two entities: an N-degron form of BIR1 domain and BIR2-RING module. The N-degron form of BIR1 degrades pro-apoptotic proteins such as Rpr, Grim, and DrICE in an Ubr1-dependent manner (right scheme). However, binding of the RHG proteins as well as DrICE to the $\Delta 20$ -DIAP1 does not facilitate their degradation in the NERD pathway-dependent manner.

It has previously been suggested that the lysines at positions 10 and 15 from the N-terminus of an N-degron are critical for ubiquitination by the N-recogin (Suzuki and Varshavsky, 1999). But recent data suggest that the lysines at position 30 and 35 of DIAP1, which correspond to the Lys-10 and -15 of the N-degron, are not responsible for the degradation of DIAP1 by the NERD pathway (Herman-Bachinsky et al., 2007). Our data was in agreement with these observations suggesting that the lysines at positions 49, 61, 77 and 79, which are a part of the BIR1 domain, could be the putative polyubiquitination sites for the degradation of BIR1 domain. Further insights can be obtained once we have a better understanding of the exact mechanism(s) by which DIAP1 is degraded by Ubr1.

Interestingly, our data suggest that in contrast to the DIAP1-BIR1, DIAP1-BIR1-BIR2 is incapable of *trans*-ubiquitinating Grim for degradation (Fig. 4.8). Initially, we hypothesized that the reason for Grim stability could be attributed to its distributed binding to both the BIR1 and BIR2 domains, which positions only a portion of Grim in close proximity to Ubr1. However, forcing most of the Grim to bind to the BIR1 domain by mutating Gly-269 to Ser did not enhance the *trans*-ubiquitination of Grim (McGonigal, *thesis in preparation*). This argues that cleavage of DIAP1 by Dronc at Asp-205 is essential for targeting Grim for degradation by the NERD pathway. One of the possible explanations for this result could be that the BIR1 domain, unlike DIAP1, which contains both BIR domains, orients Grim in a conformation that supports polyubiquitination by the Ubr1. These data are also in agreement with previous data, which suggests that cleavage of Dronc enhances its anti-apoptotic activity (Muro et al.,

2005). Therefore, cleavage of DIAP1 by both DrICE and Dronc creates two entities of DIAP1, which differentially degrade pro-apoptotic proteins either through the NERD pathway or through RING-dependent ubiquitination. Previous work by Yokokura et al. (2004) suggested that RING-dependent ubiquitination takes precedence over N-end rule pathway. As Dronc cleavage of DIAP1 separates the BIR1 domain from the influence of RING domain, it can be argued that RING-dependent ubiquitination overrides N-end rule pathway only in the uncleaved state (Illustration 4.2). It will be interesting to see if Dronc-dependent cleavage of DIAP1 also enhances ubiquitination by the RING domain.

In summary, we have shown that Grim is *trans*-ubiquitinated by the NERD pathway in a caspase-dependent manner (Fig 4.3). However, it remains unclear if a similar mechanism exists for DrICE. We have also shown that degradation of DIAP1 by the NERD pathway occurs in an Ubr1-dependent manner (Fig 4.6). But, it still remains to be determined if Ubr1 directly ubiquitinates the *trans*-targeted proteins or if it recruits other E3 ligases for this task. Gaining further insight will help us understand a novel mechanism by which IAPs regulate the IAP antagonists.

Chapter 5: Concluding remarks

Apoptosis is essential for normal development and maintenance of tissue homeostasis (Opferman and Korsmeyer, 2003). It is an evolutionarily-conserved form of cell death with many common players in different organisms such as *C. elegans*, *Drosophila*, and mammals (Kornbluth and White, 2005). In *C. elegans*, the regulatory network is rather simple with four main players: (1) CED-3, a cysteine protease (caspase), (2) CED-4, the adaptor protein, (3) EGL-1, the pro-apoptotic Bcl-2 family member, and (4) CED-9, the anti-apoptotic Bcl-2 family member (Lettre and Hengartner, 2006). Disruption of the CED-9:CED-4 interaction by EGL-1 is required to initiate the apoptotic pathway, and CED-4, subsequently binds to and activates CED-3. Once activated, CED-3 then cleaves several cellular substrates resulting in apoptosis (Lettre and Hengartner, 2006). In mammals, similar core components including caspases (mammalian homologs of CED-3), the adaptor protein Apaf-1 (mammalian homologs of CED-4), and Bcl-2 family members regulate apoptosis (Jiang and Wang, 2004). In contrast to *C. elegans*, mammalian Bcl-2 family members contribute to caspase activation by regulating MOMP, rather than directly binding to Apaf-1 (Danial and Korsmeyer, 2004). As a consequence of MOMP, cytochrome c is released into cytosol, where it induces formation of the apoptosome, an oligomeric complex that acts as a platform for the activation of caspases (Riedl and Salvesen, 2007). In mammals, IAPs and IAP antagonists impart a second layer of caspase regulation (Salvesen and Duckett, 2002). IAPs bind to and inhibit active caspases whereas IAP antagonists displace IAP-bound

caspases (Salvesen and Duckett, 2002). The *Drosophila* apoptotic regulatory machinery is very similar to that of mammals consisting of caspases, Dark (fly homolog of mammalian Apaf-1), Bcl-2 family members, IAPs, and IAP antagonists (Hay and Guo, 2006). Despite several similarities, key differences exist between mammalian and fly cell death mechanisms (Kornbluth and White, 2005). Therefore, gaining further insights into the *Drosophila* apoptotic mechanisms is essential to understand the evolutionarily-conserved nature of this process.

One of the unresolved questions regarding *Drosophila* apoptotic mechanisms is the role of mitochondria in caspase activation. As mentioned earlier, MOMP and the subsequent release of cytochrome c are prerequisites for the activation of mammalian initiator caspase-9 (Riedl and Salvesen, 2007). Moreover, release of the mammalian IAP antagonists into cytosol, regulates caspase activity by inhibiting the function of IAPs (Vaux and Silke, 2005). There is also evidence demonstrating that cytochrome c is required for caspase activation in flies in a tissue-specific manner (Arama et al., 2003; Arama et al., 2006). However, several lines of evidence suggest that activation of Dronc, the fly homolog of mammalian caspase-9, occurs independent of MOMP and cytochrome c release (Dorstyn et al., 2004; Means et al., 2006; Muro et al., 2002; Zimmermann et al., 2002). Additionally, the cytosolic localization of *Drosophila* IAP antagonists Rpr, Hid, and Grim undermine the role of mitochondria in fly apoptosis further strengthening this controversy (Kornbluth and White, 2005). Therefore, in order to gain a better understanding of mitochondrial function in *Drosophila* apoptosis, we identified and characterized the role of dOmi, a fly homolog of the mammalian IAP antagonist

Omi/Htra2 (chapter 3). We have demonstrated that various apoptotic stimuli such as STS and UV irradiation can induce MOMP and thereby cause the release of both dOmi and cytochrome c into the cytosol. Once released, the mature forms of dOmi potentiate cell death primarily through their protease activities. The role of cytochrome c will require further characterization. Nevertheless, we observed that based upon the nature of the apoptotic stimulus, MOMP occurs either in a caspase-dependent or -independent manner. This is not surprising as even in mammals, MOMP can occur either prior to or after caspase-9 activation depending on the stimulus. For instance, in the intrinsic pathway, MOMP is required for apoptosome formation and subsequent caspase-9 activation (Jiang and Wang, 2004). On the other hand, following death receptor stimulation, activation of caspase-8 leads to MOMP, which in turn leads to caspase-9 activation (Budihardjo et al., 1999). Therefore, our data suggests that in *Drosophila*, similar to mammals, MOMP can occur either in a caspase-dependent or -independent manner.

Although we have successfully established that *Drosophila* mitochondria can be permeabilized upon the receipt of an apoptotic stimulus, the factors that contribute to this process are yet to be determined. It will be interesting to see if the *Drosophila* Bcl-2 family members, Debcl and Buffy, similar to their mammalian counterparts, modulate MOMP and subsequent release of mitochondrial resident proteins, such as cytochrome c and dOmi, into the cytosol (Danial and Korsmeyer, 2004; Igaki and Miura, 2004). Apart from the Bcl-2 family members, the GH3 domain of IAP antagonists like Reaper and Grim also plays an important role in mitochondrial permeabilization (Claveria et al., 2002; Olson et al., 2003a). It will be interesting to see if GH3 domain-dependent

mitochondrial permeabilization can cause release of dOmi and cytochrome c. Therefore, it could be speculated that dOmi plays an important role in further enhancing the GH3-dependent cell death mechanisms. Additional characterization of the role of *Drosophila* Bcl-2 family members and the GH3 containing IAP antagonists in regulating MOMP should enhance our understanding of the role of mitochondria in fly apoptosis. With respect to caspase-dependent MOMP, the identity of the caspases, as well as their substrates required for mitochondrial permeabilization, remains to be determined.

We have demonstrated that dOmi, once released into cytosol, enhances caspase activity and potentiates cell death. However, RNAi of dOmi does not completely inhibit caspase activation. These data suggest that apart from dOmi, other pro-apoptotic molecules that are released into the cytosol as a consequence MOMP may also contribute to caspase activation. As cytochrome c can bind to the WD40 repeats of DARK (Kanuka et al., 1999b), it remains a possibility that some of the caspase activity observed upon MOMP may be attributed to apoptosome-dependent Dronc activation. Further studies using RNAi approaches are required to study the effects of cytochrome c, Dronc, and Dark on caspase activation following MOMP. In the case of mammals, a redundancy exists with respect to the number of mitochondrial IAP antagonists (Vaux and Silke, 2005). Thus, caspase activation in the fly could also be due to other unknown IAP antagonists that are released into cytosol following MOMP. Identification and characterization of other mitochondrial pro-apoptotic molecules would certainly reinforce the role of mitochondria in *Drosophila* apoptosis.

In *Drosophila*, loss of DIAP1 triggers spontaneous and unrestrained caspase activity, suggesting that, unlike in mammals, IAPs act upstream of caspases (Yoo et al., 2002; Zimmermann et al., 2002). The caspase activation that occurs as a consequence of DIAP1 depletion also requires the adaptor protein, Dark. These observations have led to the proposal that the *Drosophila* apoptosome is constitutively active and that displacement of DIAP1-bound Dronc is sufficient to trigger caspase activation without a prior requirement for MOMP (Kornbluth and White, 2005). In support of this hypothesis, expression of the cytosolic RHG proteins can trigger cell death. However, cytosolic expression of the catalytically inactive mature forms of dOmi, that are capable of displacing BIR2 domain-bound Dronc, could not potentiate cell death. Therefore, our results suggest that mere displacement of DIAP1-bound Dronc by dOmi is not sufficient to potentiate fly apoptosis. One potential explanation for this discrepancy is that the RHG proteins apart from displacing DIAP1-bound caspases, also play an important role in mitochondrial permeabilization (Abdelwahid et al., 2007; Chai et al., 2003a; Yan et al., 2004b). In addition, Reaper and Grim play an important role in translational inhibition (Colon-Ramos et al., 2006; Holley et al., 2002). Therefore, cell death caused by over expression of RHG proteins could be a manifestation of its multiple functions, including, caspase-displacement, mitochondrial permeabilization, and translational suppression. Thus, relying upon the ability of RHG proteins to cause cell death as evidence for a constitutively active apoptosome needs to be reconsidered.

Recent structural data of the *Drosophila* apoptosome has often been cited as evidence for a lack of mitochondrial involvement in fly cell death mechanisms. The

structural data demonstrates that the fly apoptosome is an octameric RING-like structure and is formed in the absence of cytochrome c (Yu et al., 2006). However, several questions regarding the fly apoptosome remain unanswered. In mammals, binding of cytochrome c to the WD-40 repeats is a prerequisite for oligomerization, as it results in an altered conformation of the monomeric Apaf-1 and leads to the formation of the heptameric structure (Riedl and Salvesen, 2007). The structural data for the fly apoptosome does not provide a mechanistic explanation for oligomerization. Additionally, the functionality of the proposed structure is yet to be determined. *In vitro* reconstitution experiments will be required to determine if the octameric *Drosophila* apoptosome can lead to the activation of Dronc. Additionally, it will be interesting to see if endogenous Dark exists in an oligomeric state without an apoptotic stimulus. Even if cytochrome c is not required for formation of the *Drosophila* apoptosome, it does not preclude the role of mitochondria in fly cell death mechanisms. It is possible that another mitochondrial molecule(s) may substitute for cytochrome c in promoting formation of the fly apoptosome. Therefore, identifying and characterizing putative molecules that interact with Dark will be crucial in corroborating the role of mitochondria in *Drosophila* apoptosis and will further our understanding of the mammalian apoptosome.

Similar to its mammalian counterpart, dOmi potentiates cell death mainly through its serine protease activity. We have demonstrated that DIAP1 is a dOmi substrate and that degradation of DIAP1 contributes to the caspase activation. However, dOmi potentiates cell death through both caspase-dependent and -independent mechanisms. These data suggest that dOmi can potentiate cell death by cleaving additional cytosolic

substrates. Therefore, identifying other cytosolic substrates of dOmi, using a combination of genetic and biochemical techniques, will aid in understanding the complete role of dOmi in promoting cell death.

Omi/HtrA2 plays a neuroprotective role and loss of its protease function results in mice with neurodegenerative and Parkinsonian symptoms (Jones et al., 2003; Martins et al., 2004). In addition, mutations in Omi/HtrA2 have been linked to German patients with Parkinson's disease (Strauss et al., 2005). Therefore, it will be important to better understand the mechanisms by which Omi/HtrA2 contributes to the survival of neurons. Identifying the intermembrane space substrates is also essential for understanding Omi/HtrA2's role in mitochondria. The *Drosophila* model system should also serve as a good model system to study dOmi's mitochondrial functions.

Similar to dOmi, cleavage of DIAP1 by caspases also regulates the stability and function of DIAP1 (Ditzel et al., 2003; Muro et al., 2005). Cleavage by DrICE at Asp-20 transforms DIAP1 into a substrate for the NERD pathway, thereby reducing its stability. Interestingly, loss of DIAP1 by the NERD pathway enhances its anti-apoptotic pathway with respect to Rpr-induced cell death (Ditzel et al., 2003). So far the mechanisms by which the NERD pathway modulates DIAP1 function remain unknown. We have demonstrated that Grim, when bound to the BIR1 domain in DIAP1, is *trans* ubiquitinated by NERD pathway. Our data suggest that similar to RING domain-dependent ubiquitination, the NERD pathway also regulates the stability of some pro-apoptotic proteins. Although, we have only demonstrated the effect of the NERD pathway on Grim, its influence on Rpr, Hid, and DrICE should be studied. Interestingly,

we observed that the BIR1 domain of DIAP1, formed as a result of DRONC cleavage, efficiently degrades Grim in an N-end rule-dependent manner when compared to full-length DIAP1. We hypothesize that binding of Grim to the BIR1 fragment of DIAP1 orients it for *trans*-ubiquitination by Ubr1, the E3 ubiquitin ligase of the NERD pathway. Based on these data, we speculate that Dronc cleavage may also enhance RING-dependent ubiquitination of the RHG proteins bound to the BIR2 domain. Studying the kinetics of RING-dependent degradation of RHG proteins, in the presence of either full-length or cleaved forms of DIAP1, will be required to understand the significance of Dronc cleavage.

The role of NERD pathway in the regulation of apoptosis has been reported only in *Drosophila* (Ditzel et al., 2003). However, its role in mammalian apoptotic pathways is currently under investigation. Based on the knowledge gained from fly model, we hypothesize that cleavage of various substrates by caspases may convert them from pro-N-degron to N-degron forms. If so, rapid loss of caspase substrates may enhance the rate of cell death. As mentioned previously, an Alanine residue at the N-terminus of a protein is considered stable with respect to the NERD pathway in yeast (Varshavsky, 1996). However, in mammals, an N-terminal Alanine is a destabilizing residue. Based on this, we speculate that the NERD pathway may also regulate the stability of mammalian mitochondrial IAP antagonists, characterized by an N-terminal Alanine, once they are released into cytosol. Thus, the role of NERD pathway in the degradation of mammalian IAP antagonists should be investigated.

In conclusion, we have studied the regulation of DIAP1 function by dOmi and the NERD pathway. By implicating dOmi in DIAP1 regulation we have underscored the importance of mitochondria for apoptosis in the fly. Through our N-end rule studies we have demonstrated a novel regulation of the IAP and IAP antagonist function. Despite our contributions, there are still many more interesting questions that remain unanswered which will enhance our understanding of the evolutionarily-conserved apoptotic process.

References

- Abdelwahid, E., Yokokura, T., Krieser, R.J., Balasundaram, S., Fowle, W.H. and White, K. (2007) Mitochondrial disruption in *Drosophila* apoptosis. *Dev Cell*, **12**, 793-806.
- Acehan, D., Jiang, X., Morgan, D.G., Heuser, J.E., Wang, X. and Akey, C.W. (2002) Three-dimensional structure of the apoptosome: implications for assembly, procaspase-9 binding, and activation. *Mol Cell*, **9**, 423-432.
- Alnemri, E.S., Livingston, D.J., Nicholson, D.W., Salvesen, G., Thornberry, N.A., Wong, W.W. and Yuan, J. (1996) Human ICE/CED-3 protease nomenclature. *Cell*, **87**, 171.
- Arama, E., Agapite, J. and Steller, H. (2003) Caspase activity and a specific cytochrome C are required for sperm differentiation in *Drosophila*. *Dev Cell*, **4**, 687-697.
- Arama, E., Bader, M., Srivastava, M., Bergmann, A. and Steller, H. (2006) The two *Drosophila* cytochrome C proteins can function in both respiration and caspase activation. *Embo J*, **25**, 232-243.
- Bates, P.A., Kelley, L.A., MacCallum, R.M. and Sternberg, M.J. (2001) Enhancement of protein modeling by human intervention in applying the automatic programs 3D-JIGSAW and 3D-PSSM. *Proteins*, **Suppl 5**, 39-46.
- Brach, M.A., deVos, S., Gruss, H.J. and Herrmann, F. (1992) Prolongation of survival of human polymorphonuclear neutrophils by granulocyte-macrophage colony-stimulating factor is caused by inhibition of programmed cell death. *Blood*, **80**, 2920-2924.
- Brachmann, C.B., Jassim, O.W., Wachsmuth, B.D. and Cagan, R.L. (2000) The *Drosophila* bcl-2 family member dBorg-1 functions in the apoptotic response to UV-irradiation. *Curr Biol*, **10**, 547-550.

- Bratton, S.B., Lewis, J., Butterworth, M., Duckett, C.S. and Cohen, G.M. (2002) XIAP inhibition of caspase-3 preserves its association with the Apaf-1 apoptosome and prevents CD95- and Bax-induced apoptosis. *Cell Death Differ*, **9**, 881-892.
- Bratton, S.B., Walker, G., Srinivasula, S.M., Sun, X.M., Butterworth, M., Alnemri, E.S. and Cohen, G.M. (2001) Recruitment, activation and retention of caspases-9 and -3 by Apaf-1 apoptosome and associated XIAP complexes. *Embo J*, **20**, 998-1009.
- Brimmell, M., Mendiola, R., Mangion, J. and Packham, G. (1998) BAX frameshift mutations in cell lines derived from human haemopoietic malignancies are associated with resistance to apoptosis and microsatellite instability. *Oncogene*, **16**, 1803-1812.
- Budihardjo, I., Oliver, H., Lutter, M., Luo, X. and Wang, X. (1999) Biochemical pathways of caspase activation during apoptosis. *Annu Rev Cell Dev Biol*, **15**, 269-290.
- Cain, K., Bratton, S.B. and Cohen, G.M. (2002) The Apaf-1 apoptosome: a large caspase-activating complex. *Biochimie*, **84**, 203-214.
- Cain, K., Bratton, S.B., Langlais, C., Walker, G., Brown, D.G., Sun, X.M. and Cohen, G.M. (2000) Apaf-1 oligomerizes into biologically active approximately 700-kDa and inactive approximately 1.4-MDa apoptosome complexes. *J Biol Chem*, **275**, 6067-6070.
- Cain, K., Brown, D.G., Langlais, C. and Cohen, G.M. (1999) Caspase activation involves the formation of the aposome, a large (approximately 700 kDa) caspase-activating complex. *J Biol Chem*, **274**, 22686-22692.
- Chai, J., Du, C., Wu, J.W., Kyin, S., Wang, X. and Shi, Y. (2000) Structural and biochemical basis of apoptotic activation by Smac/DIABLO. *Nature*, **406**, 855-862.
- Chai, J., Shiozaki, E., Srinivasula, S.M., Wu, Q., Datta, P., Alnemri, E.S. and Shi, Y. (2001a) Structural basis of caspase-7 inhibition by XIAP. *Cell*, **104**, 769-780.

- Chai, J., Wu, Q., Shiozaki, E., Srinivasula, S.M., Alnemri, E.S. and Shi, Y. (2001b) Crystal structure of a procaspase-7 zymogen: mechanisms of activation and substrate binding. *Cell*, **107**, 399-407.
- Chai, J., Yan, N., Huh, J.R., Wu, J.W., Li, W., Hay, B.A. and Shi, Y. (2003a) Molecular mechanism of Reaper-Grim-Hid-mediated suppression of DIAP1-dependent Dronc ubiquitination. *Nat Struct Biol*, **10**, 892-898.
- Chai, J., Yan, N., Huh, J.R., Wu, J.W., Li, W., Hay, B.A. and Shi, Y. (2003b) Molecular mechanism of Reaper-Grim-Hid-mediated suppression of DIAP1-dependent Dronc ubiquitination. *Nat. Struct. Biol.*, **10**, 892-898.
- Chen, P., Nordstrom, W., Gish, B. and Abrams, J.M. (1996) grim, a novel cell death gene in Drosophila. *Genes Dev*, **10**, 1773-1782.
- Chen, P., Rodriguez, A., Erskine, R., Thach, T. and Abrams, J.M. (1998) Dredd, a novel effector of the apoptosis activators reaper, grim, and hid in Drosophila. *Dev Biol*, **201**, 202-216.
- Chew, S.K., Akdemir, F., Chen, P., Lu, W.J., Mills, K., Daish, T., Kumar, S., Rodriguez, A. and Abrams, J.M. (2004) The apical caspase dronc governs programmed and unprogrammed cell death in Drosophila. *Dev Cell*, **7**, 897-907.
- Chinnaiyan, A.M., O'Rourke, K., Lane, B.R. and Dixit, V.M. (1997) Interaction of CED-4 with CED-3 and CED-9: a molecular framework for cell death. *Science*, **275**, 1122-1126.
- Christich, A., Kauppila, S., Chen, P., Sogame, N., Ho, S.I. and Abrams, J.M. (2002) The damage-responsive Drosophila gene sickle encodes a novel IAP binding protein similar to but distinct from reaper, grim, and hid. *Curr Biol*, **12**, 137-140.
- Clausen, T., Southan, C. and Ehrmann, M. (2002) The HtrA family of proteases: implications for protein composition and cell fate. *Mol Cell*, **10**, 443-455.
- Claveria, C., Caminero, E., Martinez, A.C., Campuzano, S. and Torres, M. (2002) GH3, a novel proapoptotic domain in Drosophila Grim, promotes a mitochondrial death pathway. *Embo J*, **21**, 3327-3336.

- Clem, R.J. and Miller, L.K. (1994) Control of programmed cell death by the baculovirus genes p35 and iap. *Mol Cell Biol*, **14**, 5212-5222.
- Colon-Ramos, D.A., Shenvi, C.L., Weitzel, D.H., Gan, E.C., Matts, R., Cate, J. and Kornbluth, S. (2006) Direct ribosomal binding by a cellular inhibitor of translation. *Nat Struct Mol Biol*, **13**, 103-111.
- Colotta, F., Re, F., Polentarutti, N., Sozzani, S. and Mantovani, A. (1992) Modulation of granulocyte survival and programmed cell death by cytokines and bacterial products. *Blood*, **80**, 2012-2020.
- Colussi, P.A., Quinn, L.M., Huang, D.C., Coombe, M., Read, S.H., Richardson, H. and Kumar, S. (2000) Debcl, a proapoptotic Bcl-2 homologue, is a component of the *Drosophila melanogaster* cell death machinery. *J Cell Biol*, **148**, 703-714.
- Conradt, B. and Horvitz, H.R. (1998) The *C. elegans* protein EGL-1 is required for programmed cell death and interacts with the Bcl-2-like protein CED-9. *Cell*, **93**, 519-529.
- Creagh, E.M., Murphy, B.M., Duriez, P.J., Duckett, C.S. and Martin, S.J. (2004) Smac/Diablo antagonizes ubiquitin ligase activity of inhibitor of apoptosis proteins. *J Biol Chem*, **279**, 26906-26914.
- Daish, T.J., Mills, K. and Kumar, S. (2004) *Drosophila* caspase DRONC is required for specific developmental cell death pathways and stress-induced apoptosis. *Dev Cell*, **7**, 909-915.
- Danial, N.N. and Korsmeyer, S.J. (2004) Cell death: critical control points. *Cell*, **116**, 205-219.
- Ditzel, M., Wilson, R., Tenev, T., Zachariou, A., Paul, A., Deas, E. and Meier, P. (2003) Degradation of DIAP1 by the N-end rule pathway is essential for regulating apoptosis. *Nat Cell Biol*, **5**, 467-473.
- Dorstyn, L., Colussi, P.A., Quinn, L.M., Richardson, H. and Kumar, S. (1999a) DRONC, an ecdysone-inducible *Drosophila* caspase. *Proc Natl Acad Sci U S A*, **96**, 4307-4312.

- Dorstyn, L., Mills, K., Lazebnik, Y. and Kumar, S. (2004) The two cytochrome c species, DC3 and DC4, are not required for caspase activation and apoptosis in *Drosophila* cells. *J Cell Biol*, **167**, 405-410.
- Dorstyn, L., Read, S., Cakouros, D., Huh, J.R., Hay, B.A. and Kumar, S. (2002) The role of cytochrome c in caspase activation in *Drosophila melanogaster* cells. *J Cell Biol*, **156**, 1089-1098.
- Dorstyn, L., Read, S.H., Quinn, L.M., Richardson, H. and Kumar, S. (1999b) DECAP, a novel *Drosophila* caspase related to mammalian caspase-3 and caspase-7. *J Biol Chem*, **274**, 30778-30783.
- Doumanis, J., Quinn, L., Richardson, H. and Kumar, S. (2001) STRICA, a novel *Drosophila melanogaster* caspase with an unusual serine/threonine-rich prodomain, interacts with DIAP1 and DIAP2. *Cell Death Differ*, **8**, 387-394.
- Du, C., Fang, M., Li, Y., Li, L. and Wang, X. (2000) Smac, a mitochondrial protein that promotes cytochrome c-dependent caspase activation by eliminating IAP inhibition. *Cell*, **102**, 33-42.
- Duckett, C.S., Nava, V.E., Gedrich, R.W., Clem, R.J., Van Dongen, J.L., Gilfillan, M.C., Shiels, H., Hardwick, J.M. and Thompson, C.B. (1996) A conserved family of cellular genes related to the baculovirus iap gene and encoding apoptosis inhibitors. *Embo J*, **15**, 2685-2694.
- Ellis, H.M. and Horvitz, H.R. (1986) Genetic control of programmed cell death in the nematode *C. elegans*. *Cell*, **44**, 817-829.
- Fadeel, B. and Orrenius, S. (2005) Apoptosis: a basic biological phenomenon with wide-ranging implications in human disease. *J Intern Med*, **258**, 479-517.
- Fraser, A.G. and Evan, G.I. (1997) Identification of a *Drosophila melanogaster* ICE/CED-3-related protease, drICE. *Embo J*, **16**, 2805-2813.
- Fraser, A.G., McCarthy, N.J. and Evan, G.I. (1997) drICE is an essential caspase required for apoptotic activity in *Drosophila* cells. *Embo J*, **16**, 6192-6199.

- Fuentes-Prior, P. and Salvesen, G.S. (2004) The protein structures that shape caspase activity, specificity, activation and inhibition. *Biochem J*, **384**, 201-232.
- Gorski, S. and Marra, M. (2002) Programmed cell death takes flight: genetic and genomic approaches to gene discovery in *Drosophila*. *Physiol Genomics*, **9**, 59-69.
- Goyal, L., McCall, K., Agapite, J., Hartwig, E. and Steller, H. (2000) Induction of apoptosis by *Drosophila* reaper, hid and grim through inhibition of IAP function. *Embo J*, **19**, 589-597.
- Grether, M.E., Abrams, J.M., Agapite, J., White, K. and Steller, H. (1995) The head involution defective gene of *Drosophila melanogaster* functions in programmed cell death. *Genes Dev*, **9**, 1694-1708.
- Hawkins, C.J., Yoo, S.J., Peterson, E.P., Wang, S.L., Vernooy, S.Y. and Hay, B.A. (2000) The *Drosophila* caspase DRONC cleaves following glutamate or aspartate and is regulated by DIAP1, HID, and GRIM. *J Biol Chem*, **275**, 27084-27093.
- Hay, B.A. and Guo, M. (2006) Caspase-dependent cell death in *Drosophila*. *Annu Rev Cell Dev Biol*, **22**, 623-650.
- Hay, B.A., Wassarman, D.A. and Rubin, G.M. (1995) *Drosophila* homologs of baculovirus inhibitor of apoptosis proteins function to block cell death. *Cell*, **83**, 1253-1262.
- Hays, R., Wickline, L. and Cagan, R. (2002) Morgue mediates apoptosis in the *Drosophila melanogaster* retina by promoting degradation of DIAP1. *Nat Cell Biol*, **4**, 425-431.
- Hegde, R., Srinivasula, S.M., Zhang, Z., Wassell, R., Mukattash, R., Cilenti, L., DuBois, G., Lazebnik, Y., Zervos, A.S., Fernandes-Alnemri, T. and Alnemri, E.S. (2002) Identification of Omi/HtrA2 as a mitochondrial apoptotic serine protease that disrupts inhibitor of apoptosis protein-caspase interaction. *J Biol Chem*, **277**, 432-438.

- Hengartner, M.O. (1996) Programmed cell death in invertebrates. *Curr Opin Genet Dev*, **6**, 34-38.
- Hengartner, M.O., Ellis, R.E. and Horvitz, H.R. (1992) *Caenorhabditis elegans* gene *ced-9* protects cells from programmed cell death. *Nature*, **356**, 494-499.
- Herman-Bachinsky, Y., Ryoo, H.D., Ciechanover, A. and Gonen, H. (2007) Regulation of the *Drosophila* ubiquitin ligase DIAP1 is mediated via several distinct ubiquitin system pathways. *Cell Death Differ*, **14**, 861-871.
- Holley, C.L., Olson, M.R., Colon-Ramos, D.A. and Kornbluth, S. (2002) Reaper eliminates IAP proteins through stimulated IAP degradation and generalized translational inhibition. *Nat Cell Biol*, **4**, 439-444.
- Huang, Y., Park, Y.C., Rich, R.L., Segal, D., Myszka, D.G. and Wu, H. (2001) Structural basis of caspase inhibition by XIAP: differential roles of the linker versus the BIR domain. *Cell*, **104**, 781-790.
- Huh, J.R., Foe, I., Muro, I., Chen, C.H., Seol, J.H., Yoo, S.J., Guo, M., Park, J.M. and Hay, B.A. (2007) The *Drosophila* inhibitor of apoptosis (IAP) DIAP2 is dispensable for cell survival, required for the innate immune response to gram-negative bacterial infection, and can be negatively regulated by the reaper/hid/grim family of IAP-binding apoptosis inducers. *J Biol Chem*, **282**, 2056-2068.
- Huh, J.R., Guo, M. and Hay, B.A. (2004a) Compensatory proliferation induced by cell death in the *Drosophila* wing disc requires activity of the apical cell death caspase Dronc in a nonapoptotic role. *Curr Biol*, **14**, 1262-1266.
- Huh, J.R., Vernooy, S.Y., Yu, H., Yan, N., Shi, Y., Guo, M. and Hay, B.A. (2004b) Multiple apoptotic caspase cascades are required in nonapoptotic roles for *Drosophila* spermatid individualization. *PLoS Biol*, **2**, E15.
- Hultmark, D. (2003) *Drosophila* immunity: paths and patterns. *Curr Opin Immunol*, **15**, 12-19.

- Igaki, T., Kanuka, H., Inohara, N., Sawamoto, K., Nunez, G., Okano, H. and Miura, M. (2000) Drob-1, a Drosophila member of the Bcl-2/CED-9 family that promotes cell death. *Proc Natl Acad Sci U S A*, **97**, 662-667.
- Igaki, T. and Miura, M. (2004) Role of Bcl-2 family members in invertebrates. *Biochim Biophys Acta*, **1644**, 73-81.
- Igaki, T., Yamamoto-Goto, Y., Tokushige, N., Kanda, H. and Miura, M. (2002) Down-regulation of DIAP1 triggers a novel Drosophila cell death pathway mediated by Dark and DRONC. *J Biol Chem*, **277**, 23103-23106.
- Jiang, X. and Wang, X. (2004) Cytochrome C-mediated apoptosis. *Annu Rev Biochem*, **73**, 87-106.
- Jin, S., Kalkum, M., Overholtzer, M., Stoffel, A., Chait, B.T. and Levine, A.J. (2003) CIAP1 and the serine protease HTRA2 are involved in a novel p53-dependent apoptosis pathway in mammals. *Genes Dev*, **17**, 359-367.
- Johnson, E.S., Gonda, D.K. and Varshavsky, A. (1990) cis-trans recognition and subunit-specific degradation of short-lived proteins. *Nature*, **346**, 287-291.
- Jones, J.M., Datta, P., Srinivasula, S.M., Ji, W., Gupta, S., Zhang, Z., Davies, E., Hajnoczky, G., Saunders, T.L., Van Keuren, M.L., Fernandes-Alnemri, T., Meisler, M.H. and Alnemri, E.S. (2003) Loss of Omi mitochondrial protease activity causes the neuromuscular disorder of mnd2 mutant mice. *Nature*, **425**, 721-727.
- Kaiser, W.J., Vucic, D. and Miller, L.K. (1998) The Drosophila inhibitor of apoptosis D-IAP1 suppresses cell death induced by the caspase drICE. *FEBS Lett*, **440**, 243-248.
- Kanuka, H., Sawamoto, K., Inohara, N., Matsuno, K., Okano, H. and Miura, M. (1999a) Control of the cell death pathway by Dapaf-1, a Drosophila Apaf-1/CED-4-related caspase activator. *Mol. Cell*, **4**, 757-769.

- Kanuka, H., Sawamoto, K., Inohara, N., Matsuno, K., Okano, H. and Miura, M. (1999b) Control of the cell death pathway by Dapaf-1, a *Drosophila* Apaf-1/CED-4-related caspase activator. *Mol Cell*, **4**, 757-769.
- Kerr, J.F., Wyllie, A.H. and Currie, A.R. (1972) Apoptosis: a basic biological phenomenon with wide-ranging implications in tissue kinetics. *Br J Cancer*, **26**, 239-257.
- Kiessling, S. and Green, D.R. (2006) Cell survival and proliferation in *Drosophila* S2 cells following apoptotic stress in the absence of the APAF-1 homolog, ARK, or downstream caspases. *Apoptosis*, **11**, 497-507.
- Kornbluth, S. and White, K. (2005) Apoptosis in *Drosophila*: neither fish nor fowl (nor man, nor worm). *J Cell Sci*, **118**, 1779-1787.
- Krajewska, M., Krajewski, S., Banares, S., Huang, X., Turner, B., Bubendorf, L., Kallioniemi, O.P., Shabaik, A., Vitiello, A., Peehl, D., Gao, G.J. and Reed, J.C. (2003) Elevated expression of inhibitor of apoptosis proteins in prostate cancer. *Clin Cancer Res*, **9**, 4914-4925.
- Lauber, K., Blumenthal, S.G., Waibel, M. and Wesselborg, S. (2004) Clearance of apoptotic cells: getting rid of the corpses. *Mol Cell*, **14**, 277-287.
- Laundrie, B., Peterson, J.S., Baum, J.S., Chang, J.C., Fileppo, D., Thompson, S.R. and McCall, K. (2003) Germline cell death is inhibited by P-element insertions disrupting the *dcp-1/pita* nested gene pair in *Drosophila*. *Genetics*, **165**, 1881-1888.
- Lettre, G. and Hengartner, M.O. (2006) Developmental apoptosis in *C. elegans*: a complex CEDnario. *Nat Rev Mol Cell Biol*, **7**, 97-108.
- Leulier, F., Lhocine, N., Lemaitre, B. and Meier, P. (2006) The *Drosophila* inhibitor of apoptosis protein DIAP2 functions in innate immunity and is essential to resist gram-negative bacterial infection. *Mol Cell Biol*, **26**, 7821-7831.

- Li, P., Nijhawan, D., Budihardjo, I., Srinivasula, S.M., Ahmad, M., Alnemri, E.S. and Wang, X. (1997) Cytochrome c and dATP-dependent formation of Apaf-1/caspase-9 complex initiates an apoptotic protease cascade. *Cell*, **91**, 479-489.
- Li, W., Srinivasula, S.M., Chai, J., Li, P., Wu, J.W., Zhang, Z., Alnemri, E.S. and Shi, Y. (2002) Structural insights into the pro-apoptotic function of mitochondrial serine protease HtrA2/Omi. *Nat Struct Biol*, **9**, 436-441.
- Lisi, S., Mazzon, I. and White, K. (2000) Diverse domains of THREAD/DIAP1 are required to inhibit apoptosis induced by REAPER and HID in *Drosophila*. *Genetics*, **154**, 669-678.
- Liu, Z., Sun, C., Olejniczak, E.T., Meadows, R.P., Betz, S.F., Oost, T., Herrmann, J., Wu, J.C. and Fesik, S.W. (2000) Structural basis for binding of Smac/DIABLO to the XIAP BIR3 domain. *Nature*, **408**, 1004-1008.
- MacFarlane, M., Merrison, W., Bratton, S.B. and Cohen, G.M. (2002) Proteasome-mediated degradation of Smac during apoptosis: XIAP promotes Smac ubiquitination *in vitro*. *J Biol Chem*, **277**, 36611-36616.
- Martins, L.M., Iaccarino, I., Tenev, T., Gschmeissner, S., Totty, N.F., Lemoine, N.R., Savopoulos, J., Gray, C.W., Creasy, C.L., Dingwall, C. and Downward, J. (2002) The serine protease Omi/HtrA2 regulates apoptosis by binding XIAP through a reaper-like motif. *J Biol Chem*, **277**, 439-444.
- Martins, L.M., Morrison, A., Klupsch, K., Fedele, V., Moiso, N., Teismann, P., Abuin, A., Grau, E., Geppert, M., Livi, G.P., Creasy, C.L., Martin, A., Hargreaves, I., Heales, S.J., Okada, H., Brandner, S., Schulz, J.B., Mak, T. and Downward, J. (2004) Neuroprotective role of the Reaper-related serine protease HtrA2/Omi revealed by targeted deletion in mice. *Mol Cell Biol*, **24**, 9848-9862.
- Martins, L.M., Turk, B.E., Cowling, V., Borg, A., Jarrell, E.T., Cantley, L.C. and Downward, J. (2003) Binding specificity and regulation of the serine protease and PDZ domains of HtrA2/Omi. *J Biol Chem*, **278**, 49417-49427.
- Mattson, M.P. (2000) Apoptosis in neurodegenerative disorders. *Nat Rev Mol Cell Biol*, **1**, 120-129.

- Means, J.C., Muro, I. and Clem, R.J. (2006) Lack of involvement of mitochondrial factors in caspase activation in a *Drosophila* cell-free system. *Cell Death Differ*, **13**, 1222-1234.
- Meier, P., Silke, J., Leevers, S.J. and Evan, G.I. (2000) The *Drosophila* caspase DRONC is regulated by DIAP1. *Embo J*, **19**, 598-611.
- Mendes, C.S., Arama, E., Brown, S., Scherr, H., Srivastava, M., Bergmann, A., Steller, H. and Mollereau, B. (2006) Cytochrome c-d regulates developmental apoptosis in the *Drosophila* retina. *EMBO Rep*, **7**, 933-939.
- Morizane, Y., Honda, R., Fukami, K. and Yasuda, H. (2005) X-linked inhibitor of apoptosis functions as ubiquitin ligase toward mature caspase-9 and cytosolic Smac/DIABLO. *J Biochem (Tokyo)*, **137**, 125-132.
- Muro, I., Berry, D.L., Huh, J.R., Chen, C.H., Huang, H., Yoo, S.J., Guo, M., Baehrecke, E.H. and Hay, B.A. (2006) The *Drosophila* caspase Ice is important for many apoptotic cell deaths and for spermatid individualization, a nonapoptotic process. *Development*, **133**, 3305-3315.
- Muro, I., Hay, B.A. and Clem, R.J. (2002) The *Drosophila* DIAP1 protein is required to prevent accumulation of a continuously generated, processed form of the apical caspase DRONC. *J Biol Chem*, **277**, 49644-49650.
- Muro, I., Means, J.C. and Clem, R.J. (2005) Cleavage of the apoptosis inhibitor DIAP1 by the apical caspase DRONC in both normal and apoptotic *Drosophila* cells. *J Biol Chem*, **280**, 18683-18688.
- Muro, I., Monser, K. and Clem, R.J. (2004) Mechanism of Dronc activation in *Drosophila* cells. *J Cell Sci*, **117**, 5035-5041.
- Nicholson, D.W., Ali, A., Thornberry, N.A., Vaillancourt, J.P., Ding, C.K., Gallant, M., Gareau, Y., Griffin, P.R., Labelle, M., Lazebnik, Y.A. and et al. (1995) Identification and inhibition of the ICE/CED-3 protease necessary for mammalian apoptosis. *Nature*, **376**, 37-43.

- Olson, M.R., Holley, C.L., Gan, E.C., Colon-Ramos, D.A., Kaplan, B. and Kornbluth, S. (2003a) A GH3-like domain in reaper is required for mitochondrial localization and induction of IAP degradation. *J Biol Chem*, **278**, 44758-44768.
- Olson, M.R., Holley, C.L., Yoo, S.J., Huh, J.R., Hay, B.A. and Kornbluth, S. (2003b) Reaper is regulated by IAP-mediated ubiquitination. *J Biol Chem*, **278**, 4028-4034.
- Opferman, J.T. and Korsmeyer, S.J. (2003) Apoptosis in the development and maintenance of the immune system. *Nat Immunol*, **4**, 410-415.
- Peterson, C., Carney, G.E., Taylor, B.J. and White, K. (2002) reaper is required for neuroblast apoptosis during Drosophila development. *Development*, **129**, 1467-1476.
- Quinn, L., Coombe, M., Mills, K., Daish, T., Colussi, P., Kumar, S. and Richardson, H. (2003) Buffy, a Drosophila Bcl-2 protein, has anti-apoptotic and cell cycle inhibitory functions. *Embo J*, **22**, 3568-3579.
- Quinn, L.M., Dorstyn, L., Mills, K., Colussi, P.A., Chen, P., Coombe, M., Abrams, J., Kumar, S. and Richardson, H. (2000) An essential role for the caspase dronc in developmentally programmed cell death in Drosophila. *J Biol Chem*, **275**, 40416-40424.
- Riedl, S.J., Renatus, M., Schwarzenbacher, R., Zhou, Q., Sun, C., Fesik, S.W., Liddington, R.C. and Salvesen, G.S. (2001) Structural basis for the inhibition of caspase-3 by XIAP. *Cell*, **104**, 791-800.
- Riedl, S.J. and Salvesen, G.S. (2007) The apoptosome: signalling platform of cell death. *Nat Rev Mol Cell Biol*, **8**, 405-413.
- Riedl, S.J. and Shi, Y. (2004) Molecular mechanisms of caspase regulation during apoptosis. *Nat Rev Mol Cell Biol*, **5**, 897-907.
- Rodriguez, A., Chen, P., Oliver, H. and Abrams, J.M. (2002) Unrestrained caspase-dependent cell death caused by loss of Diap1 function requires the Drosophila Apaf-1 homolog, Dark. *Embo J*, **21**, 2189-2197.

- Rodriguez, J. and Lazebnik, Y. (1999) Caspase-9 and APAF-1 form an active holoenzyme. *Genes Dev*, **13**, 3179-3184.
- Roy, N., Mahadevan, M.S., McLean, M., Shutler, G., Yaraghi, Z., Farahani, R., Baird, S., Besner-Johnston, A., Lefebvre, C., Kang, X. and et al. (1995) The gene for neuronal apoptosis inhibitory protein is partially deleted in individuals with spinal muscular atrophy. *Cell*, **80**, 167-178.
- Ryoo, H.D., Bergmann, A., Gonen, H., Ciechanover, A. and Steller, H. (2002) Regulation of Drosophila IAP1 degradation and apoptosis by reaper and ubcD1. *Nat Cell Biol*, **4**, 432-438.
- Ryoo, H.D., Domingos, P.M., Kang, M.J. and Steller, H. (2007) Unfolded protein response in a Drosophila model for retinal degeneration. *Embo J*, **26**, 242-252.
- Salvesen, G.S. and Duckett, C.S. (2002) IAP proteins: blocking the road to death's door. *Nat Rev Mol Cell Biol*, **3**, 401-410.
- Scott, F.L., Denault, J.B., Riedl, S.J., Shin, H., Renatus, M. and Salvesen, G.S. (2005) XIAP inhibits caspase-3 and -7 using two binding sites: evolutionarily conserved mechanism of IAPs. *Embo J*, **24**, 645-655.
- Senoo-Matsuda, N., Igaki, T. and Miura, M. (2005) Bax-like protein Drob-1 protects neurons from expanded polyglutamine-induced toxicity in Drosophila. *Embo J*, **24**, 2700-2713.
- Seshagiri, S. and Miller, L.K. (1997) Caenorhabditis elegans CED-4 stimulates CED-3 processing and CED-3-induced apoptosis. *Curr Biol*, **7**, 455-460.
- Shi, Y. (2006) Mechanical aspects of apoptosome assembly. *Curr Opin Cell Biol*, **18**, 677-684.
- Soengas, M.S., Capodieci, P., Polsky, D., Mora, J., Esteller, M., Opitz-Araya, X., McCombie, R., Herman, J.G., Gerald, W.L., Lazebnik, Y.A., Cordon-Cardo, C. and Lowe, S.W. (2001) Inactivation of the apoptosis effector Apaf-1 in malignant melanoma. *Nature*, **409**, 207-211.

- Song, Z., McCall, K. and Steller, H. (1997) DCP-1, a *Drosophila* cell death protease essential for development. *Science*, **275**, 536-540.
- Spector, M.S., Desnoyers, S., Hoepfner, D.J. and Hengartner, M.O. (1997) Interaction between the *C. elegans* cell-death regulators CED-9 and CED-4. *Nature*, **385**, 653-656.
- Srinivasula, S.M., Ahmad, M., Fernandes-Alnemri, T. and Alnemri, E.S. (1998) Autoactivation of procaspase-9 by Apaf-1-mediated oligomerization. *Mol Cell*, **1**, 949-957.
- Srinivasula, S.M., Datta, P., Fan, X.J., Fernandes-Alnemri, T., Huang, Z. and Alnemri, E.S. (2000) Molecular determinants of the caspase-promoting activity of Smac/DIABLO and its role in the death receptor pathway. *J Biol Chem*, **275**, 36152-36157.
- Srinivasula, S.M., Datta, P., Kobayashi, M., Wu, J.W., Fujioka, M., Hegde, R., Zhang, Z., Mukattash, R., Fernandes-Alnemri, T., Shi, Y., Jaynes, J.B. and Alnemri, E.S. (2002) sickle, a novel *Drosophila* death gene in the reaper/hid/grim region, encodes an IAP-inhibitory protein. *Curr Biol*, **12**, 125-130.
- Srinivasula, S.M., Gupta, S., Datta, P., Zhang, Z., Hegde, R., Cheong, N., Fernandes-Alnemri, T. and Alnemri, E.S. (2003) Inhibitor of apoptosis proteins are substrates for the mitochondrial serine protease Omi/HtrA2. *J Biol Chem*, **278**, 31469-31472.
- Srinivasula, S.M., Hegde, R., Saleh, A., Datta, P., Shiozaki, E., Chai, J., Lee, R.A., Robbins, P.D., Fernandes-Alnemri, T., Shi, Y. and Alnemri, E.S. (2001) A conserved XIAP-interaction motif in caspase-9 and Smac/DIABLO regulates caspase activity and apoptosis. *Nature*, **410**, 112-116.
- Strauss, K.M., Martins, L.M., Plun-Favreau, H., Marx, F.P., Kautzmann, S., Berg, D., Gasser, T., Wszolek, Z., Muller, T., Bornemann, A., Wolburg, H., Downward, J., Riess, O., Schulz, J.B. and Kruger, R. (2005) Loss of function mutations in the gene encoding Omi/HtrA2 in Parkinson's disease. *Hum Mol Genet*, **14**, 2099-2111.

- Sulston, J.E., Schierenberg, E., White, J.G. and Thomson, J.N. (1983) The embryonic cell lineage of the nematode *Caenorhabditis elegans*. *Dev Biol*, **100**, 64-119.
- Suzuki, T. and Varshavsky, A. (1999) Degradation signals in the lysine-asparagine sequence space. *Embo J*, **18**, 6017-6026.
- Suzuki, Y., Imai, Y., Nakayama, H., Takahashi, K., Takio, K. and Takahashi, R. (2001a) A serine protease, HtrA2, is released from the mitochondria and interacts with XIAP, inducing cell death. *Mol Cell*, **8**, 613-621.
- Suzuki, Y., Nakabayashi, Y. and Takahashi, R. (2001b) Ubiquitin-protein ligase activity of X-linked inhibitor of apoptosis protein promotes proteasomal degradation of caspase-3 and enhances its anti-apoptotic effect in Fas-induced cell death. *Proc Natl Acad Sci U S A*, **98**, 8662-8667.
- Tamm, I., Richter, S., Oltersdorf, D., Creutzig, U., Harbott, J., Scholz, F., Karawajew, L., Ludwig, W.D. and Wuchter, C. (2004) High expression levels of x-linked inhibitor of apoptosis protein and survivin correlate with poor overall survival in childhood de novo acute myeloid leukemia. *Clin Cancer Res*, **10**, 3737-3744.
- Tenev, T., Ditzel, M., Zachariou, A. and Meier, P. (2007) The antiapoptotic activity of insect IAPs requires activation by an evolutionarily conserved mechanism. *Cell Death Differ*, **14**, 1191-1201.
- Tenev, T., Zachariou, A., Wilson, R., Ditzel, M. and Meier, P. (2005) IAPs are functionally non-equivalent and regulate effector caspases through distinct mechanisms. *Nat Cell Biol*, **7**, 70-77.
- Tenev, T., Zachariou, A., Wilson, R., Paul, A. and Meier, P. (2002) Jafrac2 is an IAP antagonist that promotes cell death by liberating Dronc from DIAP1. *Embo J*, **21**, 5118-5129.
- Thompson, C.B. (1995) Apoptosis in the pathogenesis and treatment of disease. *Science*, **267**, 1456-1462.
- Uren, A.G., Pakusch, M., Hawkins, C.J., Puls, K.L. and Vaux, D.L. (1996) Cloning and expression of apoptosis inhibitory protein homologs that function to inhibit

- apoptosis and/or bind tumor necrosis factor receptor-associated factors. *Proc Natl Acad Sci U S A*, **93**, 4974-4978.
- Varkey, J., Chen, P., Jemmerson, R. and Abrams, J.M. (1999) Altered cytochrome c display precedes apoptotic cell death in *Drosophila*. *J Cell Biol*, **144**, 701-710.
- Varshavsky, A. (1996) The N-end rule: functions, mysteries, uses. *Proc Natl Acad Sci U S A*, **93**, 12142-12149.
- Varshavsky, A. (2003) The N-end rule and regulation of apoptosis. *Nat Cell Biol*, **5**, 373-376.
- Vaux, D.L. and Korsmeyer, S.J. (1999) Cell death in development. *Cell*, **96**, 245-254.
- Vaux, D.L. and Silke, J. (2003) Mammalian mitochondrial IAP binding proteins. *Biochem Biophys Res Commun*, **304**, 499-504.
- Vaux, D.L. and Silke, J. (2005) IAPs, RINGs and ubiquitylation. *Nat Rev Mol Cell Biol*, **6**, 287-297.
- Verhagen, A.M., Ekert, P.G., Pakusch, M., Silke, J., Connolly, L.M., Reid, G.E., Moritz, R.L., Simpson, R.J. and Vaux, D.L. (2000) Identification of DIABLO, a mammalian protein that promotes apoptosis by binding to and antagonizing IAP proteins. *Cell*, **102**, 43-53.
- Verhagen, A.M., Silke, J., Ekert, P.G., Pakusch, M., Kaufmann, H., Connolly, L.M., Day, C.L., Tikoo, A., Burke, R., Wrobel, C., Moritz, R.L., Simpson, R.J. and Vaux, D.L. (2002) HtrA2 promotes cell death through its serine protease activity and its ability to antagonize inhibitor of apoptosis proteins. *J Biol Chem*, **277**, 445-454.
- Vernooy, S.Y., Chow, V., Su, J., Verbrugghe, K., Yang, J., Cole, S., Olson, M.R. and Hay, B.A. (2002) *Drosophila* Bruce can potently suppress Rpr- and Grim-dependent but not Hid-dependent cell death. *Curr Biol*, **12**, 1164-1168.

- Vernooy, S.Y., Copeland, J., Ghaboosi, N., Griffin, E.E., Yoo, S.J. and Hay, B.A. (2000) Cell death regulation in *Drosophila*: conservation of mechanism and unique insights. *J Cell Biol*, **150**, F69-76.
- Vucic, D., Kaiser, W.J., Harvey, A.J. and Miller, L.K. (1997) Inhibition of reaper-induced apoptosis by interaction with inhibitor of apoptosis proteins (IAPs). *Proc Natl Acad Sci U S A*, **94**, 10183-10188.
- Vucic, D., Stennicke, H.R., Pisabarro, M.T., Salvesen, G.S. and Dixit, V.M. (2000) ML-IAP, a novel inhibitor of apoptosis that is preferentially expressed in human melanomas. *Curr Biol*, **10**, 1359-1366.
- Waldhuber, M., Emoto, K. and Petritsch, C. (2005) The *Drosophila* caspase DRONC is required for metamorphosis and cell death in response to irradiation and developmental signals. *Mech Dev*, **122**, 914-927.
- Wang, S.L., Hawkins, C.J., Yoo, S.J., Muller, H.A. and Hay, B.A. (1999) The *Drosophila* caspase inhibitor DIAP1 is essential for cell survival and is negatively regulated by HID. *Cell*, **98**, 453-463.
- Weiss, L.M., Warnke, R.A., Sklar, J. and Cleary, M.L. (1987) Molecular analysis of the t(14;18) chromosomal translocation in malignant lymphomas. *N Engl J Med*, **317**, 1185-1189.
- Wernette, C.M. and Kaguni, L.S. (1986) A mitochondrial DNA polymerase from embryos of *Drosophila melanogaster*. Purification, subunit structure, and partial characterization. *J. Biol. Chem.*, **261**, 14764-14770.
- White, K., Grether, M.E., Abrams, J.M., Young, L., Farrell, K. and Steller, H. (1994) Genetic control of programmed cell death in *Drosophila*. *Science*, **264**, 677-683.
- White, K., Tahaoglu, E. and Steller, H. (1996) Cell killing by the *Drosophila* gene reaper. *Science*, **271**, 805-807.
- Wilson, R., Goyal, L., Ditzel, M., Zachariou, A., Baker, D.A., Agapite, J., Steller, H. and Meier, P. (2002) The DIAP1 RING finger mediates ubiquitination of Dronc and is indispensable for regulating apoptosis. *Nat Cell Biol*, **4**, 445-450.

- Wing, J.P., Karres, J.S., Ogdahl, J.L., Zhou, L., Schwartz, L.M. and Nambu, J.R. (2002a) *Drosophila sickle* is a novel grim-reaper cell death activator. *Curr Biol*, **12**, 131-135.
- Wing, J.P., Schreder, B.A., Yokokura, T., Wang, Y., Andrews, P.S., Huseinovic, N., Dong, C.K., Ogdahl, J.L., Schwartz, L.M., White, K. and Nambu, J.R. (2002b) *Drosophila* Morgue is an F box/ubiquitin conjugase domain protein important for grim-reaper mediated apoptosis. *Nat Cell Biol*, **4**, 451-456.
- Wing, J.P., Schwartz, L.M. and Nambu, J.R. (2001) The RHG motifs of *Drosophila* Reaper and Grim are important for their distinct cell death-inducing abilities. *Mech Dev*, **102**, 193-203.
- Wu, D., Wallen, H.D. and Nunez, G. (1997) Interaction and regulation of subcellular localization of CED-4 by CED-9. *Science*, **275**, 1126-1129.
- Wu, G., Chai, J., Suber, T.L., Wu, J.W., Du, C., Wang, X. and Shi, Y. (2000) Structural basis of IAP recognition by Smac/DIABLO. *Nature*, **408**, 1008-1012.
- Wu, J.W., Cocina, A.E., Chai, J., Hay, B.A. and Shi, Y. (2001) Structural analysis of a functional DIAP1 fragment bound to grim and hid peptides. *Mol Cell*, **8**, 95-104.
- Xu, D., Li, Y., Arcaro, M., Lackey, M. and Bergmann, A. (2005) The CARD-carrying caspase Dronc is essential for most, but not all, developmental cell death in *Drosophila*. *Development*, **132**, 2125-2134.
- Xu, D., Wang, Y., Willecke, R., Chen, Z., Ding, T. and Bergmann, A. (2006) The effector caspases drICE and dcp-1 have partially overlapping functions in the apoptotic pathway in *Drosophila*. *Cell Death Differ*, **13**, 1697-1706.
- Xue, D., Shaham, S. and Horvitz, H.R. (1996) The *Caenorhabditis elegans* cell-death protein CED-3 is a cysteine protease with substrate specificities similar to those of the human CPP32 protease. *Genes Dev*, **10**, 1073-1083.
- Yan, N., Gu, L., Kokel, D., Chai, J., Li, W., Han, A., Chen, L., Xue, D. and Shi, Y. (2004a) Structural, biochemical, and functional analyses of CED-9 recognition by the proapoptotic proteins EGL-1 and CED-4. *Mol Cell*, **15**, 999-1006.

- Yan, N., Huh, J.R., Schirf, V., Demeler, B., Hay, B.A. and Shi, Y. (2006) Structure and activation mechanism of the *Drosophila* initiator caspase Dronc. *J Biol Chem*, **281**, 8667-8674.
- Yan, N., Wu, J.W., Chai, J., Li, W. and Shi, Y. (2004b) Molecular mechanisms of DrICE inhibition by DIAP1 and removal of inhibition by Reaper, Hid and Grim. *Nat Struct Mol Biol*, **11**, 420-428.
- Yang, Q.H., Church-Hajduk, R., Ren, J., Newton, M.L. and Du, C. (2003) Omi/HtrA2 catalytic cleavage of inhibitor of apoptosis (IAP) irreversibly inactivates IAPs and facilitates caspase activity in apoptosis. *Genes Dev*, **17**, 1487-1496.
- Yang, Y., Fang, S., Jensen, J.P., Weissman, A.M. and Ashwell, J.D. (2000) Ubiquitin protein ligase activity of IAPs and their degradation in proteasomes in response to apoptotic stimuli. *Science*, **288**, 874-877.
- Yokokura, T., Dresnek, D., Huseinovic, N., Lisi, S., Abdelwahid, E., Bangs, P. and White, K. (2004) Dissection of DIAP1 functional domains via a mutant replacement strategy. *J Biol Chem*, **279**, 52603-52612.
- Yoo, S.J., Huh, J.R., Muro, I., Yu, H., Wang, L., Wang, S.L., Feldman, R.M., Clem, R.J., Muller, H.A. and Hay, B.A. (2002) Hid, Rpr and Grim negatively regulate DIAP1 levels through distinct mechanisms. *Nat Cell Biol*, **4**, 416-424.
- Yu, X., Wang, L., Acehan, D., Wang, X. and Akey, C.W. (2006) Three-dimensional structure of a double apoptosome formed by the *Drosophila* Apaf-1 related killer. *J Mol Biol*, **355**, 577-589.
- Yuan, J. and Horvitz, H.R. (1992) The *Caenorhabditis elegans* cell death gene *ced-4* encodes a novel protein and is expressed during the period of extensive programmed cell death. *Development*, **116**, 309-320.
- Yuan, J., Shaham, S., Ledoux, S., Ellis, H.M. and Horvitz, H.R. (1993) The *C. elegans* cell death gene *ced-3* encodes a protein similar to mammalian interleukin-1 beta-converting enzyme. *Cell*, **75**, 641-652.

- Zachariou, A., Tenev, T., Goyal, L., Agapite, J., Steller, H. and Meier, P. (2003) IAP-antagonists exhibit non-redundant modes of action through differential DIAP1 binding. *Embo J*, **22**, 6642-6652.
- Zhou, L. and Steller, H. (2003) Distinct pathways mediate UV-induced apoptosis in *Drosophila* embryos. *Dev Cell*, **4**, 599-605.
- Zimmermann, K.C., Ricci, J.E., Droin, N.M. and Green, D.R. (2002) The role of ARK in stress-induced apoptosis in *Drosophila* cells. *J Cell Biol*, **156**, 1077-1087.
- Zou, H., Henzel, W.J., Liu, X., Lutschg, A. and Wang, X. (1997) Apaf-1, a human protein homologous to *C. elegans* CED-4, participates in cytochrome c-dependent activation of caspase-3. *Cell*, **90**, 405-413.

Vita

Madhavi Malladi was born in Hyderabad, India on August 31, 1976, the daughter of Ramana Challa and Someshwara Rao Challa. After graduating from Keyes High School in 1991, she attended Ideal Junior College from 1991-1993. Madhavi then attended Acharya. N. G. Ranga Agricultural University from 1994-1998 where she graduated with Bachelor of Science in Agricultural Sciences. In 1999, Madhavi joined Texas A & M University-Kingsville where she graduated with Master of Science degree in Plant and Soil Sciences in 2001. In 2003, she received another Master of Science degree in Biology from Texas A & M University-Kingsville. In August of 2003, she entered the Graduate School at the University of Texas, Austin under the tutelage of Dr. Shawn Bratton.

Permanent address: 1-5-51, Chaitanyapuri, Hyderabad, A.P, India-500060.

This dissertation was typed by the author.